

UNIVERSITY OF SOUTHAMPTON
FACULTY OF MEDICINE, HEALTH & BIOLOGICAL SCIENCES
HUMAN GENETICS DIVISION

A GENETIC INVESTIGATION INTO INHERITED VENTRICULAR ARRHYTHMIAS

Binoy Skaria

Thesis for the degree of Doctor of Medicine

February 2008

UNIVERSITY OF SOUTHAMPTON

ABSTRACT

FACULTY OF MEDICINE, HEALTH & BIOLOGICAL SCIENCES

HUMAN GENETICS DIVISION

Doctor of Medicine

A GENETIC INVESTIGATION INTO INHERITED VENTRICULAR ARRHYTHMIAS

Binoy Skaria

Inherited ventricular arrhythmias are important because a) it can cause sudden cardiac death b) affected patients are often young and c) it causes great anxiety on the family members. An understanding of the genetic factors that contribute to inherited ventricular arrhythmias may help in risk-stratification.

This study focussed on two large Caucasian families. The proband in family A presented with cardiac arrest secondary to a ventricular tachyarrhythmia and an abnormal ECG. Similar ECGs were documented in 6 other members in family A, over 3 generations, and they were further identified by electrophysiological tests to be at high risk of ventricular arrhythmias. The proband in family B presented with syncope. There was strong family history of sudden death and syncope. The resting ECGs were within normal limits. Electrophysiological testing identified 3 family members to be at high risk of ventricular arrhythmias.

Standard investigations showed affected subjects to have structurally normal hearts. The clinical characteristics did not fit with known conditions associated with sudden death in a structurally normal heart. It was therefore hypothesised that mutations in a novel gene or novel mutations in a previously identified gene caused the phenotype.

The aim was to exclude 8 candidate genes by genotyping and pedigree analysis. If any gene could not be excluded, the aim was to investigate it further. If all 8 genes were excluded, the aim was to perform a genome wide scan to identify the locus in the genome likely to harbour the gene of interest.

DNA was available on 7 affected subjects in family A and 5 affected subjects in family B. Following genotyping, 6 out of 8 genes were excluded. *TNNT2* and *RyR2*, both located on the long arm of chromosome 1, could not be excluded in family A. *RyR2* and *ANKB* could not be excluded in family B. *TNNT2* was prioritised for mutation screening. Direct sequencing of the coding exons of *TNNT2* and the intron-exon boundaries identified sequence variations in two subjects but did not demonstrate a common variation in all the affected subjects. In conclusion, it is likely that the mutated gene in family A is located at 1q. However, the genetic cause for the phenotype in the two families remains unknown and further investigations are required to identify this.

TABLE OF CONTENTS

PREFACE.....	13
CHAPTER 1- INTRODUCTION & REVIEW OF LITERATURE.....	16
1.1 SUDDEN CARDIAC DEATH	17
1.1.1 Coronary artery disease.....	19
1.1.2 Ion channelopathies.....	19
1.1.3 Cardiomyopathies	20
1.1.4 Other causes of SCD	20
1.2 ECG CHARACTERISTICS.....	22
1.2.1 Normal ECG	22
1.2.2 ECG in LQTS	24
1.2.3 ECG in SQTS.....	27
1.2.4 ECG in Brugada syndrome	29
1.2.5 ECG in CPVT	32
1.2.6 ECG in hypertrophic cardiomyopathy	34
1.2.7 ECG in ARVC	36
1.3 ION CHANNELOPATHIES.....	38
1.3.1 Cardiac action potential.....	39
1.3.2 Mechanisms of arrhythmia	41

1.3.3	Cardiac Potassium channels.....	42
1.3.4	Potassium channelopathies.....	45
1.3.4.1	LQTS	45
1.3.4.2	SQTS	51
1.3.5	Sodium channelopathies	55
1.3.5.1	LQT3	58
1.3.5.2	Brugada syndrome	60
1.3.6	Calcium channelopathies.....	62
1.3.6.1	Catecholaminergic polymorphic ventricular tachycardia	62
1.4	CARDIOMYOPATHIES	63
1.4.1	Hypertrophic cardiomyopathy.....	63
1.4.1.1	Clinical features.....	63
1.4.1.2	Genetic aspects	64
1.4.2	Dilated Cardiomyopathy (CMD)	69
1.4.3	Arrhythmogenic right ventricular cardiomyopathy	72
1.4.3.1	Clinical features.....	72
1.4.3.2	Genetic aspects	74
1.4.4	Update on the genetics of inherited arrhythmias	76
1.4.4.1	LQT7	76
1.4.4.2	LQT8	76
1.4.4.3	LQT9	76
1.4.4.4	LQT10	77
1.4.4.5	GPD1L.....	77

1.4.4.6	Sarcolipin	77
1.4.4.7	NCX.....	77
1.4.5	Channel Interacting Proteins (ChIP)	78
1.4.5.1	ANKB	78
1.4.5.2	CAV3	78
1.5	MAPPING AND CLONING DISEASE GENES	79
1.5.1	Linkage analysis	79
1.5.2	Candidate gene approach	80
1.5.3	Comparative genomics.....	81
1.5.4	Positional cloning.....	81
1.5.5	Approaches using known chromosomal abnormalities	82
1.5.6	Combination of methods to identify genes	82
1.6	HYPOTHESIS	84
1.7	AIMS	84
2.0	CHAPTER 2- MATERIALS & METHODS	85
2.1	MATERIALS	86
2.1.1	Buffers and Solutions.....	86
2.1.1.1	10× TBE	86
2.1.1.2	Ethidium Bromide staining solution	86
2.1.1.3	Ammonium persulphate.....	86
2.1.2	Gels	86
2.1.2.1	Agarose gel.....	86
2.2	METHODS	87

2.2.1	DNA extraction from whole blood	87
2.2.2	Measuring DNA concentration	87
2.2.2.1	Determination of absorbance at 260 nm	87
2.2.3	PCR amplification	88
2.2.4	Agarose gel electrophoresis	88
2.2.5	Identification and design of PCR primers	88
2.2.6	Sizing of PCR products using an ABI 377 sequencer	89
2.2.7	Direct Sequencing analysis	89
3.0	RESULTS	92
3.1	INVESTIGATIONS AND RESULTS OF FAMILY A.....	94
3.1.1	Family A ascertainment.....	94
3.1.2	Genotyping.....	101
3.1.2.1	LQT1	102
3.1.2.2	LQT2	105
3.1.2.3	LQT3	107
3.1.2.4	LQT4	109
3.1.2.5	LQT5 & LQT6	111
3.1.2.6	RyR2	113
3.1.2.7	TNNT2.....	115
3.1.3	Direct sequencing of TNNT2.....	117
3.1.3.1	Genomic structure of TNNT2	117
3.1.3.2	Results of direct sequencing	119
3.2	INVESTIGATION AND RESULTS OF FAMILY B	123

3.2.1	Family B ascertainment	123
3.2.2	Genotyping.....	127
3.2.2.1	LQT1	128
3.2.2.2	LQT2	130
3.2.2.3	LQT3	132
3.2.2.4	LQT4	134
3.2.2.5	LQT 5&6	136
3.2.2.6	RyR2.....	138
3.2.2.7	TNNT2.....	140
3.3	SUMMARY OF THE RESULTS	142
4.0	CHAPTER 4: DISCUSSION.....	143
4.1	FAMILY A.....	144
4.1.1	The clinical phenotype	144
4.1.2	Flecainide challenge test	146
4.1.3	Candidate genes in family A.....	146
4.1.4	Genotyping.....	147
4.1.5	Mutation screening of TNNT2	150
4.1.5.1	Insertion of a CTCTT sequence in intron 3.....	150
4.1.5.2	Single base substitution in exon 9	150
4.1.6	Limitations of the direct sequencing approach	151
4.2	FAMILY B.....	151
4.2.1	Candidate genes in family B.....	152
4.2.2	Genotyping.....	152

4.3	DISCUSSION ON THE APPROACH FOR GENE MAPPING	153
4.3.1	Candidate gene approach	153
4.3.2	Possible alternative approach	154
4.4	IMPORTANCE OF THE STUDY FINDINGS	155
4.5	LIMITATIONS OF THE STUDY.....	155
4.6	FUTURE WORK.....	156
APPENDIX A	157
APPENDIX B	158
APPENDIX C	160
APPENDIX D	162
APPENDIX E	166
APPENDIX F	175
APPENDIX G	176
APPENDIX H	177
APPENDIX I	178
APPENDIX J	180
APPENDIX K	185
BIBLIOGRAPHY	188

LIST OF TABLES

Table 1	Other causes of sudden death in the general population	21
Table 2	Mechanisms underlying phases of the cardiac action potential	40
Table 3	Genetic aspects of SQTS.....	53
Table 4	Genetic aspects of potassium ion channelopathies	54
Table 5	Characteristic features of genetic mutations causing HCM	65
Table 6	Genes associated with HCM	66
Table 7	Genetic aspects of dilated cardiomyopathy.....	70
Table 8	Diagnostic criteria for ARVC	73
Table 9	Genetic aspects of ARVC	75
Table 10	Examples of methods used to map genes.....	83
Table 11	Clinical features of family A	94
Table 12	Comparison table of ECG changes	145
Table 13	Echocardiographic assessment of family A	175

LIST OF FIGURES

Figure 1 Causes of sudden cardiac death in those aged <35 years	18
Figure 2 Causes of sudden cardiac death in those aged >35 years	18
Figure 3 Normal ECG	23
Figure 4 ECG in LQTS	25
Figure 5 ECG patterns in LQT syndrome	26
Figure 6 ECG in Short QT syndrome.....	28
Figure 7 ECG showing type 2 changes of Brugada syndrome	30
Figure 8 Repolarisation abnormalities in ECGs in Brugada syndrome	31
Figure 9 ECG in Catecholaminergic polymorphic ventricular tachycardia.....	33
Figure 10 ECG in hypertrophic cardiomyopathy	35
Figure 11 ECG in ARVC	37
Figure 12 The action potential of a cardiac ventricular myocyte.....	40
Figure 13 Structure of the α -subunit of potassium channels.....	43
Figure 14 General structure of cardiac potassium channels.....	44
Figure 15 Structure of KCNQ1	47
Figure 16 Structure of KCNH2	49
Figure 17 Electrophysiological basis of SQTS	52

Figure 19 Structure of α -subunit of sodium channel.....	57
Figure 20 Electrophysiologic basis of LQT3	59
Figure21 Electrophysiologic basis of Brugada syndrome.....	61
Figure 22 Components of the cardiac sarcomere	68
Figure 23 Pedigree of family A	93
Figure 24 Twelve lead ECG of proband in Family A	97
Figure 25 ECG of affected members of family A	98
Figure 26 Resting ECG of IV: 1.....	99
Figure 27 ECG of IV: 1 post Flecainide infusion	100
Figure 28 An example of a gene-scan trace	103
Figure 29 Segregation analysis of LQT1 marker in family A.....	104
Figure 30 Segregation analysis of LQT2 marker in family A.....	106
Figure 31 Segregation analysis of LQT3 marker in family A.....	108
Figure 32 Segregation analysis of LQT4 markers in family A	110
Figure 33 Segregation analysis of LQT5 & LQT6 loci in family A	112
Figure 34 Segregation analysis of RyR2 markers in family A.	114
Figure 35 Segregation analysis of TNNT2 markers in family A	116
Figure 36 Genomic structure of <i>TNNT2</i>	118
Figure 37 CTTCT insertion in intron 3 of <i>TNNT2</i>	120
Figure 38 Forward sequence of exon 9 of <i>TNNT2</i> in subject II: 1	122
Figure 39 Reverse sequence of exon 9 of <i>TNNT2</i> in subject II: 1	122
Figure 40 Pedigree of family B	124
Figure 41 Resting ECG.on family member IV: 1	125

Figure 42	Exercise ECG on family member V: 2	126
Figure 43	Segregation analysis of LQT1 marker in family B	129
Figure 44	Segregation analysis of LQT2 markers in family B	131
Figure 45	Segregation analysis of LQT3 locus in family B	133
Figure 46	Segregation analysis of LQT4 locus in family B	135
Figure 47	Segregation analysis of D21S1895 marker in family B	137
Figure 48	Segregation analysis of markers near RyR2 locus in family B	139
Figure 49	Segregation analysis of TNNT2 locus in family B	141
Figure 50	Genotyping results summary in family A	149
Figure 51	ECG of subject II: 1 in family A	167
Figure 52	ECG of subject IV: 1 in family A	168
Figure 53	ECG of subject II: 3 in family A	169
Figure 54	ECG of subject III: 3 in family A	170
Figure 55	ECG of subject III: 5 in family A	171
Figure 56	ECG of subject III: 1 in family A	172
Figure 57	ECG of subject III: 2 in family A	173
Figure 58	ECG of subject III: 6 in family A	174
Figure 59	Sequence trace of exon 3 & 4, subject IV: 1	181
Figure 60	Forward sequence trace of exon 9, subject II: 1	183
Figure 61	Reverse sequence of exon 9, subject II: 1	184

PREFACE

DECLARATION OF AUTHORSHIP

I, Binoy Skaria, declare that the thesis entitled 'A Genetic Investigation into Inherited Ventricular Arrhythmias' and the work presented in the thesis are both my own, and have been generated by me as the result of my own original research. I confirm that:

- This work was done wholly while in candidature for a research degree at this University;
- Where I have consulted the published work of others, this is always clearly attributed;
- Where I have quoted from the work of others, the source is always given. With the exception of such quotations, this thesis is entirely my own work;
- I have acknowledged all main sources of help;
- None of this work has been published before submission;
- All references were consulted by me and the literature search was upto date as of

Februrary 2008.

Binoy Skaria

Acknowledgements:

I am grateful to all the patients for participating in this study. I thank my supervisors- Profs. David Wilson, Anneke Lucassen and John Morgan for their supervision throughout this study. I thank David especially for his constant motivation and understanding. I thank the clinicians for the tests done on the families prior to the start of the study. I thank my colleagues at the University of Southampton- Mirella, Tom, Dave, Emily, Karen, Vicky, Lee, Neil and all the other members of the group who have in some way helped me during this period. I thank Tim and Raj for helping me with 'Coreldraw'. I thank John Holloway for his expertise with the ABI 377 sequencer, Patricia and her colleagues for their help with DNA quantification using the PicoGreen method, Andy Collins and members of the Genetic Epidemiology Group for helping me to understand the basics of statistical genetics. I thank the University of Southampton and the School of Medicine for all the help. I thank BUPA for the fellowship which enabled me to do this research.

I thank my wife- Nija, my children – Maria, Matthew & Joel, my parents and all my well wishers for their support. Finally, I thank God for His guidance.

February 2008

LIST OF ABBREVIATIONS

SCD- Sudden cardiac death
ECG- Electrocardiogram
CAD- Coronary Atery Disease
LQTS- Long QT Syndrome
SQTS- Short QT Syndrome
JLNS- Jervell Lange Nielsen syndrome
CPVT- Catecholaminergic Polymorphic Ventricular Tachycardia
HCM- Hypertrophic Cardiomyopathy
CMD- Dilated Cardiomyopathy
ARVC- Arrhythmogenic Right Ventricular Cardiomyopathy
SCD- Sudden Cardiac Death
RBBB- Right Bundle Branch Block
LVH- Left Ventricular Hypertrophy
MRI- Magnetic Resonance Imaging
SSCP- Single Strand Conformation Polymorphism
DNA- Deoxyribonucleic acid
RNA- Ribonucleic acid
TNNT2- troponin T gene
TNNT2- troponin T protein
RyR2- Ryanodine receptor gene
RyR2- Ryanodine receptor protein
OMIM- Online Mendelian Inheritance in Man
bp- base pair

CHAPTER 1- INTRODUCTION & REVIEW OF LITERATURE

1.1 SUDDEN CARDIAC DEATH

Sudden cardiac death (SCD) is defined as 'natural death, from cardiac causes, characterised by abrupt loss of consciousness, within one hour of the onset of symptoms. The time and mode of death are unexpected'¹. The major mechanism leading to sudden cardiac death in most cases is ventricular arrhythmia².

Due to the inconsistencies in reporting the causes of death, studies have found it difficult to accurately estimate the incidence and prevalence of sudden cardiac death and its various causes. Based on reported studies, figures 1 and 2 show the causes of sudden cardiac death in the white Caucasian population³⁻⁵. If all ages are considered in a single chart, it looks similar to figure 2.

The incidence of SCD in England in people aged 16-64 years is estimated at 11 per 100,000 (3,500 deaths) per year⁶. Sudden Arrhythmic Death Syndrome (SADS) is a subset of SCD, when a cardiac pathologist can find no evidence of cardiac disease and the toxicology screen is negative. A survey in England estimated the annual death rate for Sudden Arrhythmic Death Syndrome (SADS) in white Caucasians aged 4 to 64 years as 0.16 per 100,000 per annum⁷.

In inherited conditions leading to sudden cardiac death, presymptomatic diagnosis is sometimes possible. Both drug therapy and implantation of cardioverter defibrillators have reduced morbidity and mortality in various patient subgroups at high risk of ventricular arrhythmias⁸.

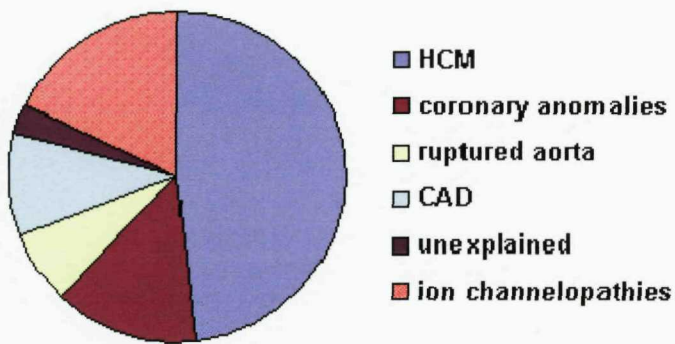


Figure 1 Causes of sudden cardiac death in those aged <35 years

The major causes of sudden cardiac death in those aged <35 years are HCM (hypertrophic cardiomyopathy), ion channelopathies, coronary anomalies, CAD (coronary artery disease), ruptured aorta and unexplained causes.

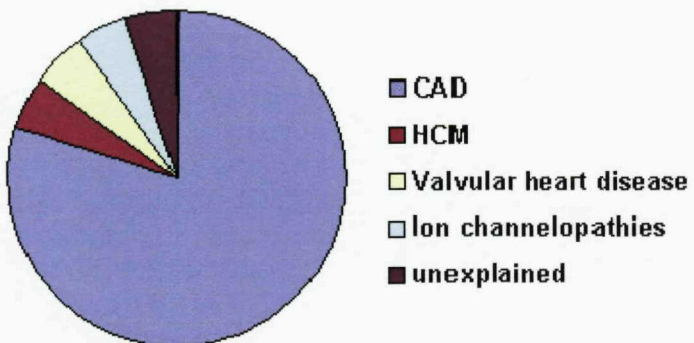


Figure 2 Causes of sudden cardiac death in those aged >35 years

The major cause of sudden cardiac death in those aged > 35 years is coronary artery disease (CAD). HCM (hypertrophic cardiomyopathy), valvular heart disease, ion channelopathies and unexplained causes account for the rest.

1.1.1 Coronary artery disease

Coronary artery disease (CAD) is characterized by accumulation of atheromatous plaques within the coronary arteries. Plaque rupture ⁹ and thrombus formation in the coronary arteries may lead to myocardial ischaemia or myocardial infarction which can induce ventricular arrhythmias and cause sudden death ¹⁰. The major risk factors for developing coronary artery disease include male sex, age, ethnicity, family history of coronary artery disease, smoking, diabetes mellitus and dyslipidemia¹¹. CAD can also lead to heart failure which in turn can cause sudden cardiac death ¹².

1.1.2 Ion channelopathies

Ion channelopathies are also called primary electrical abnormalities and cause ventricular arrhythmias in a structurally normal heart. Long QT syndrome (LQTS) is the most well known ion channelopathy. The other main cardiac ion channelopathies are Short QT syndrome (SQTS), Brugada syndrome and Catecholaminergic ventricular tachycardia (CPVT) ¹³. SQTS is a potassium channelopathy where the QT interval is shorter than 300 ms, leading to repolarisation abnormalities and ventricular arrhythmias. Brugada syndrome is a sodium channelopathy with characteristic ECG changes and high risk of ventricular arrhythmias and sudden death. CPVT is a calcium channelopathy which can lead to ventricular arrhythmias. These conditions have monogenic transmission in an autosomal dominant manner in the majority of cases¹⁴. Abnormalities in the repolarisation phase of the cardiac action potential can lead to cardiac arrhythmias like ventricular tachycardia (VT). When VT is sustained it can cause hemodynamic compromise and lead to syncope and when it degenerates into ventricular fibrillation (VF), cardiac arrest occurs.

1.1.3 Cardiomyopathies

Cardiomyopathies are disorders of the cardiac muscle. They can be inherited or acquired and can lead to ventricular arrhythmias and sudden death. The main types of cardiomyopathies are 1) hypertrophic cardiomyopathy (HCM)¹⁵ where the walls of the ventricles may become abnormally thick 2) dilated cardiomyopathy (CMD)¹⁶ where the ventricles are enlarged and pump less efficiently and 3) arrhythmogenic right ventricular cardiomyopathy (ARVC) where the ventricle, usually the right, becomes thin, because of fibrofatty deposition.

1.1.4 Other causes of SCD

Congenital heart diseases can cause secondary pulmonary hypertension (Eisenmenger syndrome) and heart failure, leading to ventricular arrhythmias and SCD¹⁷. Electrolyte abnormalities can lead to ventricular arrhythmias and sudden cardiac death especially in debilitated patients. Coronary artery anomalies like congenital lesions, coronary artery embolism, coronary arteritis and mechanical abnormalities of the coronary artery, can cause sudden cardiac death. Myocarditis often caused by viral infection can lead to cardiac dysfunction and ventricular arrhythmias. Connective tissue diseases like Marfan's syndrome can lead to aortic dissection or aneurysmal rupture and sudden death¹⁸. Aortic stenosis can cause sudden death as its first symptom. Other valvular diseases like aortic regurgitation and mitral stenosis can also lead to progressive cardiac dysfunction and sudden death. In conditions like Wolff-Parkinson-White syndrome, there is an accessory pathway in addition to the normal conducting pathways within the heart. Atrial arrhythmias like atrial fibrillation which is normally not life threatening on its own, can conduct down to the ventricles via the accessory pathway and lead to ventricular fibrillation and sudden death. Medications can lead to anaphylactic reaction. They can also cause prolonged QT intervals. Both these mechanisms can lead to sudden cardiac death. Pulmonary embolism can cause sudden death especially in people who have risk factors for thromboembolism including immobility, smoking, positive family history of thromboembolism, malignancy and hypercoagulable states. Table 1 summarises these conditions and the mechanisms by which they cause sudden cardiac death.

Condition	Mechanism causing SCD	Reference
Congenital heart disease	Heart failure & arrhythmias	¹⁷
Electrolyte abnormalities	Arrhythmias	¹⁹
Anomalous coronary arteries	Myocardial infarction or arrhythmias	²⁰
Myocarditis	Heart failure and arrhythmias	²¹
Connective tissue diseases- Marfan's syndrome	Aortic rupture	¹⁸
Valvular heart disease	Arrhythmias and Heart failure	²²
Mitral valve prolapse	Arrhythmias and heart failure	²³
Wolff-Parkinson-White Syndrome	Arrhythmias	²⁴
Medications	Arrhythmias	²⁵
Pulmonary emboli	Obstruction of the pulmonary arteries	²⁶

Table 1 Other causes of sudden death in the general population

1.2 ECG CHARACTERISTICS

1.2.1 Normal ECG

The standard 12 lead ECG is a representation of the heart's electrical activity recorded from electrodes on the body surface. Figure 3 denotes a normal ECG. The sinoatrial nodal (SAN) cells of the right atrium normally act as a pacemaker and initiates the electrical impulse which is then conveyed to all atrial myocytes because the cells are coupled via intercellular gap junctions producing coordinated depolarisation and contraction. Atrial depolarisation is reflected on the ECG as the P wave. The impulse is conveyed to the AV node and then to the bundle branches and to the Purkinje fibres, which allow for orderly ventricular depolarisation, which is observed on the ECG as the QRS complex. Repolarisation of the ventricles, which is a return to negative resting membrane potential, is reflected on the ECG by the ST segment and T wave.

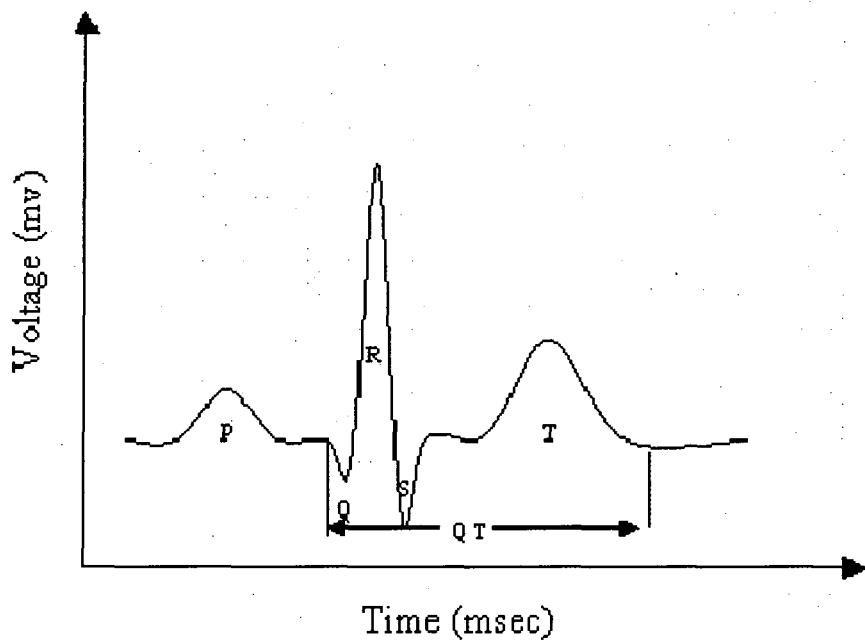


Figure 3 Normal ECG

The P wave represents the activation (depolarisation) of the right and left atria. The QRS complex represents the activation (depolarisation) of the ventricles. The ST segment & T wave represent ventricular repolarisation. PR interval indicates the time interval from the onset of atrial depolarisation to the onset of ventricular depolarisation. The QRS duration indicates the duration of ventricular depolarisation alone. The QT interval represents the duration of ventricular depolarisation and repolarisation.

1.2.2 ECG in LQTS

The QT interval is often measured in lead V2 from the onset of the QRS complex to the end of T wave, defined as the intersection of isoelectric line and the tangent of the maximal downward limb of the T wave ²⁷. A typical ECG in LQTS is shown in figure 4.

The QT interval is the total time required for depolarisation and repolarisation to occur and a prolonged QT interval indicates prolonged action potential duration at the cellular level. Males with QT interval above 440 milliseconds (ms) and females with QT interval above 460 ms when corrected to heart rate (QTc) [QTc = QT/ ($\sqrt{R-R}$ interval)] are considered to have prolonged QT intervals²⁸. About 30% of patients with genetically proven LQTS have a normal QTc²⁹. In addition to genetic causes of LQTS, acquired conditions like drugs, electrolyte imbalance and hypothermia lead to LQTS. Several different genes have been described, which, when mutated, lead to LQTS. Depending on the gene, LQTS is classified as LQT1, LQT2, LQT3, LQT4, LQT5 and LQT6. There appears to be a genotype / phenotype relationship in that certain gene mutations produce characteristic ECG patterns (figure 5). The prolonged QT interval can lead to ventricular arrhythmias (figure 6).

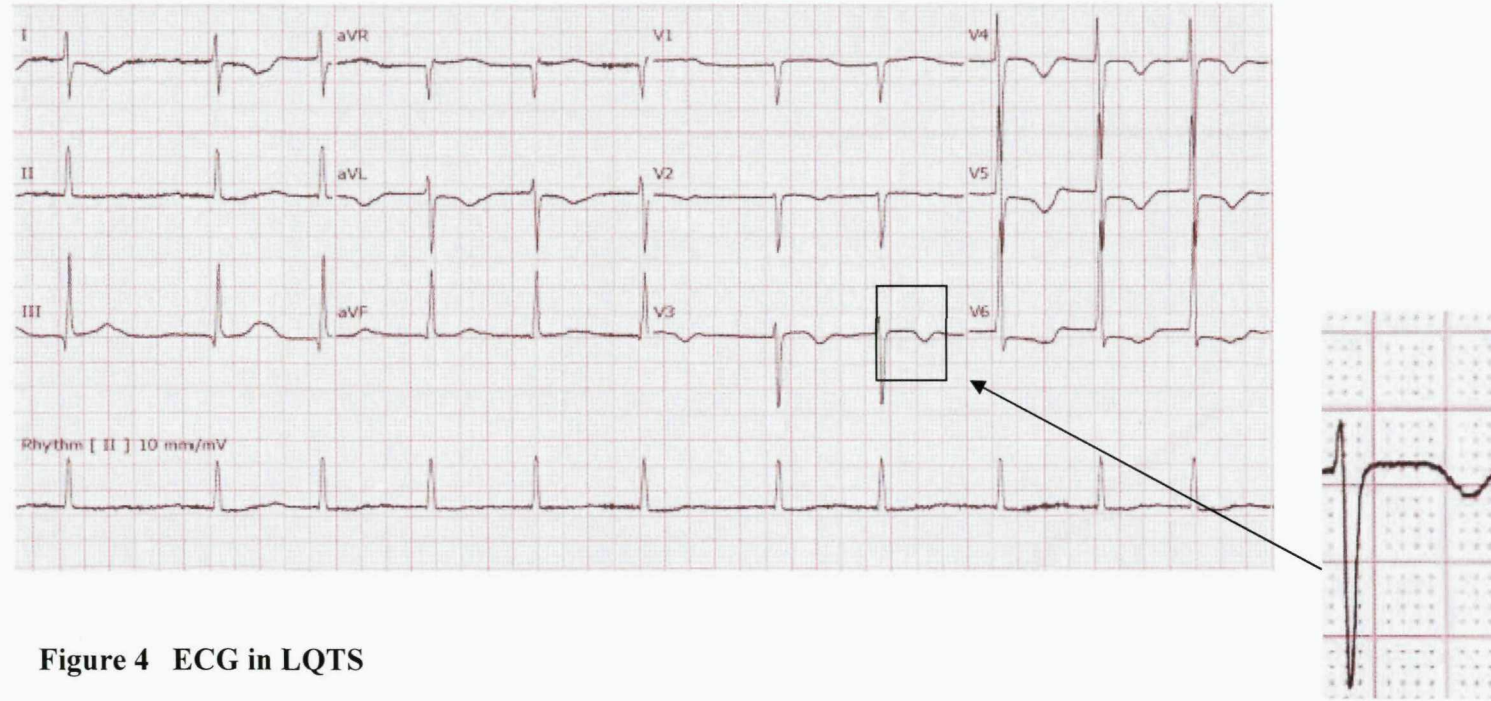


Figure 4 ECG in LQTS

12 lead ECG in a patient with LQTS. QT is 520 ms. RR interval is 0.8 s

Therefore corrected QT interval, $QTc = QT/\sqrt{RR \text{ interval}} = 584 \text{ ms}$. The arrow shows a magnified view of one of the 12 leads showing QT prolongation.

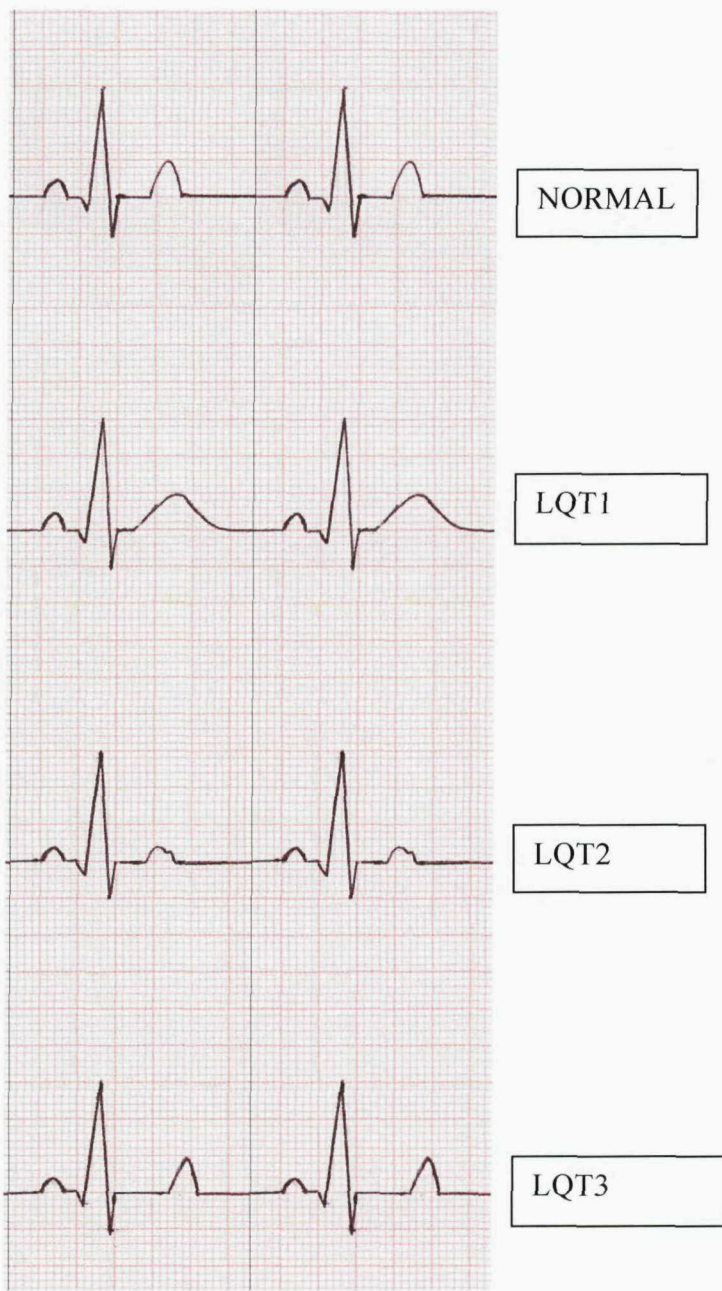


Figure 5 ECG patterns in LQT syndrome

Gene specific ECG patterns exist that may help to differentiate LQT1, LQT2 and LQT3 patients. Figure shows early onset of broad based T waves with long T wave duration in LQT1, low amplitude and often notched T wave in LQT2 and late onset T wave with normal duration and amplitude in LQT3.

1.2.3 ECG in SQTS

The ECG in SQTS shows a short QT interval (<300ms) and often the T waves appear peaked. These changes are illustrated in figure 7. In SQTS, the QT interval variability with heart rate, is much less pronounced than in normal individuals.

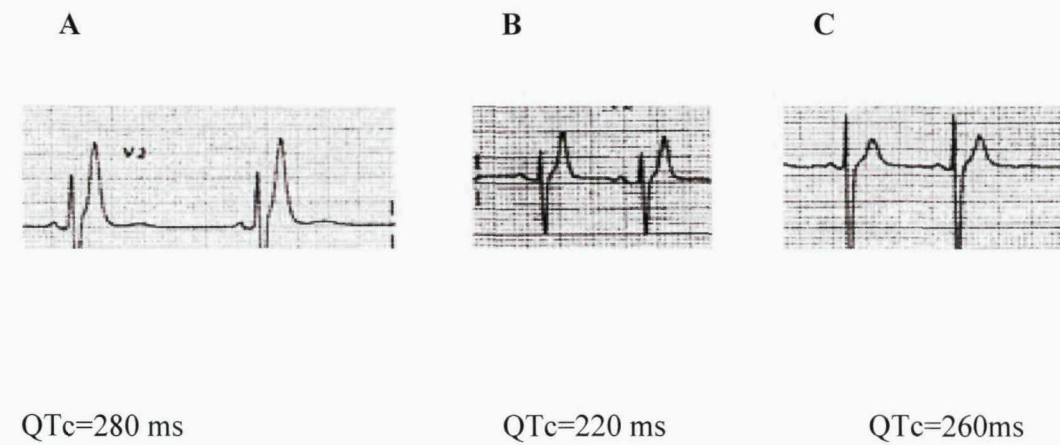


Figure 6 ECG in Short QT syndrome

A single lead (V2) ECG shows the features of short QT syndrome (short QT interval, and peaked T waves) in members A, B & C from the same family (Gaita et al Circulation, August 18, 2003).

1.2.4 ECG in Brugada syndrome

The ECG in Brugada syndrome characteristically shows features of right bundle branch block (RBBB) and ST segment elevation in the right precordial leads V1- V3 ³⁰. Three variants of the repolarisation pattern in leads V1-V3 are known. Type 1 is diagnostic of Brugada syndrome and has convex (coved) ST elevation of > 2mm followed by a negative T wave. Type 2 has a saddleback appearance with a high takeoff ST-segment elevation, with a trough showing at least 1 mm ST elevation, followed by a positive or biphasic T wave. Type 3 has either a saddleback or coved appearance with the ST segment elevated <1mm³¹. Type 2 and type 3 ECGs are not diagnostic of the Brugada syndrome. Following administration of a sodium channel blocking agent, if a type 2 or type 3 ECG changes to a type 1 ECG, it is diagnostic of Brugada syndrome. A 12 lead ECG with type 2 changes is shown in figure 8. The characteristic features of the three types of ECG changes are illustrated in figure 9. The ECG pattern may change over time and a random ECG can be normal.

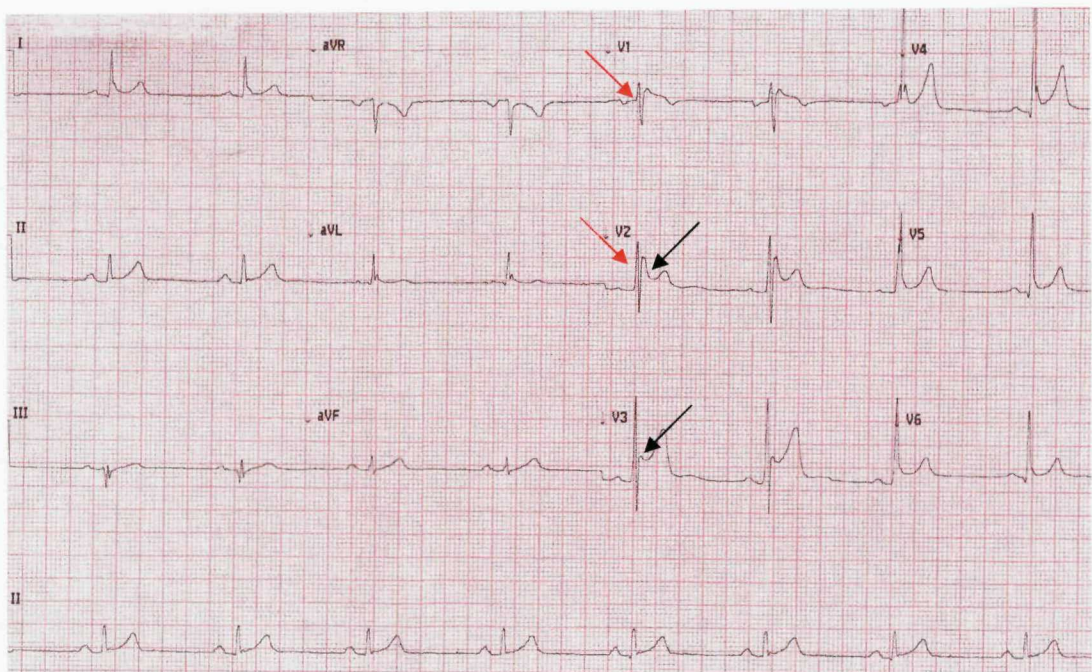


Figure 7 ECG showing type 2 changes of Brugada syndrome

Figure shows a 12 lead ECG with features of concave ST elevation in V2 and V3, >1mm (type 2 changes, shown with black arrows) and RBBB pattern (shown with red arrows).



Figure 8 Repolarisation abnormalities in ECGs in Brugada syndrome

In type 1 pattern, the ST segment elevation is convex $>2\text{mm}$ followed by a negative T wave. In type 2 pattern, the ST segment elevation has a saddleback appearance and is $>1\text{mm}$. In type 3 pattern, the ST segment is elevated $<1\text{mm}$ (A.A.M.Wilde et al, Proposed diagnostic criteria for the Brugada syndrome, European Heart Journal, 2002, 23, 1648, by permission of Oxford University Press).

1.2.5 ECG in CPVT

In CPVT, the ECG at rest may be normal, but during exercise or emotion, ventricular tachycardia with right bundle branch morphology can occur. Also the QRS axis can demonstrate a beat-to-beat variation (figure 10). The QT interval is normal at rest and on exercise.

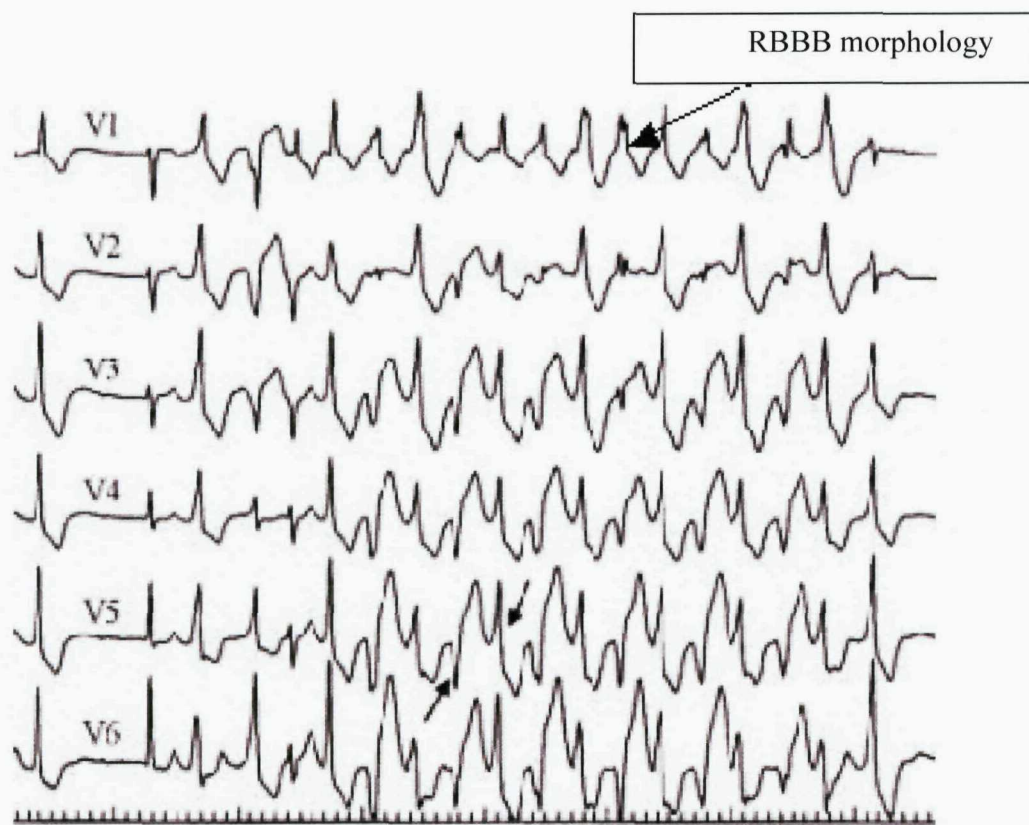


Figure 9 ECG in Catecholaminergic polymorphic ventricular tachycardia

Ventricular tachycardia with right bundle branch (RBBB) morphology (M pattern in V1) and beat- to- beat alternating QRS axis (arrowed in V5) is shown (Ngai-Shing Mok et al, Chinese Medical Journal 2006, Vol.119 No.24, 2130, by permission).

1.2.6 ECG in hypertrophic cardiomyopathy

In hypertrophic cardiomyopathy, the ECG can show features of left ventricular hypertrophy. Classically this includes tall R waves in leads V5 and V6 and tall S waves in V1 and V2. T wave inversion and ST segment depression may be seen, which again is due to the voltage changes caused by the cardiac hypertrophy (figure 11).

The basic mechanism responsible for ST segment depression is an abnormality in the current flow in the subendocardial region³². ST depression can be – a) upward sloping b) planar c) sagging and d) downward sloping. Of these, downward sloping ST depression is pathologically the most significant. Although abnormalities in ST segments and T waves are most commonly seen in coronary artery disease, they may be abnormal in left ventricular hypertrophy where there is left ventricular systolic overload and the hypertrophied left ventricle is under strain because of relative left ventricular ischemia.

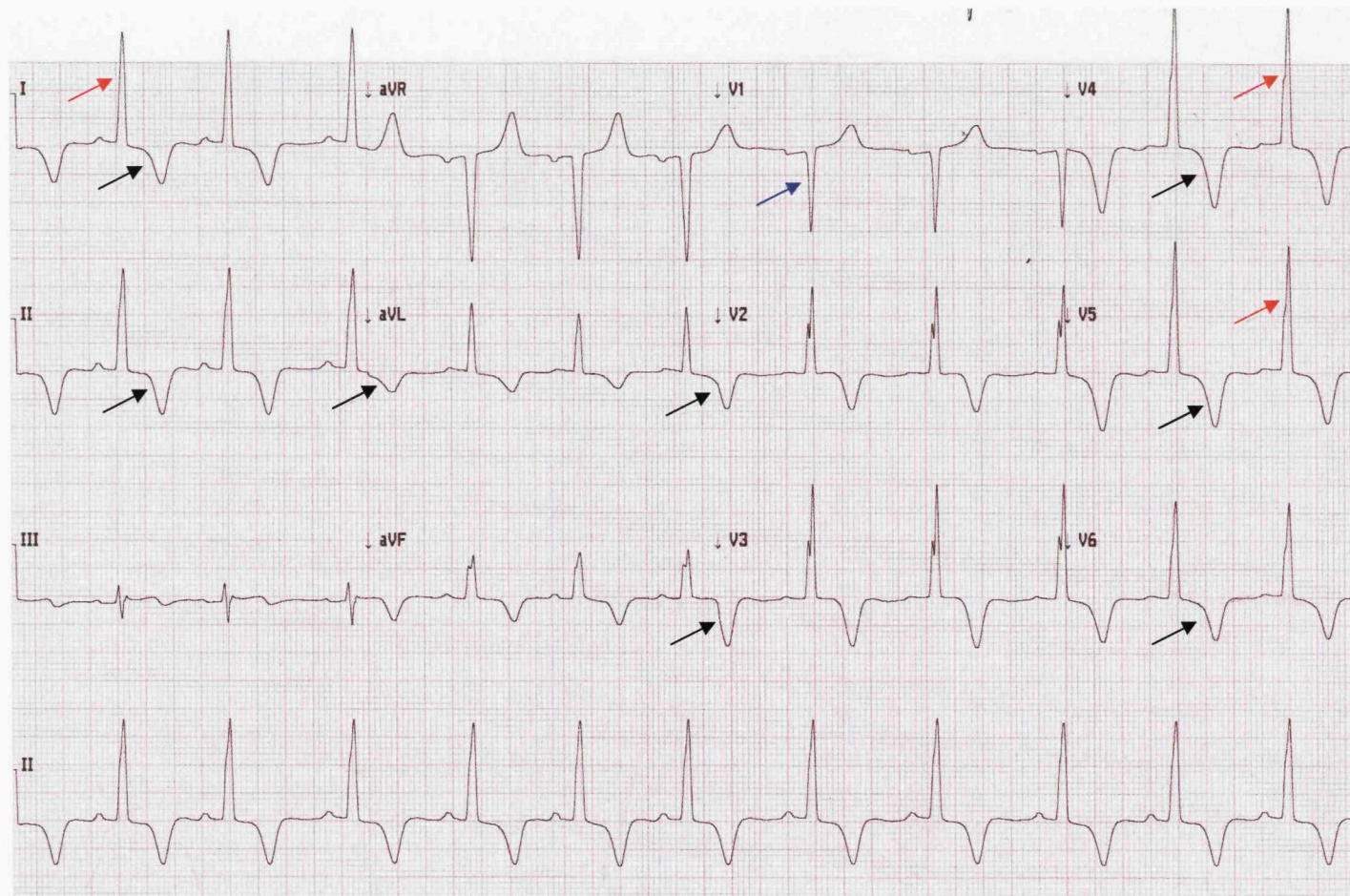


Figure 10 ECG in hypertrophic cardiomyopathy

Typical ECG in hypertrophic cardiomyopathy shows features of left ventricular hypertrophy (LVH) -tall R waves in I, V4 & V5 (shown with red arrows) and deep S wave in V1 (shown with blue arrow) and deep T wave inversion in most leads (shown with black arrows).

1.2.7 ECG in ARVC

The resting ECG may be normal or it may show non-specific T wave inversion and epsilon waves. Epsilon waves represent late potentials resulting from late activation of myocytes in the right ventricle. In ARVC, myocytes are replaced with fat, producing islands of the viable myocytes surrounded by fat. This causes a delay in excitation of some of the myocytes of the right ventricle and causes the small delayed activity during the ST segment of the ECG³³. They are best seen in leads V₁ and V₂.

These ECG features in ARVC are demonstrated in figure 12.

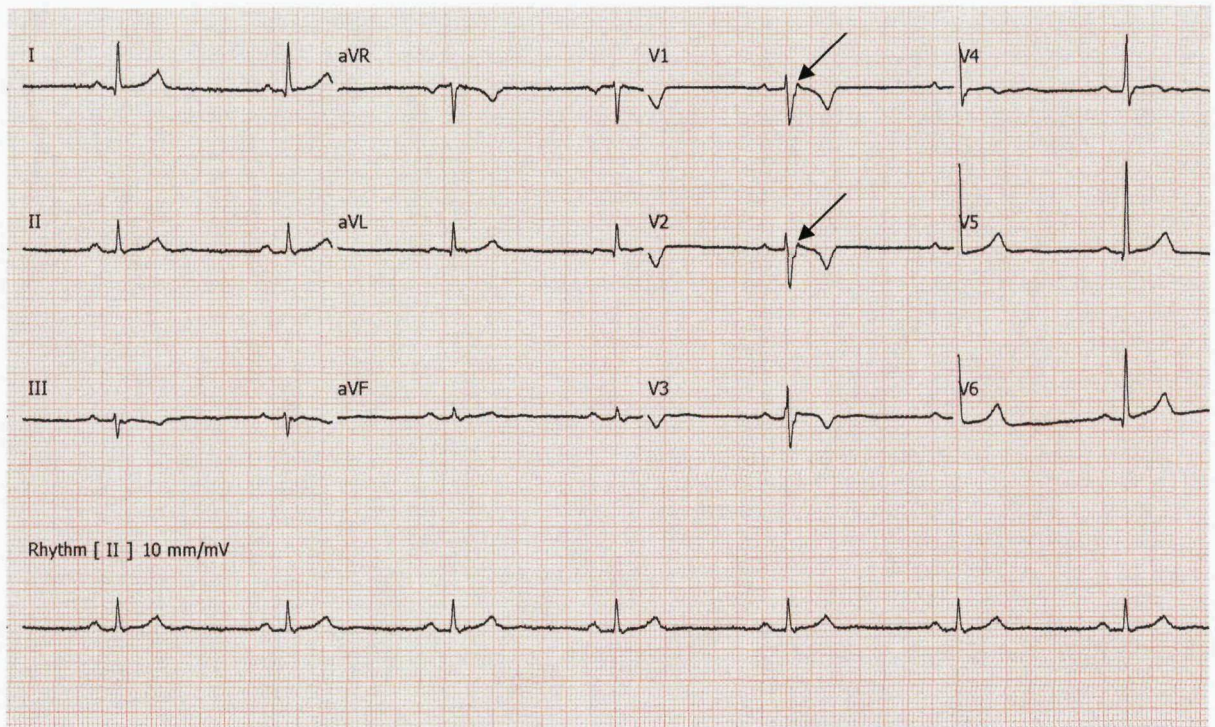


Figure 11 ECG in ARVC

12 lead ECG in a patient with ARVC showing T wave inversion in leads III, V1-V4 and epsilon waves in leads V1 & V2 (shown with arrows).

1.3 ION CHANNELOPATHIES

Ion channels are pore-forming proteins through which ions move in and out of cells. Diseases caused by mutations in genes that encode ion channel subunits or regulatory proteins that contribute to cardiac action potential currents or the process of excitation-contraction coupling are referred to as ion channelopathies. They are an important cause of sudden cardiac death and can be classified as potassium, sodium and calcium channelopathies.

1.3.1 Cardiac action potential

The cardiac action potential characteristics are variable within the heart in keeping with the specific electrical characteristics of the different types of cells. The cardiac action potential in the ventricular myocyte consists of five phases (Phases 0-4)³⁴ (figure 13). Phase 0 is the rapid depolarisation which is due to rapid activation of voltage gated Na channels and lead to inward movement of sodium ions. During phase 1 (early or partial repolarisation) the Na channels close and I_{to} (transient outward channel) opens. Phase 2 (prolonged depolarisation or plateau phase), is the result of slowly decreasing inward Ca²⁺ (mainly via L-type calcium channels) and increasing outward potassium currents. This phase is especially long in ventricular myocytes and Purkinje fibres (Purkinje fibres are specialised fibres, just beneath the endocardium, which can rapidly conduct impulses). The sodium channels enter a non-conducting inactivated state during the plateau phase. The net current during the plateau phase is small and therefore, small changes in ion current during this phase can have a major impact on action potential duration and the ECG during this phase is at baseline. Phase 3 (rapid repolarisation) occurs due to activation of outward K currents (I_{kr} and I_{ks}). At this stage, the outward currents are more than the inward currents. In a ventricular myocyte, phase 4 is the resting membrane potential and describes the membrane potential when the cell is not being stimulated. Once the ventricular myocyte is electrically stimulated (typically by an electric current from an adjacent cell), it begins a sequence of actions involving the movement of ions across the ion channels to produce the action potential of the cell. The adjacent cells are then electrically stimulated. Table 2 summarises the mechanism for each phase of the cardiac action potential.

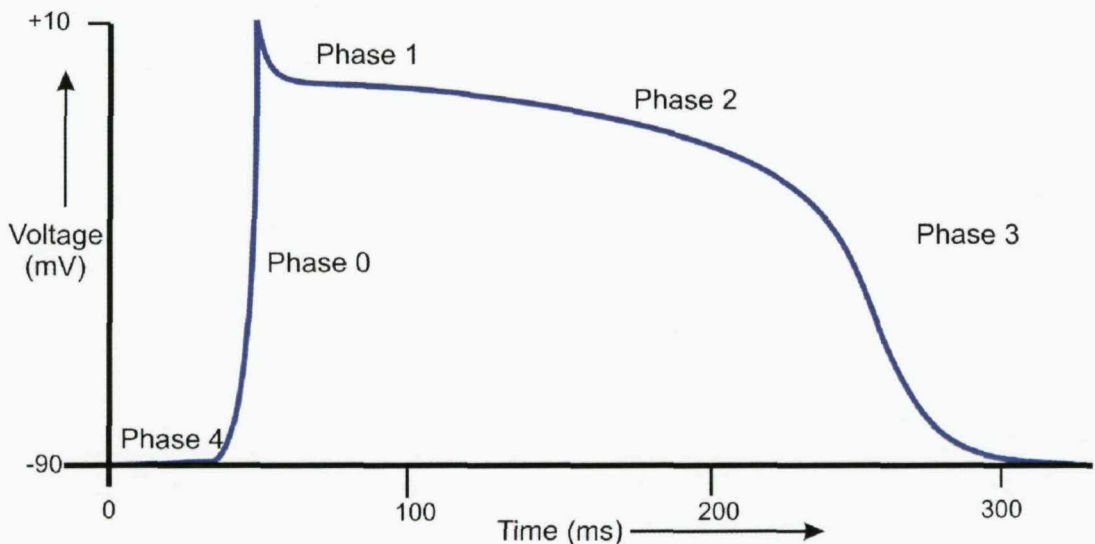


Figure 12 The action potential of a cardiac ventricular myocyte

Figure shows phases of the cardiac action potential of a ventricular myocyte- phase 0- rapid depolarisation, phase 1- early repolarisation, phase 2- plateau phase, phase 3- rapid repolarisation and phase 4- slow diastolic depolarisation.

Phase	Name of phase	Mechanism
0	Rapid depolarisation	Rapid activation of voltage gated sodium channels
1	Early repolarisation	Inactivation of Na channels & activation of transient outward K current (I _{to})
2	Plateau	Slowly decreasing inward calcium currents & increasing outward potassium currents (I _{kr} & I _{ks})
3	Rapid repolarisation	Outward potassium currents (I _{kr} , I _{ks}) and inward rectifier potassium current (I _{ki})
4	Slow diastolic depolarisation	Automaticity

Table 2 Mechanisms underlying phases of the cardiac action potential

The table shows the mechanisms responsible for each phase of the action potential.

1.3.2 Mechanisms of arrhythmia

When repolarisation is delayed (as manifested by a prolonged QT interval on the ECG), there is dispersion of refractoriness throughout the myocardium which can lead to unidirectional block of electrical excitation. The arrhythmia is then triggered by spontaneous secondary depolarisations (early after-depolarisations) due to reactivation of calcium channels during the late repolarisation phase.

When the sympathetic nervous system is activated, the inward currents carried by the calcium channels can increase, and increase the chance of early after-depolarisations, which can then trigger an arrhythmia. Once the arrhythmia is triggered, it can form a circuit by passing through relatively inexcitable tissue (re-entry phenomenon). The development of multiple re-entrant circuits within the heart can lead to ventricular fibrillation and sudden cardiac death.

1.3.3 Cardiac Potassium channels

The potassium (K⁺) channels in the heart help to maintain the resting membrane potential, modulate action potential duration and determine pacemaker activity ³⁵. K⁺ channels can be functionally classified as a) voltage gated channels and b) inward rectifying channels. The cardiac K⁺ channels are formed by the assembly of 4 principal subunits with auxiliary subunits (figure 15).

The α -subunit of a voltage gated potassium channel has six membrane spanning domains (S1-S6), a voltage sensor (S4) and a pore sequence between S5 & S6. The α -subunit of an inward rectifying potassium channel has two membrane spanning domains M1 and M2 (figure 14).

Cardiac potassium channels are formed by the assembly of four voltage gated or inward rectifier pore forming α -subunits with accessory β - subunits and regulatory proteins³⁶ (figure 15). I_{ks} and I_{kr} are examples of cardiac voltage gated potassium channels. I_{ks} conducts the slowly activating delayed rectifier potassium current in the heart and I_{kr} conducts the rapidly activating delayed rectifier potassium current. I_{ks} is formed by four KvLQT1 α -subunits (encoded by *KCNQ1*) assembling with MinK (β - subunits encoded by *KCNE1*). I_{kr} is formed by four HERG (KCNH2) α -subunits (encoded by *KCNH2*) assembling with MiRP1 (β - subunit encoded by *KCNE2*) (figure 15). Mutations in *KCNQ1*, *KCNE1*, *KCNH2* or *KCNE2* can lead to reduction in I_{ks} or I_{kr} and prolong repolarisation ³⁷ which in turn prolongs QT interval and predisposes the heart to ventricular arrhythmias.

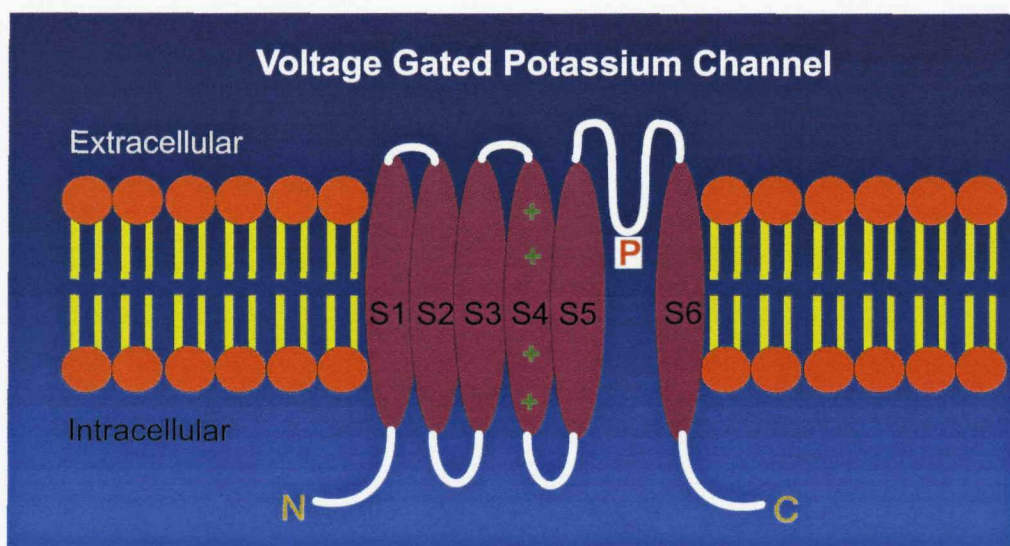


Fig:14(a)

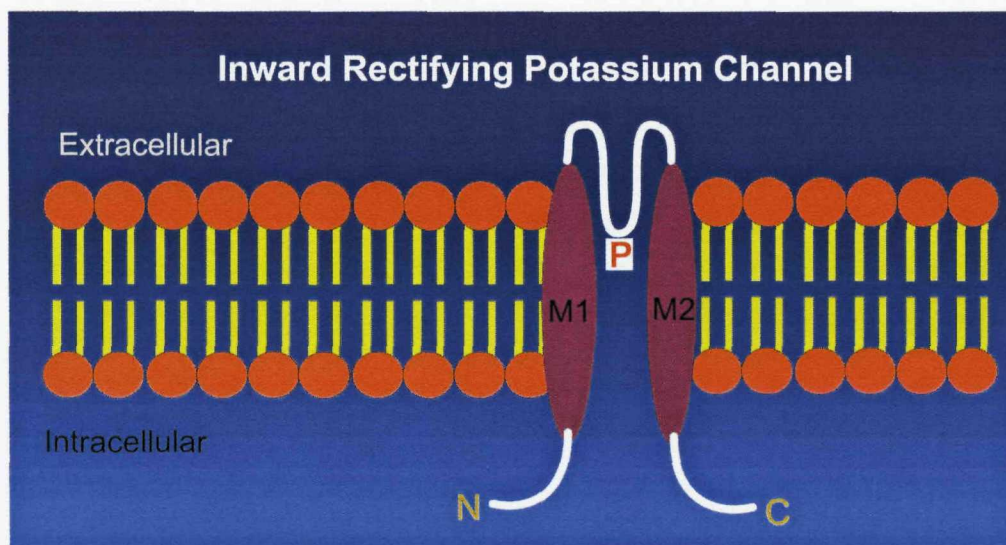


Fig:14(b)

Figure 13 Structure of the α -subunit of potassium channels

Figure 14(a) shows the α -subunit of a voltage gated potassium channel with six transmembrane segments (S1-S6). Segment S4 of the voltage gated channel acts as the voltage sensor and has + signs marked on it. The pore (P) sequence is located between S5 & S6. Figure 14(b) shows the α -subunit of the inward rectifying potassium channel with 2 transmembrane segments (M1 & M2) and an intervening pore forming domain. N and C denote the amino and carboxy terminals of the polypeptide chain. Four such α -subunits assemble with the auxiliary subunit to form the functional potassium channel.

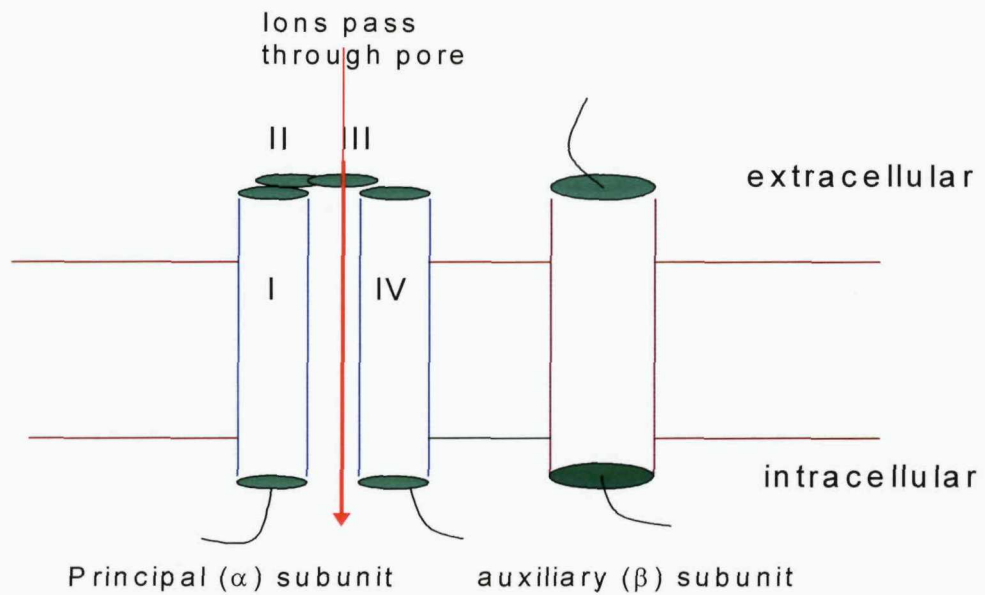


Figure 14 General structure of cardiac potassium channels

Four principal (α) subunits in association with the auxiliary (β) subunit form the functional cardiac potassium channel. For example, I_{ks} and I_{kr} are voltage gated potassium channels.

Four KvLQT1 (α -subunits) with MinK (β -subunit) form I_{ks} channel.

Four HERG (α -subunits) with MiRP1 (β -subunit) form I_{kr} channel.

1.3.4 Potassium channelopathies

Mutations in the genes which encode the α -subunits of the voltage gated potassium channels (*KCNQ1* and *KCNH2*) account for the majority of the potassium channelopathies. Mutations in genes which code for the potassium channel β - subunits (*KCNE1* and *KCNE2*) and mutations in *KCNJ2* which encodes the inward rectifier potassium channel α -subunit account for less than 1% of the total cases of the cardiac potassium channelopathies. The various potassium channelopathies are described below and their genetic aspects are summarised in table 4.

The disorders are transmitted with variable penetrance and expressivity. (Penetrance is the frequency with which a specific phenotype is expressed by those subjects with a specific genotype and expressivity is defined as the severity of the phenotype). For example, LQTS has a penetrance of only 25%²⁹.

1.3.4.1 LQTS

LQTS can be congenital or acquired. Congenital LQTS can be transmitted in an autosomal dominant or autosomal recessive manner. The autosomal dominant form of LQTS is also known as Romano Ward syndrome. Mutations in one of 3 different genes account for the majority of cases of congenital LQTS (LQT1, LQT2 & LQT3). The autosomal recessive form of LQTS is also called as Jervell- Lange-Nielsen syndrome (JLNS). Patients affected with JLNS are homozygous for mutations in either *KCNQ1*³⁸ or *KCNE1*³⁹, which leads to loss of I_{ks} and prolonged QT interval. Since I_{ks} is important for the proper functioning of hair cells in the inner ear, these patients have associated deafness⁴⁰.

LQT1

KCNQ1 encodes the α (pore-forming) subunit, that co-assembles with minK- the β subunit to form the channel responsible for the I_{ks} (slow component of the delayed rectifier) current. Mutations in *KCNQ1* can lead to decrease in the repolarising I_{ks} current and cause prolongation of ventricular repolarisation and lengthening of the QT interval (LQT1) (OMIM#192500). Exercise ²⁸, swimming and conditions with increased sympathetic activity may precipitate cardiac arrhythmias in subjects with LQT1 syndrome⁴¹. The structure of KCNQ1 is illustrated in figure 16.

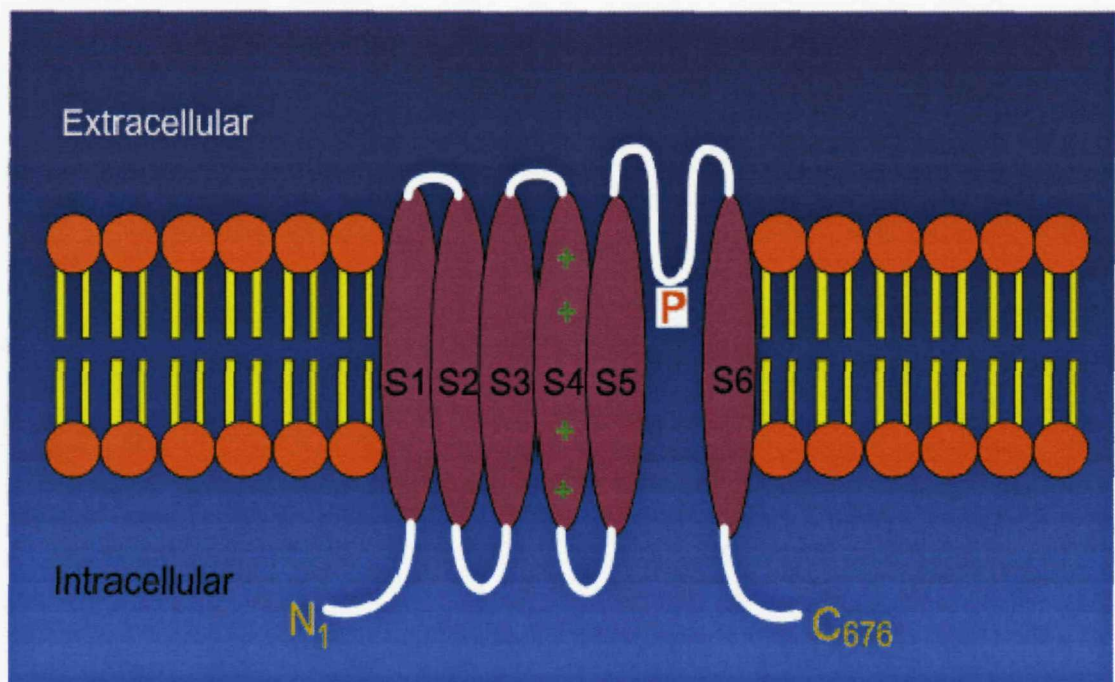


Figure shows the 6 transmembrane segments of the potassium channel subunit, dysfunction of which leads to LQT1. The polypeptide chain has 676 aminoacids; N and C denote the amino and carboxy terminals.

LQT2

KCNH2 encodes the α (pore-forming) subunit, that coassembles with MiRP1- the β subunit to form the channel responsible for the Ikr (rapid component of the delayed rectifier) current. Mutations in *KCNH2* can lead to decrease in the repolarising Ikr current and cause prolongation of ventricular repolarisation and lengthening of the QT interval (LQT2) (OMIM+152427)⁴². Cardiac events in LQT2 syndrome patients are associated with arousal or conditions in which patients are startled, like the sudden ringing of an alarm⁴³. The structure of KCNH2 is illustrated in figure 17.

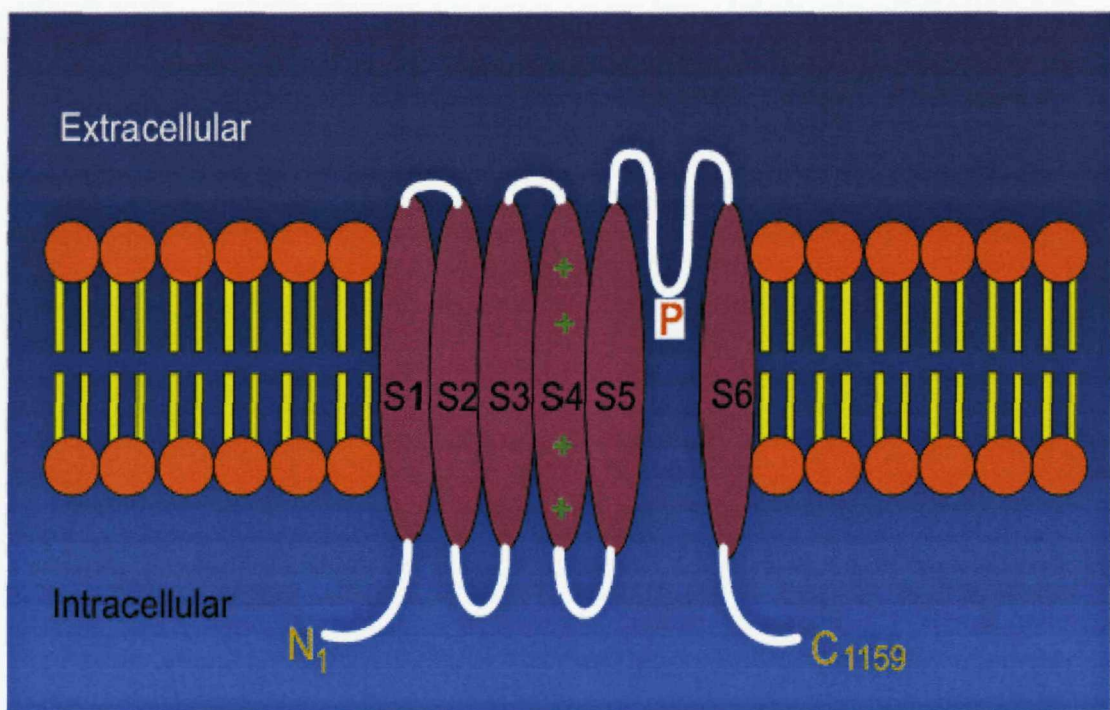


Figure shows the structure of KCNH2 with its 6 transmembrane domains and the polypeptide chain with 1159 aminoacids. N and C denote the amino and carboxy terminals.

LQT4

LQT4 (OMIM#600919) is characterised by prolonged QT interval and disturbed sinus-node function⁴⁴, manifested often as sinus bradycardia on the ECG. It is secondary to mutations in *ANKB* which encodes ankyrin-B. Ankyrin B is an adapter protein (An adapter protein acts as a connecting molecule and is critical to intermolecular interactions and plays a role in the regulation of signal transduction) and is important for the optimum spatial orientation of the sodium pump, the sodium/calcium exchanger, and inositol-1,4,5-trisphosphate receptors, which are all ankyrin-B-binding proteins⁴⁵. *ANKB* mutations can also lead to altered calcium signalling that can result in abnormal depolarisations known as after-depolarisations, which in turn can trigger arrhythmias⁴⁵. Cardiac arrhythmias are precipitated by physical exertion and emotional stress.

LQT5

KCNE1 encodes the β subunit (minK) that co-assembles with KVLQT1, the α subunit to form the channel responsible for the I_{ks} current⁴⁶. Mutations in *KCNE1* can reduce I_{ks} and thereby delay myocyte repolarisation, leading to arrhythmia susceptibility and LQT5 (OMIM+176261)³⁹.

LQT6

KCNE2 encodes the β subunit (MiRP1) that co-assembles with KCNH2 (HERG), the α subunit to form the channel responsible for the I_{kr} current⁴⁶. Mutations in *KCNE2* can reduce I_{kr} and thereby delay myocyte repolarisation, leading to arrhythmia susceptibility and lead to LQT6 (OMIM+603796) ⁴⁷.

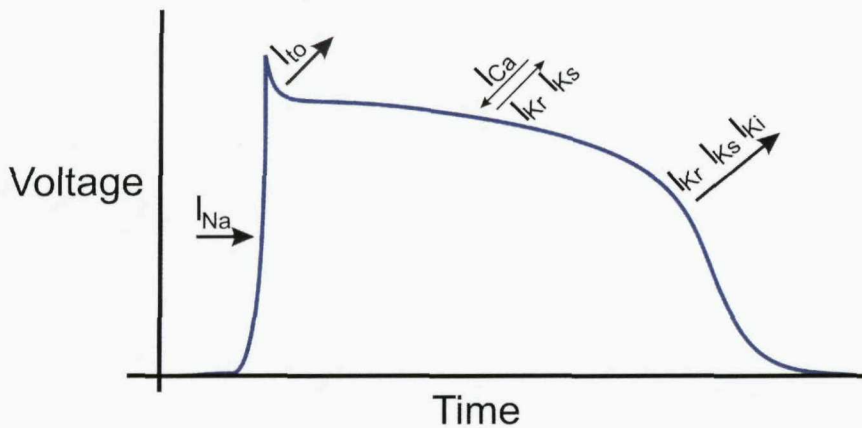
1.3.4.2 SQTS

SQTS is characterised by abnormally short repolarisation (QT interval < 300ms). The first report of this condition was made in 2003⁴⁸. No information is available on specific triggers that may precipitate arrhythmias. The first identified SQTS gene was *KCNH2*. The other genes subsequently identified were *KCNQ1* and *KCNJ2*. Depending on the underlying genetic cause, SQTS is classified into SQTS1 (OMIM#609620)⁴⁹, SQTS2 (OMIM#609621)⁵⁰ and SQTS3 (OMIM#609622)⁵¹. SQTS1 is secondary to mutation in *KCNH2* (OMIM152427), SQTS2 is due to mutations in *KCNQ1* (OMIM607542) and SQTS3 is due to mutations in *KCNJ2* (OMIM600681). The genetic aspects of SQTS are summarised in table 3.

KCNH2 encodes KCNH2 (HERG) that makes up the potassium channel responsible for the rapidly activating rectifier outward current (I_{kr}). Some mutations of *KCNH2* induce a "gain of function" in the I_{kr} current, thus shortening the action potential. *KCNQ1* encodes a subunit of the protein responsible for the slowly activating delayed outward potassium current (I_{ks}). *KCNQ1* mutations can cause gain-of-function and shorten the action potential. *KCNJ2* encodes the protein responsible for the inward rectifier current I_{Ki}. *KCNJ2* mutations can lead to channels that generate electrical currents which do not rectify or decrease as much as those of the normal channels. Thus, gain-of-function defects in any of these 3 genes can result in larger outward potassium currents which can lead to shortening of repolarisation and shortened QT interval. This mechanism is illustrated in figure 18⁵².

Normal Action Potential

Figure18(a)



SQT Action Potential

Figure18(b)

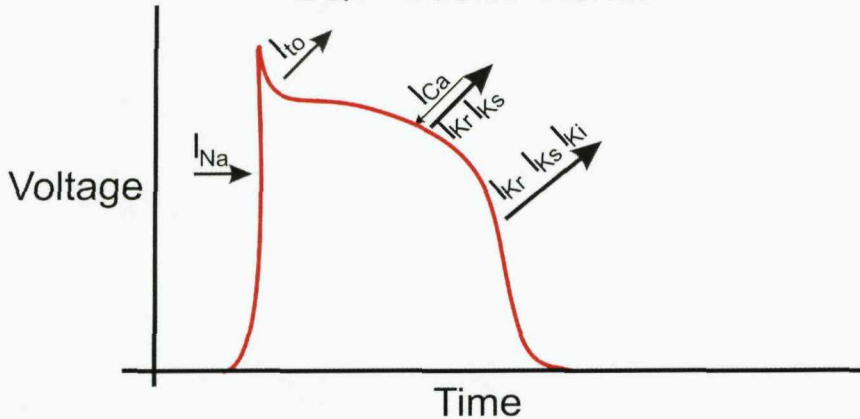


Figure 17 Electrophysiological basis of SQTS

Figure 18 (a) represents the normal action potential and the flux of ions (top) and the normal QT interval associated with it. Figure 18 (b) shows that with gain-of-function mutations in any of 3 different potassium channels, the net outward current in the repolarisation phase increases and shortens the cardiac action potential and the QT interval.

Disease	OMIM	Gene	OMIM	Location	Protein	Reference
SQTS1	#609620	<i>KCNH2</i>	152427	7q35-q36	Ikr α subunit (HERG)	⁴⁹
SQTS2	#609621	<i>KCNQ1</i>	607542	11p15.5	Iks α subunit (KvLQT1)	⁵⁰
SQTS3	#609622	<i>KCNJ2</i>	600681	17q23.1-q24.2	Ik1 (Kir 2.1)	⁵¹

Table 3 Genetic aspects of SQTS

The table shows the 3 types of short QT syndrome identified so far (along with the OMIM reference numbers for the disease & the mutated gene), and the protein coded by the gene.

Disease	Gene	OMIM	Location	Protein	Protein function	Ref
LQT1, SQT2, JLNS1	<i>KCNQ1</i>	607542	11p15.5	Iks α -subunit	KvLQT1 assembles with MinK to form Iks	⁵³
LQT2, SQT1	<i>KCNH2</i>	152427	7q35-36	Ikr α -subunit	HERG assembles with MiRP1 to form Ikr	⁵⁴
LQT5, JLNS2	<i>KCNE1</i>	176261	21q22.1	Iks β -subunit	MinK assembles with KvLQT1 to form Iks	³⁹
LQT6	<i>KCNE2</i>	603796	21q22.1	Ikr β -subunit	MiRP1 assembles with HERG to form Ikr	⁴⁷

Table 4 Genetic aspects of potassium ion channelopathies

Ikr denotes the rapidly activating delayed rectifier potassium current and Iks denotes the slowly activating component of the delayed rectifier potassium current.

1.3.5 Sodium channelopathies

The cardiac sodium channel is voltage gated and consist of a pore-forming α -subunit complexed with 1 or 2 smaller accessory β subunits. The structure of the α -subunit is shown in figure 20. *SCN5A* (OMIM *600163) encodes the α -subunit of the sodium channel and mutations in this gene can lead to ventricular arrhythmias. The sodium channels are important for the generation of cardiac action potentials, especially phase 0 of the action potential.

The principal cardiac sodium channelopathies are long QT syndrome type 3 (LQT3, OMIM#603830)⁵⁵ and Brugada syndrome (BS-1, OMIM#601144)⁵⁶. Mutations in *SCN5A* can also lead to idiopathic VF (IVF, OMIM#603827)⁵⁷, progressive familial heart block type 1 (PFHB1, OMIM#113900)⁵⁸, sick sinus node syndrome (SSS1, OMIM#608567)⁵⁹ and atrial standstill(OMIM#108770)⁶⁰. Some of the *SCN5A* mutations that cause these conditions are shown in figure 19. *SCN5A* mutations characteristically trigger cardiac events during sleep or rest⁶¹.

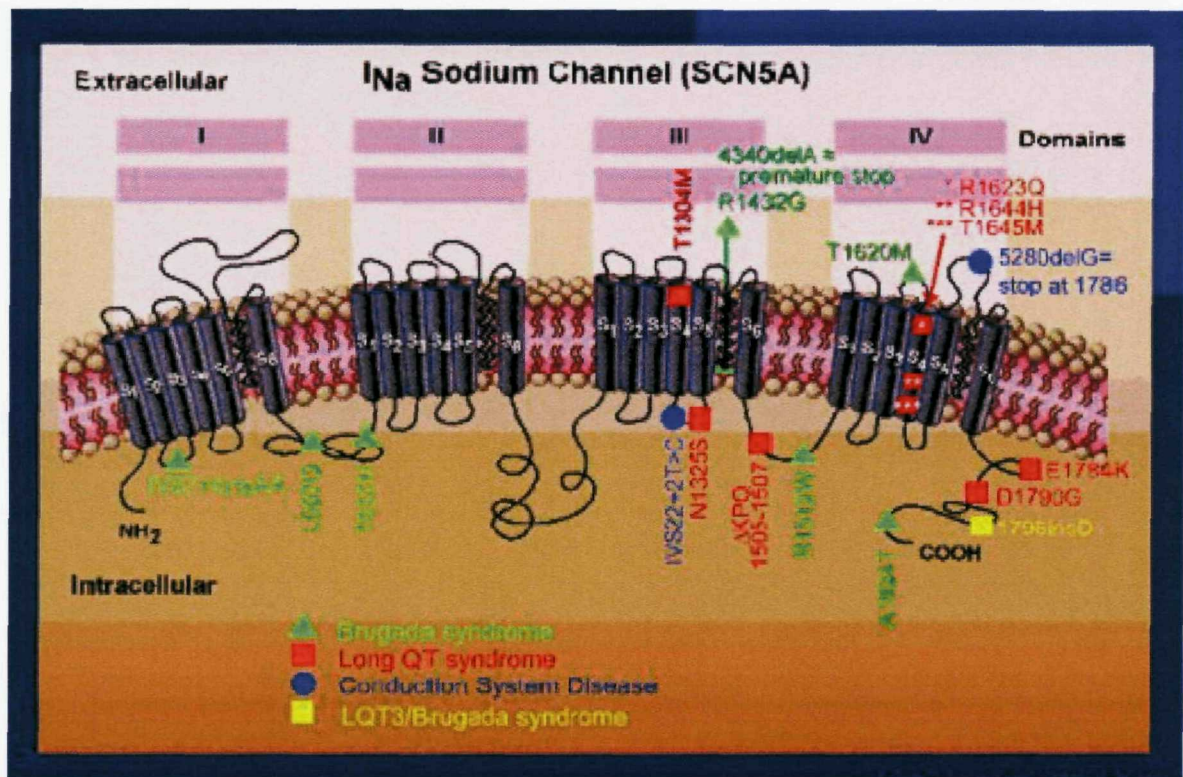


Figure 18 SCN5A mutations

Figure shows some of the identified mutations in SCN5A that lead to Brugada syndrome, LQT3 and conduction system disease. Figure reproduced with permission from Nature publishing group, Chen Q et al, Genetic basis and molecular mechanism for idiopathic ventricular fibrillation, 1998.

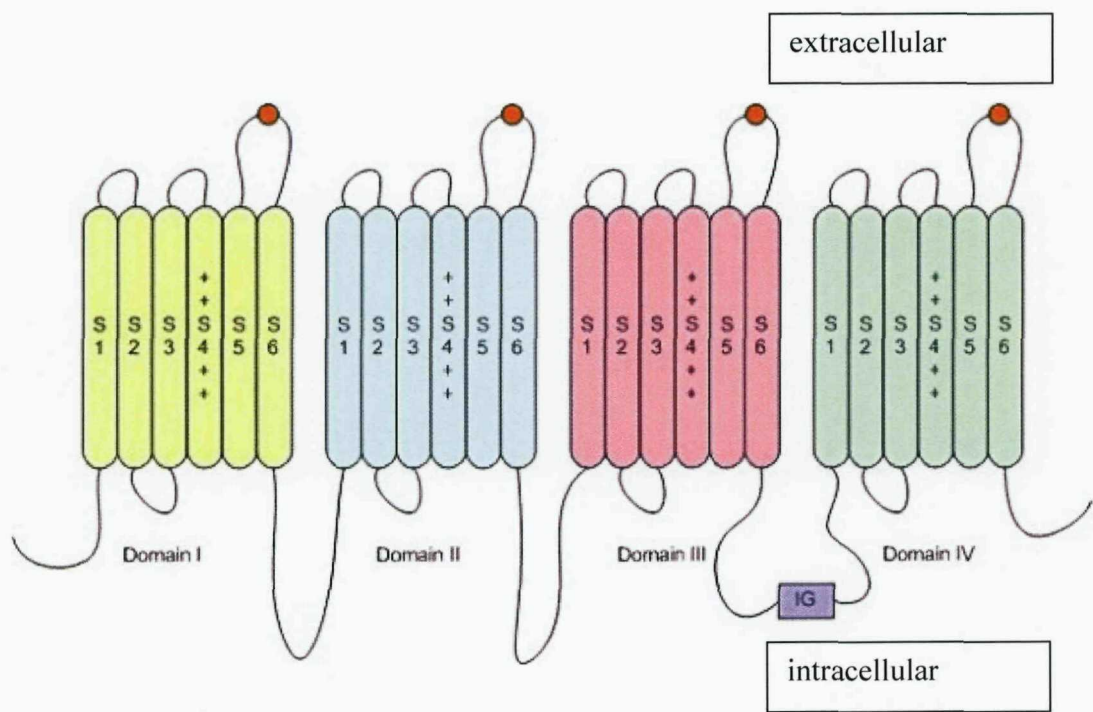


Figure 19 Structure of α -subunit of sodium channel

The α -subunit has 4 domains. Each domain has 6 membrane spanning regions (S1-S6). Domains I-IV are arranged as a tetramer to give a central ion channel. (figure reproduced with permission from Tim Smith). The S4 region of the domain forms the actual voltage sensor. The pore is between S5 and S6. IG- inactivation gate between domains III and IV, which mediates sodium channel inactivation. There are long loops linking the domains I- II, II- III, III- IV and shorter extracellular loops.

1.3.5.1 LQT3

Mutations in *SCN5A* can lead to non-inactivation of the sodium channel subunit and lead to persistent inward sodium current. This will delay onset of repolarisation since it depends on the balance between the inward and outward currents. The action potential duration is lengthened and thus the corresponding QT interval⁶². This is demonstrated in figure 21. LQT3 has the most malignant prognosis among LQTS patients. LQT3 subjects experience lower number of syncopal episodes, yet when events do occur, they are more likely to be fatal⁶³.

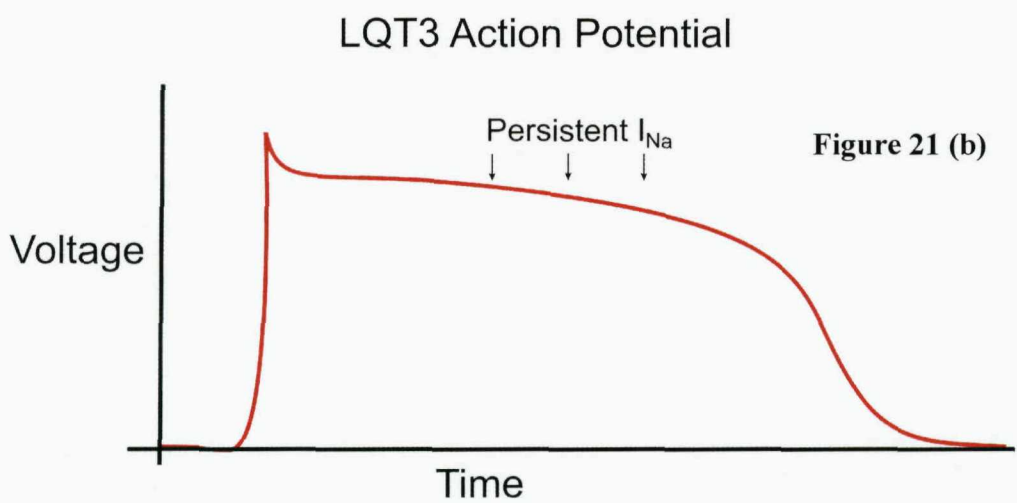
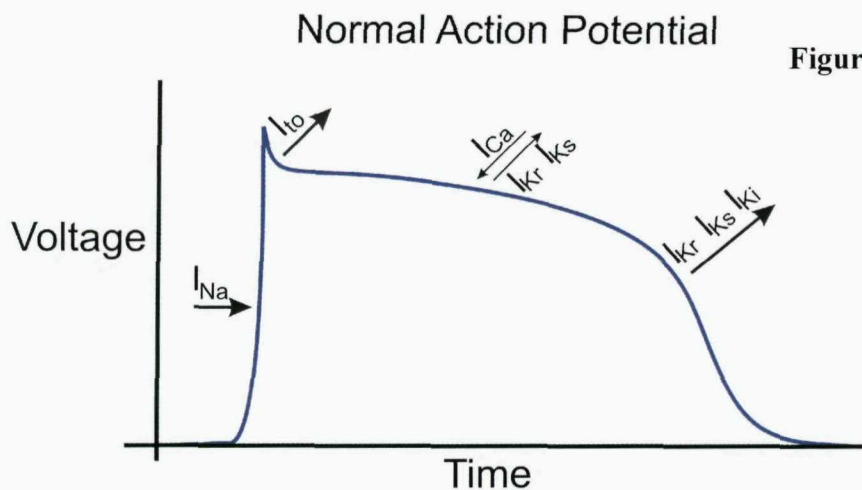


Figure 20 Electrophysiologic basis of LQT3

Figure 21(a) shows the normal ECG and the corresponding phases of the cardiac action potential. Individual ionic currents responsible for different phases of the action potential are labelled. Figure 21(b) shows the ECG in LQT3, which is due to SCN5A mutation and which leads to persistent sodium current which leads to prolongation of the repolarisation phase. I_{Na} - sodium current; I_{Ca} -calcium current; I_{Ki} -inward rectifier current; I_{Kr} -rapid component of delayed rectifier current; I_{Ks} -slow component of delayed rectifier current; I_{to} - transient outward current.

1.3.5.2 Brugada syndrome

This condition is characterised by ST segment elevation in the right precordial ECG leads V1-V3 and a right bundle branch block pattern, but normal QT intervals and a structurally normal heart³⁰. Administration of sodium channel blockers like flecainide may expose this ECG pattern in latent cases³⁰. A family history of unexplained sudden death is often present.

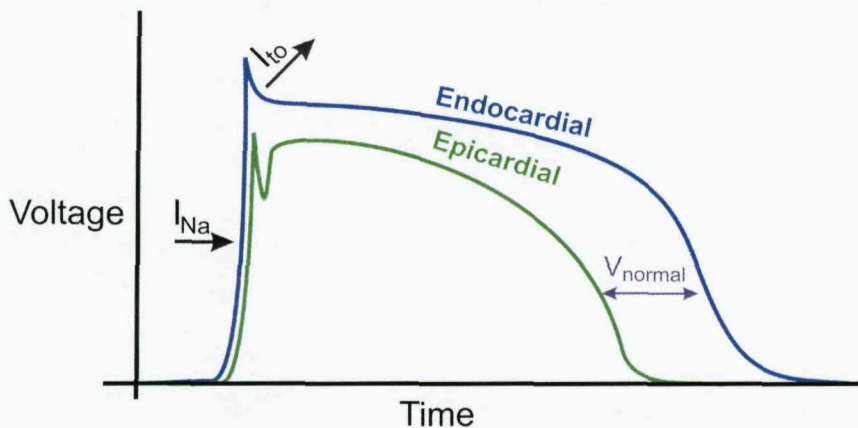
A definitive diagnosis of Brugada syndrome can be made when a type 1 ST-segment elevation (figure 9) is observed in the right precordial leads (V1 to V3) in the presence or absence of a sodium channel-blocking agent, and in conjunction with one of the following: documented ventricular fibrillation, polymorphic ventricular tachycardia, a family history of sudden cardiac death, coved-type ECGs in family members, inducibility of VT with programmed electrical stimulation or syncope³¹.

Electrophysiologic basis of Brugada syndrome:

SCN5A mutations in Brugada syndrome can lead to reduced myocardial sodium current which can lead to exaggerated transmural voltage gradient (figure 22). This can lead to dispersion of repolarisation and arrhythmias. The predominance of ECG changes in the right precordial leads (V1-V3) may be due to transmural differences in action potential configuration, especially in the right ventricular outflow tract⁶⁴, which in turn may be related to variable expression of ion currents.

Normal Action Potential

Figure 22(a)



Brugada Action Potential

Figure 22(b)

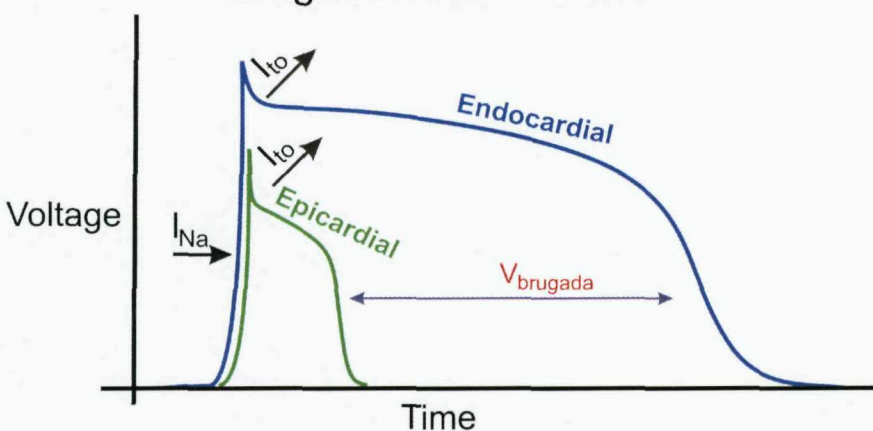


Figure 21 Electrophysiologic basis of Brugada syndrome

I_{Na} -sodium current, I_{to} - transient outward current, V_{normal} - normal transmural voltage gradient, $V_{brugada}$ - transmural voltage gradient in Brugada syndrome. Figure 22(a) shows endocardial and epicardial action potentials in the normal heart. The epicardial action potential is shorter because of large transient outward current. Figure 22(b) shows endocardial and epicardial action potentials in Brugada syndrome. Reduced sodium current causes disproportionate shortening of epicardial action potentials with resulting exaggeration of the transmural voltage gradient.

1.3.6 Calcium channelopathies

The cardiac ryanodine receptors (RyR2) are calcium-induced calcium release channels located in cardiac sarcoplasmic reticulum. These channels are activated by calcium which enters the cell through the L-type calcium channels during cardiac myocyte depolarisation. When RyR2 channels open, they allow release of calcium from the sarcoplasmic reticulum, which initiates activation of the contractile apparatus⁶⁵. Mutations in the *RyR2* gene can lead to defective RyR channels which can result in defective calcium ion release. This can impair contractility or contribute to diastolic depolarisations (after-depolarisations) that can trigger ventricular arrhythmias and cause catecholaminergic polymorphic ventricular tachycardia (CPVT) (OMIM#604772)⁶⁶.

1.3.6.1 Catecholaminergic polymorphic ventricular tachycardia

Catecholaminergic polymorphic ventricular tachycardia (CPVT) usually occurs in children and young adults and is characterised by stress or emotion induced (adrenergic) syncope⁶⁷. There are two patterns of inheritance for CPVT. Mutations in the ryanodine type-2 receptor (*RYR2*) gene (OMIM180902), located on chromosome 1q42, cause the more common autosomal dominant CPVT (CPVT1)⁶⁶. A rare, recessive form of CPVT (CPVT2) can occur due to mutations in calsequestrin 2 gene (*CASQ2*), (OMIM#114251), which codes for a calcium ion binding protein⁶⁸. Both RYR2 and CASQ2 play a crucial role in the excitation-contraction coupling, by their involvement in the storage and release of calcium ions from the sarcoplasmic reticulum. There is often a characteristic ECG pattern of bi-directional ventricular tachycardia, which may be reproduced by exercise. The resting electrocardiogram may be normal. Therefore clinical assessment alone is not reliable to detect CPVT⁶⁷. Beta blockers may reduce syncope and implantation of a defibrillator is often indicated⁶⁹.

1.4 CARDIOMYOPATHIES

The main familial cardiomyopathies are hypertrophic cardiomyopathy (HCM), dilated cardiomyopathy (DCM) and arrhythmogenic right ventricular cardiomyopathy (ARVC)⁷⁰. Mutations in the β -myosin heavy chain gene were first identified as responsible for familial hypertrophic cardiomyopathy⁷¹. Since then, mutations in 12 genes have been found to cause hypertrophic cardiomyopathy (table 6) and mutations in other genes have been identified that cause dilated cardiomyopathy and arrhythmogenic right ventricular cardiomyopathy.

1.4.1 Hypertrophic cardiomyopathy

Hypertrophic cardiomyopathy (HCM) (OMIM#192600) is a primary disorder of the myocardium. The estimated prevalence of HCM in the western population is about 1 in 500⁷². Often there is myocardial hypertrophy (in the absence of conditions like aortic stenosis and hypertension, which by themselves can cause myocardial hypertrophy), which can involve the inter-ventricular septum, and lead to obstruction of flow through the left ventricular outflow tract. The obstructive form of HCM occurs in <25% of affected individuals. Some patients have systolic dysfunction and most patients have diastolic dysfunction⁷³. The major mechanism for sudden death is ventricular arrhythmia related to myofibrillar disarray, abnormal Ca^{2+} homeostasis, myocardial ischemia, left ventricular diastolic dysfunction or left ventricular outflow tract obstruction.

1.4.1.1 Clinical features

Patients may be asymptomatic or have symptoms ranging from palpitations and dizziness to syncope and sudden death. The age of onset of symptoms can vary between different HCM genes. For example, mutations in cardiac myosin binding protein C (*cMyBPC*), tend to present after the fifth decade of life and mutations in *cTNNT2* or β -MHC tend to present early in life.

1.4.1.2 Genetic aspects

Twelve different genes have been identified which, if mutated, can cause HCM. Most of the disease-causing mutations have been identified in the gene encoding sarcomeric proteins like β -myosin heavy chain, α -tropomyosin, troponin I, troponin T and actin. Table 6 summarises the genetic aspects of HCM. The majority of mutations occur in *MYH7* and *MYBPC3*. The characteristic features of certain gene mutations leading to HCM are shown in table 5. Patients with *TNNT2* mutations may have a high risk of sudden death in the absence of ventricular hypertrophy⁷⁴. The diagnostic yield of genetic testing in familial HCM is around 60%⁷⁵. Genetic testing should be considered for patients with a firm clinical diagnosis of hypertrophic cardiomyopathy as a means of cascade screening of relatives, 'since ECG or echocardiographic abnormalities may be absent, subtle or develop late in life'⁷⁶.

Gene	Features	Reference
β -MHC	Typically present in first two decades. Moderate or severe hypertrophy	77
<i>cMyBPC</i>	Asymptomatic until the fifth or sixth decades	78
<i>cTNNT</i>	Mild or clinically undetectable hypertrophy	79
<i>cTNNI</i>	Hypertrophy often localized to the left ventricular apex	80
<i>ACTC1</i>	Hypertrophy often localized to midcavity	81
<i>MYL-2</i>	Hypertrophy often localized to midcavity	82

Table 5 Characteristic features of genetic mutations causing HCM

Table shows the characteristic features of some of the genetic mutations that cause HCM. β -MHC- β -myosin heavy chain, *cMyBPC*- cardiac myosin binding protein C, *cTNNT*-cardiac troponinT, *cTNNI*- cardiac troponin I, *ACTC1*- actin, *MYL-2*-myosin light chain

Locus	Gene	OMIM	Reference	Protein
1q32	<i>TNNT2</i>	191045	⁸³	Cardiac troponin T
2q31	<i>TTN</i>	188840	⁸⁴	Titin
3p21	<i>MYL3</i>	608751	⁸²	Essential myosin light chain
3p14	<i>TNNC1</i>	191040	⁸⁵	Cardiac troponin C
7q36	<i>PRKAG2</i>	600858	⁸⁶	AMP-activated protein kinase
11p11	<i>MYBPC3</i>	115197	⁸⁷	Cardiac myosin binding protein C
11p15	<i>CLP</i>	600824	⁸⁸	Cardiac muscle LIM protein
12q24	<i>MYL2</i>	160781	⁸⁹	Regulatory myosin light chain
14q12	<i>MYH7</i>	160760	⁷⁷	β-Myosin heavy chain
15q14	<i>ACTC1</i>	102540	⁸¹	Cardiac actin
15q22	<i>TPM1</i>	115196	⁹⁰	Tropomyosin
19q13	<i>TNNI3</i>	191044	⁹¹	Cardiac troponin I

Table 6 Genes associated with HCM

Table summarises the various genes identified in hypertrophic cardiomyopathy, their OMIM coding, location and the proteins they code.

In general, each affected family has a unique mutation. Mutations in the 12 known disease genes account for 50-70% of all cases of HCM, suggesting that there are other as yet unidentified genes, which if mutated can lead to HCM.

Cardiac troponin T

Troponin T is a protein of the thin filament of the sarcomere and forms the troponin complex with troponin I, troponin C and tropomyosin, that regulates cardiac muscle contraction (figure 23)⁹², in response to alterations in intracellular calcium ion concentration. Mutations in the gene which codes for troponin T (*TNNT2*) is associated with familial hypertrophic cardiomyopathy as well as dilated cardiomyopathy⁹³.

Troponin T is expressed in heart and in developing skeletal muscle. Transcripts for this gene undergo alternative splicing that results in many tissue-specific isoforms⁹⁴. In the human heart, four cTnT isoforms are expressed (cTnT1 through cTnT4, numbered in the order of decreasing molecular size). cTnT1 and cTnT2 are expressed in the fetal heart, cTnT4 is expressed in the fetal heart and is re-expressed in heart failure and cTnT3 is the dominant isoform in the adult human heart⁹⁵.

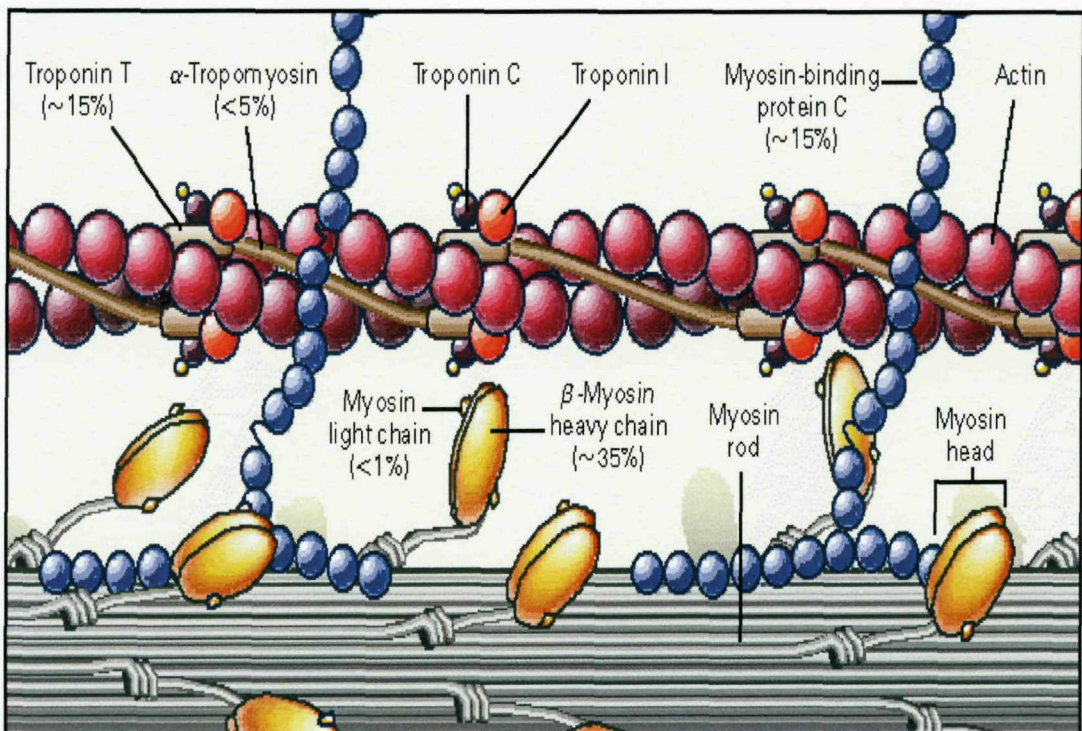


Figure 22 Components of the cardiac sarcomere

Figure shows components of the cardiac sarcomere. Percentages represent the estimated frequency with which a mutation on the corresponding gene causes hypertrophic cardiomyopathy (Paolo Spirito et al, NEJM Mar 13,1997; 336 (11) page 775, by permission from the Massachusetts Medical Society).

1.4.2 Dilated Cardiomyopathy (CMD)

Dilated cardiomyopathy is clinically defined by dilatation and dysfunction of the ventricles. The main causes of dilated cardiomyopathy are ischaemic heart disease, alcohol excess, viral infection and genetic. Clues to genetic causes are familial nature and early age of onset of the disease (usually in the second or third decade of life). The genetic causes account for approximately 20% of all the causes for dilated cardiomyopathy⁹⁶.

CMD1A is a form of dilated cardiomyopathy caused by mutation in the lamin A/C gene (*LMNA*). It is often associated with AV block⁹⁷. The locus for CMD1B has been identified at 9q13-q22, but the gene has not been found yet⁹⁸. Dilated cardiomyopathy with or without left ventricular noncompaction (CMD1C) is caused by mutation in *LDB3*⁹⁹. CMD1D is the form of dilated cardiomyopathy which maps to 1q32 and is due to mutation in the gene encoding cardiac troponin T¹⁰⁰. CMD1E is caused by mutation in the *SCN5A*¹⁰¹. The locus for CMD1F is at 6q23 but the gene has not been isolated yet¹⁰². CMD1G is caused by mutations in the titin gene (*TTN*) on 2q31¹⁰³. The locus for CMD1H is at 2q14-q22 but the gene has not been identified yet¹⁰⁴. CMD1I is caused by mutations in the desmin gene (*DES*) on 2q35¹⁰⁵. CMD1J is caused by mutation in *EYA4*¹⁰⁶ on 6q23-24. The locus for CMD1K is at 6q12-q16 but the gene has not been isolated yet¹⁰⁷. CMD1L is caused by mutation in *SGCD* on 5q33¹⁰⁸. CMD1M is caused by mutation in *CSRP3* encoding cysteine- and glycine-rich protein-3 on 11p15.1¹⁰⁹. CMD1N is caused by mutation in *TCAP* on 17q12¹⁰⁹. CMD1O is caused by mutation in *ABCC9* on 12p12.1¹¹⁰; CMD1P is caused by mutation in *PLN* on 6q22.1¹¹¹; The locus for CMD1Q is at 7q22.3-q31.1 but the gene has not been isolated yet¹¹². CMD1R is caused by mutation in *ACTC* on 15q14¹¹³; CMD1S is caused by mutation in *MYH7* on 14q12¹¹⁴; CMD1T is caused by mutation in *TMPO* on chromosome 12q22¹¹⁵; CMD1U, is caused by mutation in *PSEN1* on 14q24.3¹¹⁶; CMD1V is caused by mutation in *PSEN2* on 1q31-q42¹¹⁶; CMD1W is caused by mutation in the gene encoding metavinculin (*VCL*) on 10q22-q23¹¹⁷ and CMD1X, is caused by mutation in *FKTN* encoding fukutin on 9q31¹¹⁸; Mutation in *MYBPC3* is also a possible cause of CMD¹¹⁹.

	Locus	OMIM	Gene	OMIM	Reference
CMD1A	1q21.2-q21.3	#115200	<i>LMNA</i>	150330	⁹⁷
CMD1B	9q13-q22	#600884	-	-	⁹⁸
CMD1C	10q22.2-q23.3	#601493	<i>LDB-3</i>	605906	⁹⁹
CMD1D	1q32	#601494	<i>TNNT2</i>	191045	¹⁰⁰
CMD1E	3p	#601154	<i>SCN5A</i>	600163	¹⁰¹
CMD1F	6q23	#602067	-	-	¹⁰²
CMD1G	2q31	#604145	<i>TTN</i>	188840	¹⁰³
CMD1H	2q14-q22	#604288	-	-	¹⁰⁴
CMD1I	2q35	#604765	<i>DES</i>	125660	¹⁰⁵
CMD1J	6q23-24	#605362	<i>EYA4</i>	603550	¹⁰⁶
CMD1K	6q12-q16	#605582	-	-	¹⁰⁷
CMD1L	5q33	#606685	<i>SGCD</i>	601411	¹⁰⁸
CMD1M	11p15.1	#607482	<i>CSRP3</i>	600824	¹⁰⁹
CMD1N	17q12	#607487	<i>TCAP</i>	604488	¹⁰⁹
CMD1O	12p12.1	#608569	<i>ABCC9</i>	601439	¹¹⁰
CMD1P	6q22.1	#609909	<i>PLN</i>	172405	¹¹¹
CMD1Q	7q22.3-q31.1	#609915	<i>CHRM</i>	-	¹¹²
CMD1R	15q14	-	<i>ACTC</i>	102540	¹¹³
CMD1S	14q12	-	<i>MYH7</i>	160760	¹¹⁴
CMD1T	12q22	-	<i>TMPO</i>	188380	¹¹⁵
CMD1U	14q24.3	-	<i>PSEN1</i>	104311	¹¹⁶
CMD1V	1q31-1q42	-	<i>PSEN2</i>	600759	¹¹⁶
CMD1W	10q22-q23	#611407	<i>VCL</i>	193065	¹¹⁷
CMD1X	9q31	-	<i>FKTN</i>	607440	¹¹⁸
	11p11	-	<i>MYBPC3</i>	115197	¹¹⁹

Table 7 Genetic aspects of dilated cardiomyopathy

Table 7 summarises the different genetic causes of dilated cardiomyopathy and their loci. The OMIM coding for the conditions and the genes are also shown. CMD- Cardiomyopathy

Dilated (dilated cardiomyopathy), *LMNA*-lamin A/C, *LDB*-LIM Domain Binding, *TNNT2*-troponin T, *SCN5A*- sodium channel gene, *TTN*-titin, *DES*-desmin, *EYA*- Eyes Absent gene, *SGCD*- δ sarcoglycan, *CSRP*- cysteine and glycine rich protein, *TCAP*- Titin cap; *ABCC9*-ATP Binding Cassette subfamily C, *PLN*- phospholamban, *CHRM* – muscarinic acetylcholine receptor, *ACTC*-cardiac actin, *MYH7*- β -myosin heavy chain, *TMPO*-thymopoietin, *PSEN*- Presenilin, *VCL*-metavinculin, *FKTN*-fukutin, *MYBPC3*- cardiac myosin binding protein C.

1.4.3 Arrhythmogenic right ventricular cardiomyopathy

Arrhythmogenic right ventricular cardiomyopathy (ARVC) is a familial cardiomyopathy characterised by myocyte loss with fibrofatty replacement (hence also sometimes referred to as ARVDysplasia), and predisposes the subject to ventricular arrhythmias, heart failure and sudden death. The pathological process predominantly affects the right ventricle but can also involve the left ventricle¹²⁰. Autosomal dominant inheritance is observed most commonly. An autosomal recessive form of ARVC has been reported in association with palmo-plantar keratoderma and woolly hair (Naxos disease)¹²¹.

1.4.3.1 Clinical features

The diagnosis of ARVC is based on the detection of structural, histologic, electrocardiographic, arrhythmic and genetic factors. The important feature is the presence of structural and functional alterations of the right ventricle and the diagnosis can be made when a subject has two major criteria, one major and two minor criteria, or four minor criteria (table 8).

Major criteria	Minor criteria
Severe structural abnormalities in the right ventricle	Mild to moderate structural abnormalities of the right ventricle
Fatty infiltration in the right ventricle	-
Repolarisation abnormalities on the ECG	Minor ECG abnormalities
Conduction abnormalities on the ECG	Ventricular arrhythmias on ECG or 24 hour tape
Family history of ARVC	Family history of sudden cardiac death

Table 8 Diagnostic criteria for ARVC

The diagnosis of ARVC is made when two major criteria, or one major and two minor criteria or four minor criteria are fulfilled.

1.4.3.2 Genetic aspects

ARVC is a genetically heterogeneous disorder. Twelve chromosomal loci have been identified in families with ARVC and seven genes identified (Table 9). Clinical expression of various mutations is heterogeneous among members of the same family, ranging from being totally asymptomatic to being severely affected.

Mutations in 7 genes have been identified so far, that cause ARVC. Mutations in *RyR2* causes ARVC2, which is characterised by effort induced polymorphic ventricular tachycardia. In ARVC2, structural abnormalities are limited to mild regional wall motion abnormalities of the right ventricle and the phenotype has a resemblance to familial catecholaminergic ventricular tachycardia, which is also associated with mutations in *RyR2*¹²².

Mutations in desmoplakin, plakophilin, desmoglein, desmocollin and plakoglobin can directly lead to dysfunction of desmosomes and mutations in β type transforming growth factor can indirectly lead to abnormal desmosomal function and lead to ARVC. Table 9 summarises the genetic aspects of ARVC.

Condition	OMIM	Locus	Gene	OMIM	Protein	Reference
ARVC1	107970	14q23-q24	<i>TGFB3</i>	190230	β type transforming growth factor	^{123,124}
ARVC2	600996	1q42-q43	<i>RYR2</i>	180902	Ryanodine receptor	^{125,126}
ARVC3	602086	14q12-q22	?	-	?	
ARVC4	602087	2q32.1-q32.3	?	-	?	¹²⁷
ARVC5	604400	3p23	?	-	?	¹²⁸
ARVC6	604401	10p12-p14	?	-	?	
ARVC7	609160	10q22	?	-	?	¹²⁹
ARVC8	607450	6p24	<i>DSP</i>	125647	Desmoplakin	¹³⁰
ARVC9	609040	12p11	<i>PKP2</i>	602861	Plakophilin-2	^{131,132}
ARVC10	610193	18q12.1-q12	<i>DSG2</i>	125671	Desmoglein-2	¹³³
ARVC11	610476	18q12.1	<i>DSC2</i>	125645	Desmocollin	¹³⁴
ARVC12	611528	17q21	<i>JUP</i>	173325	Plakoglobin	¹³⁵
Naxos disease	601214	17q21	<i>JUP</i>	173325	Plakoglobin	¹³⁶

Table 9 Genetic aspects of ARVC

The table shows the 10 loci identified so far as having genetic mutations that lead to ARVC. *TGFB3*- transforming growth factor beta-3, *RYR2*- ryanodine receptor-2, *DSP*- desmoplakin, *PKP*- plakophilin, *DSG*-desmoglein, *DSC*- desmocollin, *JUP*-plakoglobin.

1.4.4 Update on the genetics of inherited arrhythmias

Mutations in several other genes can lead on to ventricular arrhythmias in a structurally normal heart. These genes are described below.

1.4.4.1 LQT7

LQT7 is associated with ventricular arrhythmias, periodic paralysis and skeletal deformities. The severity of the periodic paralysis and skeletal deformities can be mild. *KCNJ2* encodes for the inward rectifier potassium channel Kir2.1 and contribute to I_{K_i} ¹³⁷. Mutations in *KCNJ2* reduce the inward rectifier K^+ channel current (I_{K_i}) and slows down the return of the membrane to the resting potential.

1.4.4.2 LQT8

LQT8 (Timothy syndrome) is due to mutations in *CACNA1c* which codes for the α -subunit of the L-type calcium channel (Cav1.2), which is important in excitation contraction coupling in the heart. Patients have varying clinical manifestations including prolonged QT interval, ventricular arrhythmias, congenital heart disease, webbing of fingers and toes and autism¹³⁸.

1.4.4.3 LQT9

LQT9 is secondary to mutations in *CAV3* which is located on 3p25. Similar to *SCN5A* mutations causing LQT3, mutations in *CAV3* can increase late sodium current and impair cellular repolarisation, leading to long QT interval¹³⁹.

1.4.4.4 LQT10

LQT10 is secondary to mutations in *SCN4B* which is located on 11q23.3 and which encodes the protein Nav β 4 (the sodium channel auxiliary subunit to the pore forming subunit) of the voltage gated sodium channel of the heart¹⁴⁰.

Mutations in *KCNQ1*, *KCNH2* and *SCN5A* account for nearly 75% of congenital LQTS (LQT1, LQT2, and LQT3) and about 5 % of LQTS are due to mutations involving ankyrin-B, KCNE1, KCNE2, KCNJ2, *CACNA1c*, CAV3 and *SCN4B* (LQT4, LQT5, LQT6, LQT7, LQT8, LQT9 and LQT10).

1.4.4.5 GPD1L

A second locus for Brugada syndrome (OMIM 611777) was identified on chromosome 3 at 3p25-p22¹⁴¹. The gene has been identified as the *GPD1L* (glycerol-3-phosphate dehydrogenase 1-like) gene (OMIM 611778) and mutations in this gene reduce the inward sodium current during the cardiac action potential¹⁴².

1.4.4.6 Sarcolipin

Following cardiac contraction, cytoplasmic calcium is transported back to sarcoplasmic reticulum by a Ca²⁺ ATPase (SERCA2) located in the sarcoplasmic reticulum membrane. The function of SERCA2 is regulated by two polypeptides-phospholamban (PLN) and sarcolipin (SLN). Mutations in *PLN* can cause dilated cardiomyopathy¹⁴³. No disease associated mutations have been described in *SLN* but remains possible¹⁴⁴.

1.4.4.7 NCX

After the voltage dependent Ca²⁺ channels have inactivated, the terminal portion of the plateau of the action potential is maintained by inward current through the Na⁺/ Ca²⁺

exchanger which is encoded by the gene *NCX1* on 2p21-23¹⁴⁵. Dysfunction of this gene can lead to poorly controlled cytoplasmic Ca^{2+} and result in triggered arrhythmias.

1.4.5 Channel Interacting Proteins (ChIP)

Defective protein-protein interactions or targeting mechanisms contribute to arrhythmogenesis. Specifically, proteins that interact with ion channel function are called ChIPs. The interaction can secondarily disrupt ion channel function (like their localisation, post translational modification, trafficking, and electrophysiology) and can lead to arrhythmias¹⁴⁶. ANKB and caveolin-3 are two examples of a potentially large group of such proteins in the heart.

1.4.5.1 ANKB

The gene *ANKB* or *ANK2* codes for ankyrin-B which is an adapter protein. An adapter protein acts as a connecting molecule and is critical to intermolecular interactions and plays a role in the regulation of signal transduction. It is important for the optimal spatial orientation of Na-K ATPase, inositol triphosphate (IP3) receptor and Na/Ca exchanger to their appropriate membrane microdomains⁴⁵.

1.4.5.2 CAV3

The gene *CAV3* codes for CAV3 (caveolin 3), an important scaffolding protein of caveolae. Scaffold proteins in general bring together various other proteins in a signalling pathway and allows for their interaction. Voltage-gated Na^+ channel (Nav1.5)¹⁴⁷, voltage gated K^+ channel (Kv1.5)¹⁴⁸ and the L-type calcium channel¹⁴⁹ are localised to caveolae. Caveolin-3 in particular helps to localize key signalling molecules of the $\beta 2$ adrenergic receptor cascade like G proteins, adenyl cyclase, and protein kinase-A and thus helps to modulate the sympathetic response in the heart. *CAV3* mutation can therefore lead to dysfunction of these ion channels and signalling pathways. This in turn can lead to abnormalities in repolarisation and ventricular arrhythmias.

1.5 MAPPING AND CLONING DISEASE GENES

Mapping of genes specify the location of a chromosome region likely to harbour the gene. Genes can be mapped by genetic and physical techniques. In genetic mapping, linkage analysis is used to determine the relative position of a gene on a chromosome. In physical mapping, techniques like fluorescent in-situ hybridization are used to determine the position of the gene on a chromosome. Once the gene is mapped, the gene can be cloned and its DNA sequence and protein product studied.

1.5.1 Linkage analysis

Linkage analysis is a method for locating the position of a gene, mutations in which has caused the disease, relative to the known location of genetic markers in the genome. The genetic markers used in linkage analysis are DNA sequence variations (often microsatellites and SNPs) with a high degree of polymorphism. Alleles at loci near each other often cosegregate together (recombination event is less likely) and this principle is used to track the transmission of genomic regions in a family. After typing multiple markers for each family member in an informative pedigree, it is possible to observe the segregation of groups of alleles (haplotypes) with the disease status, provided the affected and non-affected status of the subjects are unambiguous. Haplotype analysis helps to narrow down the genomic region of interest. The statistical method used to estimate the proximity between the hypothetical disease locus and the loci of the genetic markers is the LOD score method, that is based on calculation of the likelihood of the observed pedigree data, given assumed parameter

values¹⁵⁰. A LOD score of 3 often suggests significant linkage and a LOD score of -2 excludes linkage. Linkage analyses can be performed on single large families or on several small families if the disease is unambiguously caused by the same gene in all the families. Linkage analysis strategies are effective but labour intensive.

1.5.2 Candidate gene approach

In this approach, certain assumptions about the pathophysiology of the disorder are initially made and possible candidate genes are listed. Genetic tests are done to look for segregation of alleles with the disease, to see if the candidate gene tested is the likely source of mutation. For example, in Jervell-Lange-Nielsen syndrome, patients have deafness and prolonged QT interval. Ion channels are important in normal hearing and also for cardiac repolarisation. Therefore genes that encode ion channels are candidate genes for further investigation. Polymorphic markers that lie within and near the candidate genes are selected for genetic tests as opposed to selecting a group of markers distributed throughout the genome. If the selected marker is close to the gene, it is unlikely for recombination to occur between the marker and the disease gene and all the affected subjects (who share the same gene mutation) will share a common allele when the corresponding genetic marker is tested. If the number of affected subjects tested is large enough, it may generate enough evidence to suggest a statistically significant linkage between the marker and the disease locus. If the number of subjects tested is not large enough, it may prove difficult to confirm linkage but at the same time, linkage cannot be excluded and further investigations may be needed. If all the affected subjects do not share a common allele, it excludes that particular locus as the disease locus (assuming that no recombination event has occurred). Once the disease gene is identified, it can be mutation screened to identify and characterize the mutation. If the affected and non- affected groups are not correctly selected, gene discovery by the candidate gene approach may be unsuccessful.

1.5.3 Comparative genomics

This strategy helps to identify the gene through an animal model. The animal mutant and a phenotypically similar human disease are identified. Then if the animal gene is cloned, its human ortholog becomes a candidate gene. Comparative genomics strategy can work if functionally conserved or structurally homologous genes affecting phenotypic variation of interest have already been confirmed in other species ¹⁵¹. This strategy however may be inefficient because of the biological difference from one species to another due to the genetic heterogeneity or evolutionary differentiation¹⁵².

1.5.4 Positional cloning

Positional cloning requires identification of the variant region of the genome as the preliminary step. All the genes in the region are identified, prioritised for mutation screening and tested in affected individuals. For Mendelian diseases, initial linkage analysis helps to define the candidate region. For non-Mendelian diseases, linkage analysis is less precise and candidate regions are typically 20 cM or more, which requires further information using techniques such as linkage disequilibrium to narrow the search.

KVLQT1 is an example of a gene identified by positional cloning methods⁵³. It was previously known that mutations leading to LQTS in a large family was linked to chromosome 11p15.5. The authors mapped the gene to a narrow region in 11p15.5 by genotype and haplotype analysis. DNA sequence analyses of the entire region revealed a portion of sequence which predicted an aminoacid sequence similar to a voltage gated potassium channel. The gene was named as *KVLQT1*. Single strand conformational polymorphism (SSCP) and DNA sequencing analyses identified the mutation⁵³.

1.5.5 Approaches using known chromosomal abnormalities

Patients with balanced chromosomal rearrangements usually have a normal phenotype. If however, they are phenotypically abnormal, it is possible that one of the chromosome breakpoints is located within a disease gene or very close to it and has inactivated the gene. The position of the breakpoint may be identified using FISH. This does not necessarily locate the gene, since occasionally the breakpoint can alter the expression of a gene located at a distance¹⁵³.

An example of the use of this approach in gene identification is demonstrated in the identification of the gene for Alstrom syndrome, which is an inherited disorder characterised by obesity, cardiomyopathy and multiorgan dysfunction. An individual with Alstrom syndrome carrying a familial balanced reciprocal chromosome translocation was studied¹⁵⁴. Previous investigators had mapped two loci for the Alstrom gene. Hearn et al used BACs containing these two loci as probes, hybridised them to metaphase chromosomes and performed FISH analysis and found that a different BAC crossed the patient's translocation breakpoint. Sequence analysis of this BAC suggested the presence of a gene of interest. The cDNA representing this gene was used for RT-PCR. Northern Blot analysis was performed and the transcript studied. This localised the 2p13 breakpoint to a long range PCR product derived from the BAC. This was then further refined by Southern blot analysis. In the same individual, a deletion was detected in the paternal allele. The individual was thus a compound heterozygote, carrying one copy of a gene disrupted by translocation and the other copy disrupted by an intragenic mutation. Other families having Alstrom syndrome were studied for mutations and *ALMS1* was confirmed as the gene underlying Alstrom syndrome.

1.5.6 Combination of methods to identify genes

For successful gene identification, a combination of methods is usually required. Often a likely candidate gene is identified which can then be tested for mutations in affected people. A combination of clinical and lab work along with computer analysis and database searching

is crucial for successful gene identification. Table 10, shows examples of the methods used to identify the genes, mutations in which are responsible for LQTS.

Gene	Method used for identification	Reference
<i>KCNQ1</i>	Positional cloning	⁵³
<i>KCNH2</i>	Linkage analysis and candidate gene approach	⁴²
<i>SCN5A</i>	Positional cloning and candidate gene approach	⁵⁵
<i>ANKB</i>	Genome wide linkage analysis	⁴⁵
<i>KCNE1</i>	Candidate gene approach	¹⁵⁵
<i>KCNE2</i>	Analysis from a candidate protein	⁴⁷

Table 10 Examples of methods used to map genes

The table shows the methods used to identify the 6 main LQT genes. *KCNQ1* - LQT1 gene, *KCNH2*- LQT2 gene, *SCN5A*- LQT3 gene, *ANKB*-LQT4 gene, *KCNE1*-LQT5 gene and *KCNE2*- LQT6 gene.

1.6 HYPOTHESIS

Two large families have been identified with a rare, cardiac phenotype. It was therefore hypothesized that a novel previously unidentified gene or novel mutations in a known candidate gene was responsible.

1.7 AIMS

- 1) To refine the phenotype of 2 large families with inherited ventricular tachyarrhythmia.
- 2) To use microsatellite markers to exclude linkage to known genes implicated in inherited ventricular tachyarrhythmias in structurally normal hearts.
- 3) To mutation screen any of these genes that cannot be excluded.

2.0 CHAPTER 2- MATERIALS & METHODS

2.1 MATERIALS

The source of materials used are given in appendix A and the source of instruments used are given in appendix B.

2.1.1 Buffers and Solutions

2.1.1.1 10× TBE

A stock solution of 10×TBE was made using Trisbase 108g, Boric Acid 55g and EDTA 9.3g, which were mixed with sufficient dH₂O and the volume was made upto 1 litre, pH 8.3. This solution was kept in the lab at room temperature for further use.

2.1.1.2 Ethidium Bromide staining solution

This was prepared by mixing 20ml of 10×TBE, 20μl of ethidium bromide and 180ml of water. It was then kept in a dark tank, since light degrades ethidium bromide. Gels were left for 30 minutes in this solution before undertaking electrophoresis.

2.1.1.3 Ammonium persulphate

A 10% solution was prepared by dissolving 1g of Ammonium persulphate in appropriate amount of water and then increasing the volume to 10ml.

2.1.2 Gels

2.1.2.1 Agarose gel

1 g of pure agarose was added to 100ml 1×TAE buffer and then heated in a microwave for 3minutes 30 seconds on high power.

2.2 METHODS

2.2.1 DNA extraction from whole blood

3-10ml of blood was transferred into a 50ml polypropylene tube. Four times the volume of reagent A (Nucleon kit) was added and the solution was mixed for 4 minutes in a rotary mixer. The solution was then centrifuged for four minutes at 1,000 rpm. To convert the speed (rpm) into relative centrifugal force (rcf) [expressed in units of gravity (times gravity or $\times g$)], the formula used is $g = (1.118 \times 10^{-5}) RS^2$, where g is the relative centrifugal force, R is the radius of the centrifuge rotor in cm and S is the speed of the rotor in rpm. The supernatant was discarded without disturbing the pellet. 2ml reagent B was added (Nucleon kit). 500 μ l of sodium perchlorate (Nucleon kit) was added and the solution mixed by gently inverting and then spun for 3 minutes at 3,600 rpm. 300 μ l of Nucleon resin was added and the tube was re-spun at 3,600 rpm for 3 minutes. The clear upper phase was transferred to a new tube using a pipette. Twice the volume of cold absolute ethanol (approximately 5ml) was added and the tube inverted several times until the DNA was precipitated. The DNA was pelleted by centrifuging at 3,600 rpm for 5 minutes. The supernatant was discarded. 2ml cold 70% ethanol was added and re-centrifuged as before. The supernatant was discarded and the pellet air-dried for 10 minutes. The DNA was re-suspended in 50 μ l dH₂O.

2.2.2 Measuring DNA concentration

2.2.2.1 Determination of absorbance at 260 nm

5 μ L DNA was added to 1ml of ultrapure water. Using the quartz cuvette, the absorbance at 260nm was measured. The absorbance obtained was multiplied by 10 to obtain the concentration of DNA in μ g/ μ L.

2.2.3 PCR amplification

Amplification was carried out in a 20 μ l reaction mix of 15% DNA polymerase buffer (Promega), 15% 2.5mM forward primer, 15% 2.5mM reverse primer, 0.5-1 μ g DNA, 0.2 μ l Taq 1u/ μ l DNA polymerase and made upto 20 μ l with distilled water. PCR cycle conditions used were-1) initial denaturation for 4 minutes at 94°C, 2) 30 cycles of 1 minute at 94 °C, 50-60°C (depending on primer Tm) for 1 minute, 72°C for 1 minute and 3) final extension at 72°C for 10 minutes. PCR was carried out using a thermocycler.

2.2.4 Agarose gel electrophoresis

PCR products were run on a 1-2% ethidium bromide agarose gel with 1 \times Ficoll Orange loading buffer. DNA was visualized using Molecular Dynamics Fluorimager- 595 or UV-illuminometer.

2.2.5 Identification and design of PCR primers

PCR primers amplifying polymorphic microsatellite markers were identified using the NCBI database (<http://www.ncbi.nlm.nih.gov>). If possible, published markers were used. However, in regions of low density, additional polymorphic markers were identified from genomic clones mapping to the region. Primers were designed flanking dinucleotide repeats larger than 20 bp in length, using DNA Star-Primer Select software. Identified primers were put into a BLAST search (<http://www.ncbi.nlm.nih.gov>) to ensure that they did not map to multiple loci. Primers were obtained from Qiagen-Operon with a fluorescent label- FAM, TET or HEX, attached to the 5' terminus of the forward primer to allow detection following gel electrophoresis. Optimisation of primer annealing temperatures was carried out on control DNA. The information on primers used for genotyping are given in appendix C and the information on primers used for sequencing *TNNT2* is given in appendix I.

2.2.6 Sizing of PCR products using an ABI 377 sequencer

PCR was carried out as outlined above. PCR products were sized using ABI-377 automated fluorescent sequencer and GeneScan software. Multiplexing of primers in each lane was possible with 2 μ l of each primer PCR product of each DNA sample being pooled and made upto 20 μ l with distilled water. Typically 6 primers could be pooled without PCR products overlapping. Similar sized fragments could be run in the same lane provided they were labelled with a different fluorescent dye. 0.5 μ l of pooled PCR sample was added to 2 μ l mix of 4 parts de-ionised formamide, 1 part Tamra size standard and 1 part loading buffer (Applied Biosystems). The samples were denatured at 94 °C for 3 minutes and placed on ice to prevent re-annealing. Gel constituents for microsatellite analysis were 15 ml Gene-page plus, 150 μ l 10% APS, 15 μ l TEMED. 2 μ l samples were loaded into each well and electrophoresis done for 80 minutes. Data was extracted from the gel and analysed using ABI Prism Genescan software. Segregation of the different alleles was determined manually.

2.2.7 Direct Sequencing analysis

PCR amplification was carried out in 30 μ l reactions. Products were run on agarose gel with 1.5 μ l of 10 \times Ficoll orange loading dye and visualised using U-V illuminometer. Gel extraction of PCR products was carried out using a Qiagen kit and protocol. PCR products were cut from the 2% agarose gel using a scalpel and placed in a 1.5ml eppendorf. 500 μ l buffer QG (provided in the Qiagen kit) was added to each eppendorf, which was then incubated in a 50°C water bath for 10 minutes. The eppendorfs were vortexed to help the agarose dissolve. The contents were transferred to QIA-quick spin column. The column was centrifuged for 1 minute at 13,000 rpm. The flow-through was discarded. 500 μ l QC were added to the column to remove any remaining traces of agarose and centrifuged as before. The flow through was discarded and 750 μ l of Buffer PE was added to the spin column. The column was left to stand for 3 minutes before centrifuging for 1 minute at 13,000rpm. The flow through was discarded and the column spun for an additional minute to remove any residual ethanol. The columns

were placed in a new eppendorf. 30 μ l distilled water was added to the centre of the column, left to stand for 1 minute and centrifuged for a minute to elute the DNA.

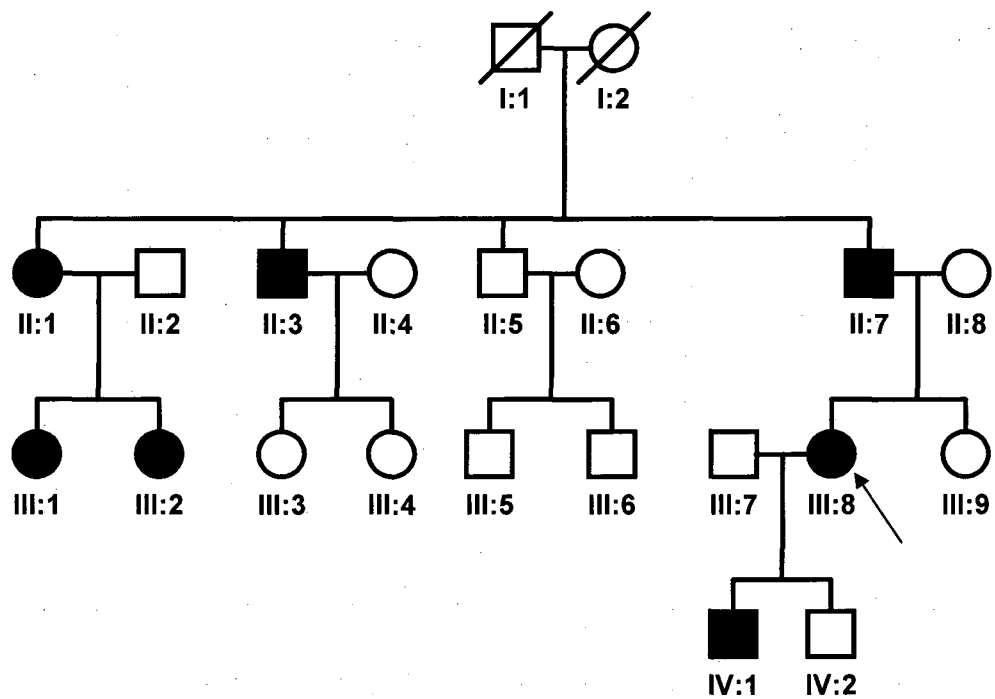
Sequencing reactions were carried out using the ABI Prism dye terminator cycle sequencing ready reaction kit (Applied Biosystems). The reaction mix consisted of 8 μ l dye terminator ready-reaction mix, 3-10ng DNA PCR product, 2 pmol of forward and reverse primers and made upto 20 μ l with distilled water. Initial denaturation was carried out for 5 minutes at 96°C. This was followed by 25 cycles of 96°C for 10 seconds, 50°C for 30 seconds and 60°C for 4 minutes. The products were held at 4°C until used. The products were precipitated with 80 μ l of 75% isopropranolol for 15 minutes, followed by centrifugation for 20 minutes at 13,200 rpm. The supernatant was aspirated using a syringe. 250 μ l of isopropanol were added to the tubes and centrifuged at 13,200 rpm for 5 minutes. The supernatants were removed using a syringe and the samples were dried in a thermocycler for 1 minute at 90°C.

PCR pellets were resuspended in 4 μ l loading mix containing 5 parts of formamide to 1 part loading buffer (ABI Prism). Products were denatured at 96°C for 3 minutes and maintained on ice. Electrophoresis of the products were done using ABI- 377 automated sequencer for 3.5 hours. Gel constituents consisted of 30ml 5% Genepage plus, 300 μ l 10% APS, 30 μ l TEMED. Sequence analysis was carried out using Chromas and DNA Star software.

CHAPTER 3 - RESULTS

3.0 RESULTS

Two large Caucasian families (A & B) were clinically identified to be at high risk of sudden cardiac death. Following approval by the Hampshire Local Research and Ethics Committee, the families were investigated. The study complied with the Declaration of Helsinki. The results of the investigations in family A is shown first followed by the results in family B. The phenotype ascertainment is followed by the genetic investigations.



Symbol definitions:



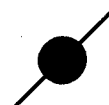
unaffected male



unaffected female



affected male



affected dead female

Figure 23 Pedigree of family A

The figure shows the pedigree of family A. The proband is identified with an arrow. The subject numberings are shown below the corresponding symbols.

3.1 INVESTIGATIONS AND RESULTS OF FAMILY A

3.1.1 Family A ascertainment

A pedigree of family A is shown in figure 24. Of the 14 members in three generations at risk of inheriting this disorder, 7 (3 males and 4 females) were affected. The clinical features of the family are summarised in table 11.

Subject no.	Age	Sex	QTc	palpitation	syncope	failed SCD	ECG	VT stim
II: 1	40	F	430 ms	-	-	-	Abnormal	Positive
II: 3	38	M	428 ms	-	-	-	Abnormal	Positive
II: 7	49	M	410 ms	+	-	-	Abnormal	Positive
III: 1	10	F	440 ms	+	-	-	Abnormal	Positive
III: 2	12	F	408 ms	-	-	-	Abnormal	Positive
III: 8	32	F	380 ms	+	+	+	Abnormal	Positive
IV: 1	14	M	436 ms	+	-	-	Abnormal	Positive
II: 5	46	M	NA	-	-	-	normal	NI
III: 3	16	F	400 ms	-	-	-	normal	NI
III: 4	13	F	NA	-	-	-	normal	NI
III: 5	15	M	418 ms	-	-	-	normal	NI
III: 6	4	M	420 ms	-	-	-	normal	NI
III: 9	34	F	NA	-	-	-	normal	NI
IV: 2	12	M	NA	-	-	-	normal	NI

Table 11 Clinical features of family A

M- male, F-female, QTc – corrected QT interval, SCD- sudden cardiac death, VT stim-
Ventricular tachycardia stimulation test, NI-not indicated, NA-not available

The proband, III: 8, presented with cardiac arrest in the community. Cardiopulmonary resuscitation was given by paramedics and she was taken to the local hospital, where she was fully resuscitated. 12 lead ECG showed abnormalities in the ST segment (figure 25). She had coronary angiography which showed normal coronary arteries and left ventricular angiogram which showed normal function and no wall motion abnormalities. Subsequent transthoracic echocardiogram and cardiac MRI showed structurally normal heart. Further electrophysiological studies were performed to assess her risk of subsequent ventricular tachyarrhythmias. Ventricular tachycardia was easily induced at standard protocol (appendix G). She was stratified as having high risk of future ventricular tachyarrhythmias. An implantable cardioverter defibrillator was implanted.

Subsequently, other members of the family were investigated using 12 lead ECGs. The ECGs of 4 family members were not available for analysis. A total of 7 individuals had abnormal ST segment changes in the resting ECG (figure 26). Electrophysiological testing confirmed inducible ventricular tachycardia in all 7 individuals which suggested high risk of ventricular arrhythmias and therefore internal cardioverter defibrillators were implanted. The 12 lead ECGs of the affected and some of the unaffected family members are shown in appendix E.

Exercise treadmill tests done on subjects II: 1, II: 3, II: 5 and II: 7 (standard Bruce protocol) were negative for symptoms and ECG changes and normal heart rate and blood pressure response were obtained. There were no exercise inducible arrhythmias.

Twenty four hour ECG monitoring performed on subjects II: 1, II: 3, II: 5 and II: 7 did not reveal arrhythmias and subjects were asymptomatic for the duration of the test.

Transthoracic echocardiography performed on the 7 affected subjects showed normal parameters (appendix F). The cardiac chambers and valves appeared normal in size and function. There was no evidence of hypertrophy of the septum or any of the cardiac chambers.

Flecainide challenge test was performed on subject IV: 1. (The protocol used for Flecainide challenge test is shown in appendix H). The pattern of ST segments following infusion of flecainide, a sodium channel blocker, was observed. Following flecainide infusion, the ST segment depression present in the resting ECG became accentuated (figures 27 and 28).

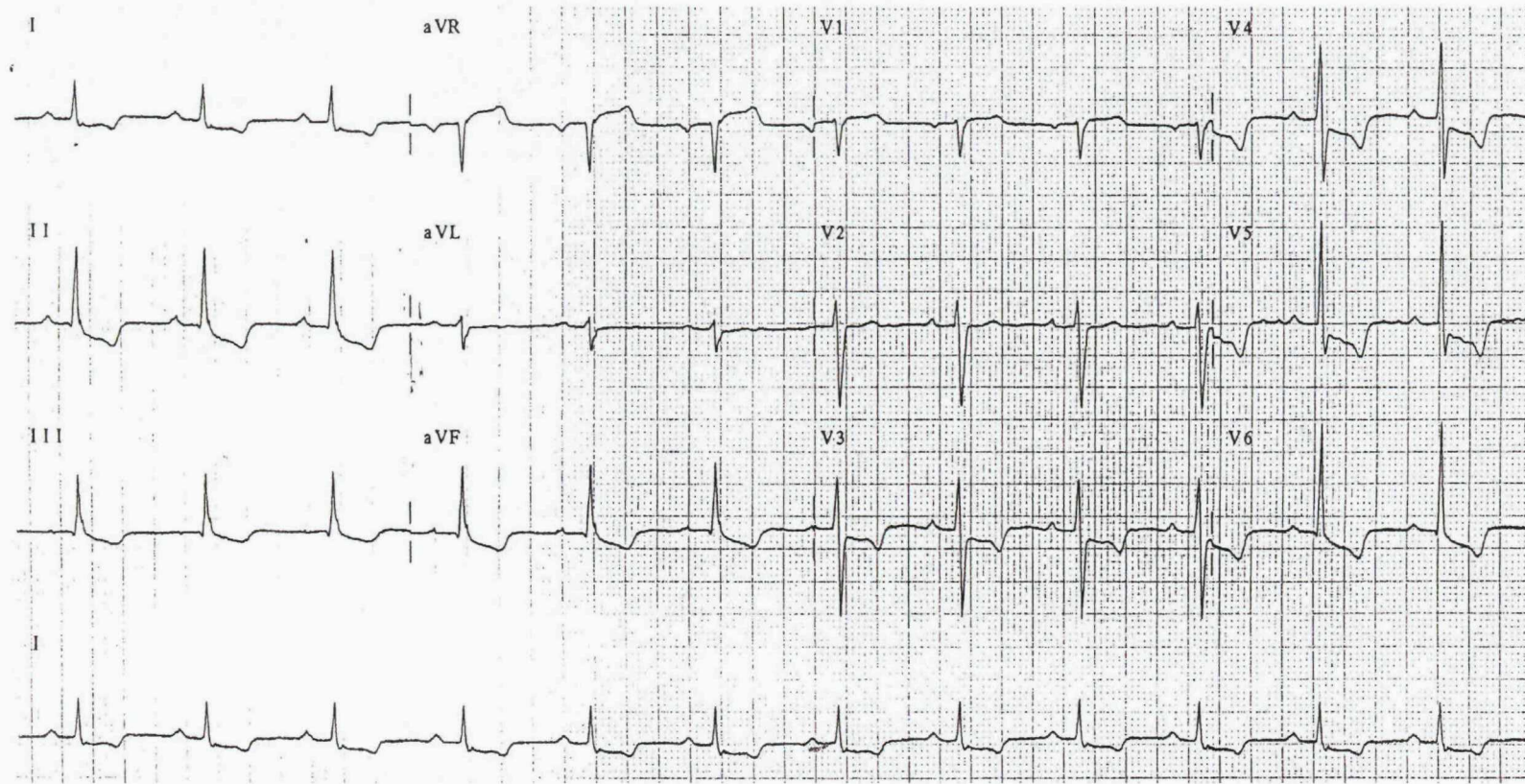


Figure 24 Twelve lead ECG of proband in Family A

Twelve lead ECG of the proband (III: 8) shows ST depression and T wave inversion in the anterior (I, V3-V6) and inferior (II, III, aVF) leads. The changes are not typical of cardiac ischaemia. Although left ventricular hypertrophy (LVH) can cause similar ECG, there was no evidence of LVH on echocardiography. Therefore, the ECG abnormalities were considered to be due to abnormalities in cardiac repolarisation.

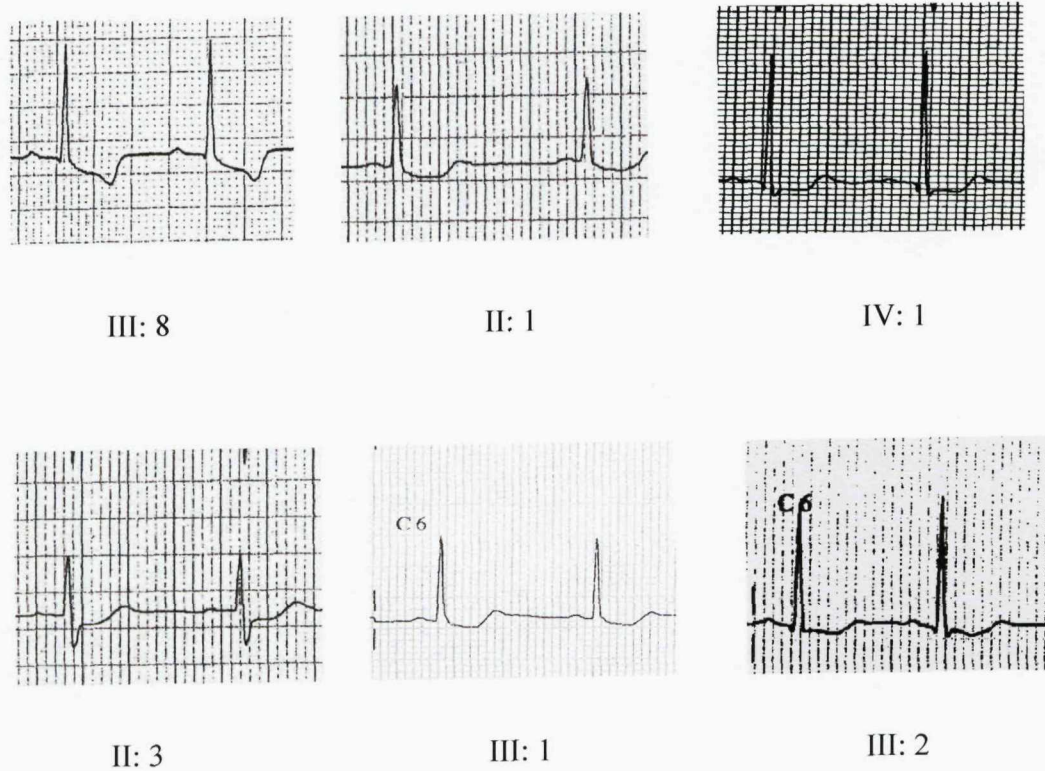


Figure 25 ECG of affected members of family A

Single lead (chest lead 6) ECG of 6 affected members of family A shows ST segment changes, suggesting abnormalities in the cardiac repolarisation. The subject number is identified at the bottom of each ECG.

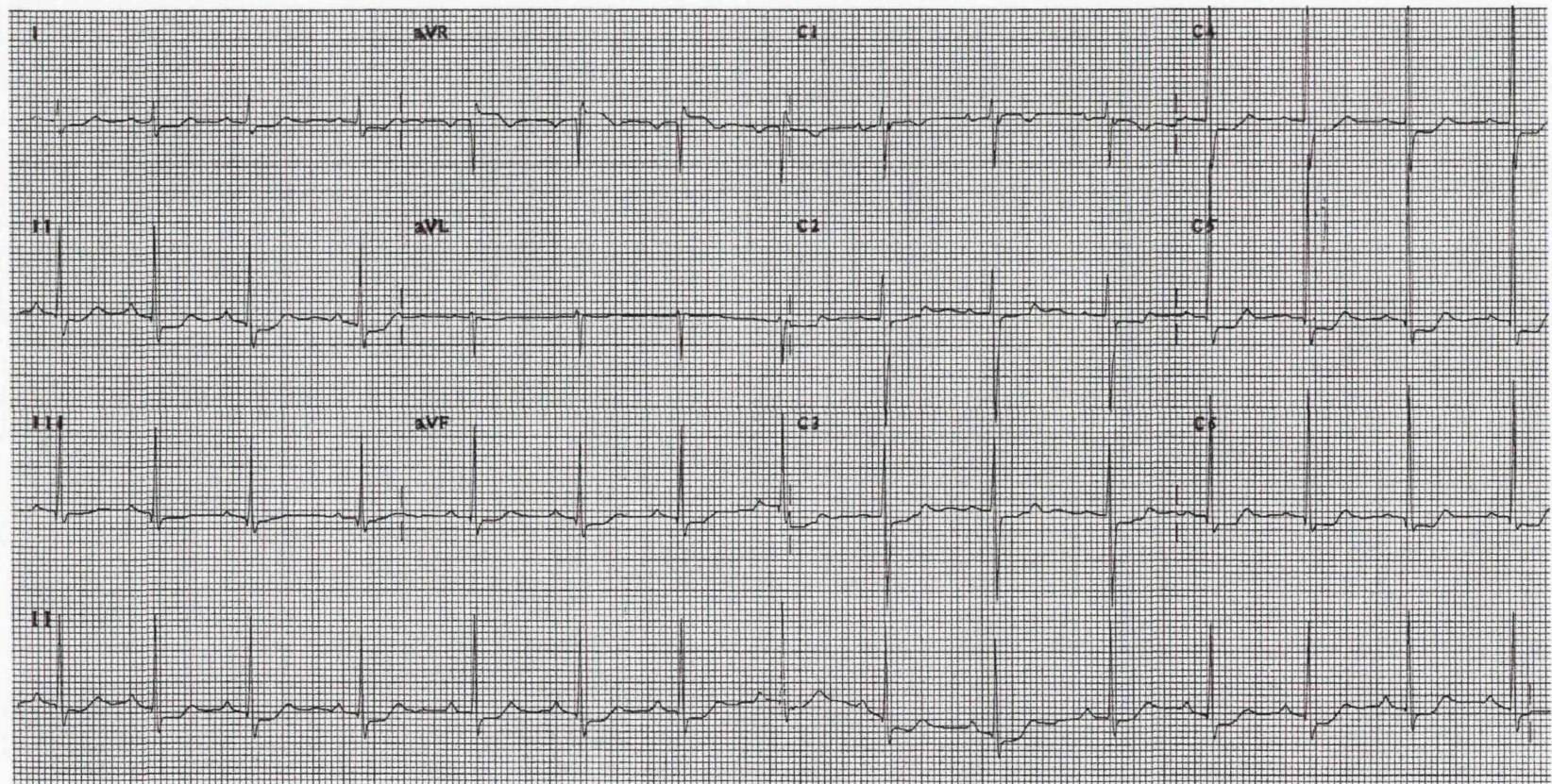


Figure 26 Resting ECG of IV: 1

12 lead ECG shows 1 mm ST segment depression in leads I, II, aVF, V2-V6 prior to Flecainide infusion.

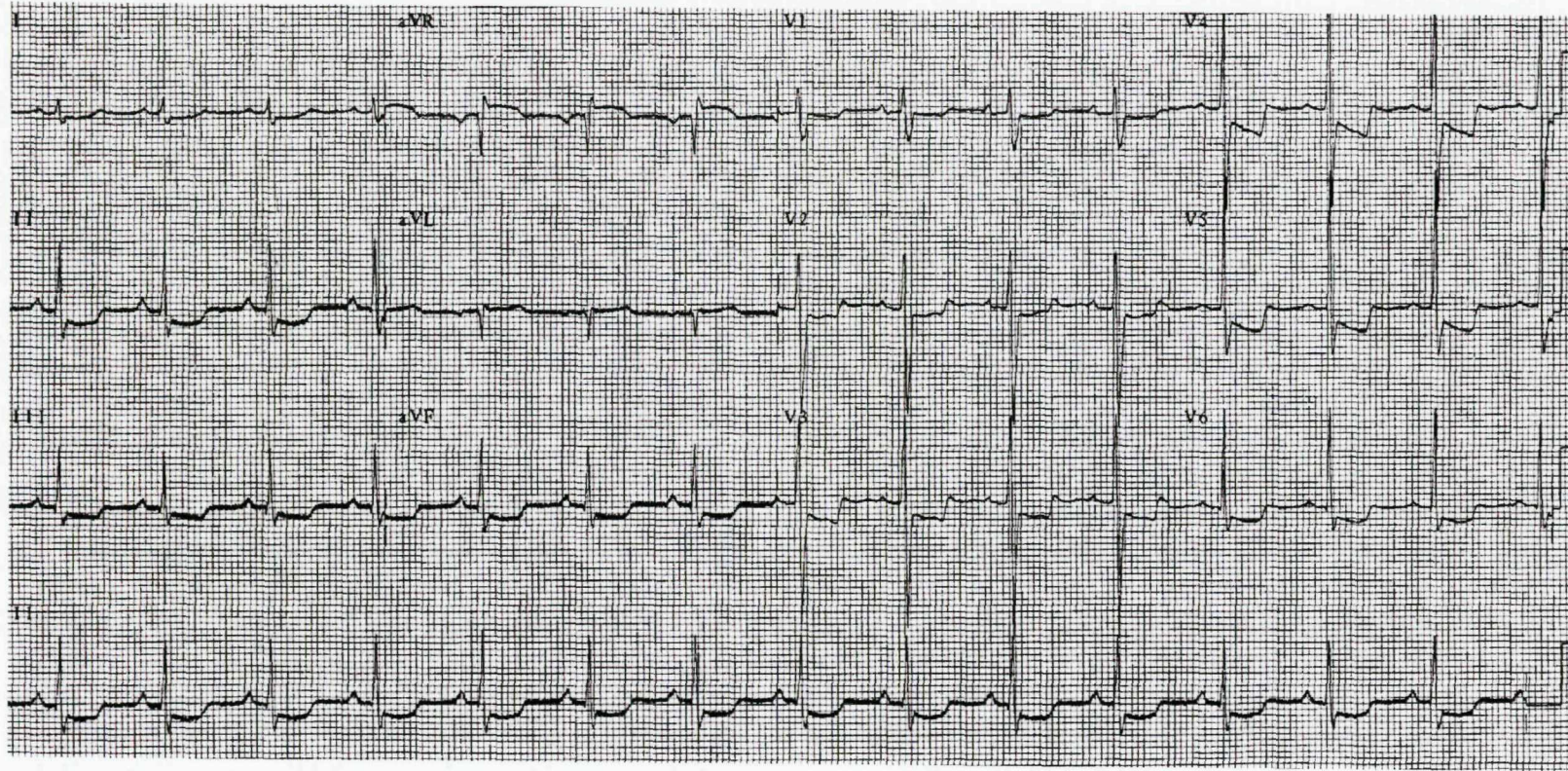


Figure 27 ECG of IV: 1 post Flecainide infusion

12 lead ECG in subject IV: 1, one minute post Flecainide infusion shows worsening ST-T wave changes in all the leads.

3.1.2 Genotyping

The main genes, mutations in which cause ventricular tachyarrhythmias and sudden cardiac death in patients with apparently normal cardiac structure, were analysed. These were the genes responsible for LQT syndrome (*KCNQ1*, *KCNH2*, *SCN5A*, *ANKB*, *KCNE1* & *KCNE2*), the *RyR2* gene responsible for Catecholaminergic Ventricular tachycardia and the *TNNT2* gene responsible for Hypertrophic cardiomyopathy.

Microsatellite markers were chosen for genotyping. Where possible, markers from Genome Database (GDB) and Genethon were used. When suitable published markers were not available, markers were designed using Primer Select software (see 2.2.5). Markers were labelled with fluorescent dyes. PCR was performed according to standard procedures (see 2.2.3) using the markers and the DNA samples followed by agarose gel electrophoresis (see 2.2.4). The appearance of bands at the expected size range confirmed whether the PCR had worked. Once confirmed, the PCR product was run on polyacrylamide gel (see 2.1.2.2) and gene-scan analysis was performed using ABI 377 and Genescan analysis software (Applied Biosystems Inc, see 2.2.6). The allele sizes obtained were plotted on the pedigree. Some markers did not work despite changing the PCR conditions. It was sometimes possible to work out which allele was obtained from the mother and the father. In situations where more than one marker gave allele sizes, thus it was sometimes possible to work out the haplotypes. Where possible, the paternal allele was written first, then the maternal allele.

3.1.2.1 LQT1

KCNQ1 (KvLQT1) is located at 2,430,350-2,834,048 bp on chromosome 11. Polymorphic microsatellite markers KvLQT1CA86 (located at 2,224,259-2,224,334 bp) and D11S4088 (located 2,719,260-2,719,466 bp) were chosen. The marker D11S4088 was intra-genic and the marker KvLQT1CA86 was located within 2 Mb of the gene. The positions of the gene and markers are obtained from the Human Genome NCBI Build 35.1. D11S4088 did not work despite altering the annealing temperatures and magnesium concentrations.

The allele sizes obtained for family A, for all the markers are shown in appendix D. The gene-scan tracing obtained with the marker KvLQT1CA86 is shown in figure 29. A subject who is homozygous for an allele will show a single peak on the tracing and a subject who is heterozygous for the alleles will show two peaks. The PCR amplification of a microsatellite locus typically produces a minor product peak shorter than the corresponding main allele peak. If the microsatellite marker is a dinucleotide repeat as in KvLQT1CA86, the minor product peak is usually 2 bp shorter than the main allele peak. This is referred to as the stutter peak and is shown in figure 29.

A common allele for the marker KvLQT1CA86 did not segregate with the disease in the family (figure 30). Since a recombination event so close to the locus is unlikely, this locus was considered excluded as containing the mutation responsible for the phenotype in this family.

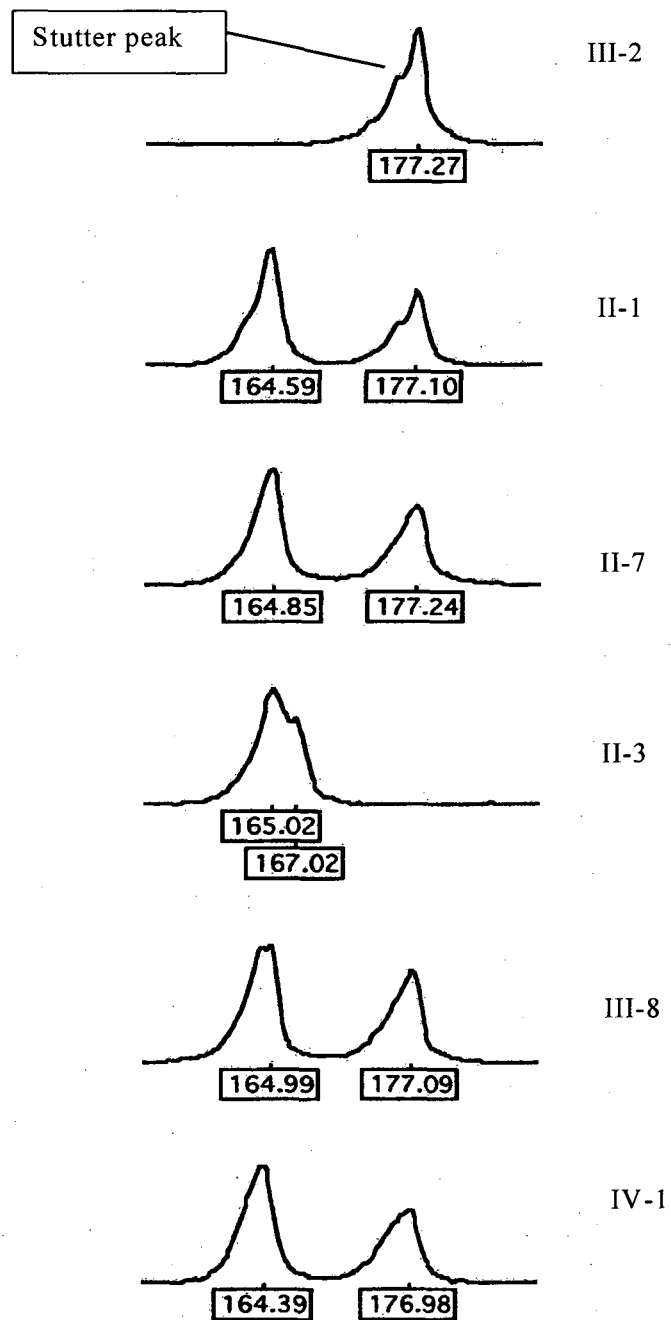


Figure 28 An example of a gene-scan trace

Figure shows the allele sizes obtained for subjects III: 2, II: 1, II: 7, II: 3, III: 8 and IV: 1 in family A with the marker KvLQT1CA86. For example, subject III: 2 is homozygous for the allele 177 and subject II: 1 is heterozygous for the alleles 165 and 177. A stutter peak is shown in the tracing for III: 2. The allele sizes for subject III: 1 was not obtained in this tracing and the gene-scan had to be done separately for this subject (tracing not shown).

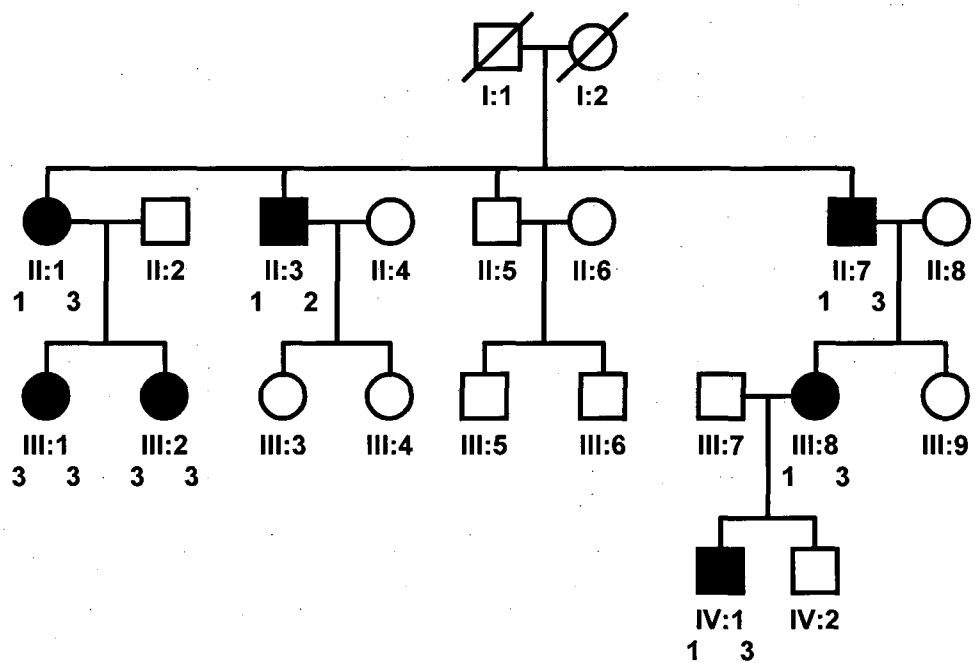


Figure 29 Segregation analysis of LQT1 marker in family A

Numbers below the subjects refer to the allele size obtained for the subject following genotyping with the marker KvLQT1CA86. Individuals III: 1 and III: 2 do not share an allele common with II: 3, and therefore excludes this locus (assuming no recombination event has taken place).

3.1.2.2 LQT2

KCNH2 is located between bp 149,956,934 and 149,989,899 on chromosome 7. D7S2439 is located at 148,634,628-148,634,782 bp, telomeric to the gene and within 1Mb. The positions of the gene and markers are obtained from the Human Genome NCBI Build 35.1. The allele sizes obtained for the marker were plotted on a pedigree and segregation analysis showed no commonly inherited alleles among all the affected members (figure 31). Since recombination was unlikely to occur so close to the gene, the locus was considered excluded as having the causative mutation in this family.

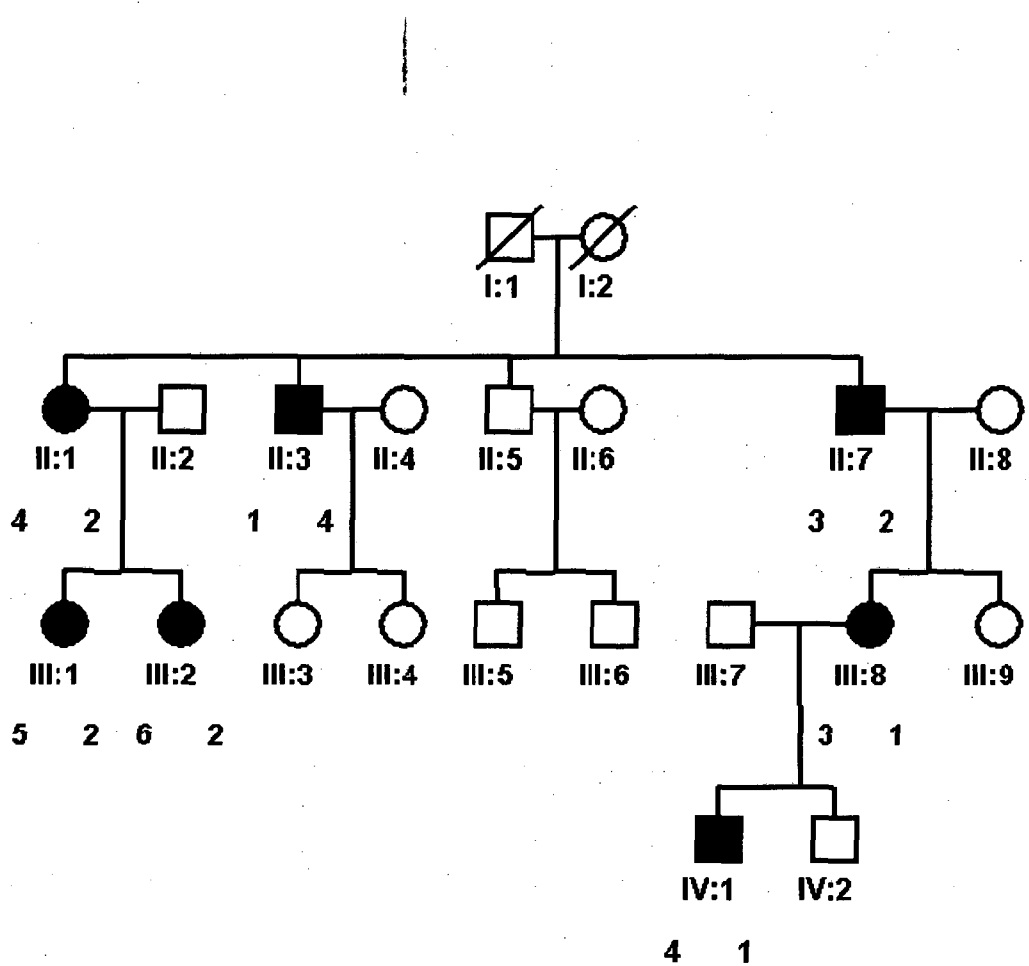


Figure 30 Segregation analysis of LQT2 marker in family A

There are no common alleles shared by all affected members for marker D7S2439. The locus is thus excluded in this family (assuming no recombination event has taken place).

3.1.2.3 LQT3

SCN5A is located at 38,564,556-38,666,166 base pairs on chromosome 3. The microsatellite marker SCN5AGTExon16, located at 38,587,884 bp is intragenic. The positions of the gene and markers are obtained from the Human Genome NCBI Build 35.1. There was no commonly inherited allele among the affected subjects (figure 32). Since a recombination event was unlikely, the locus was considered excluded.

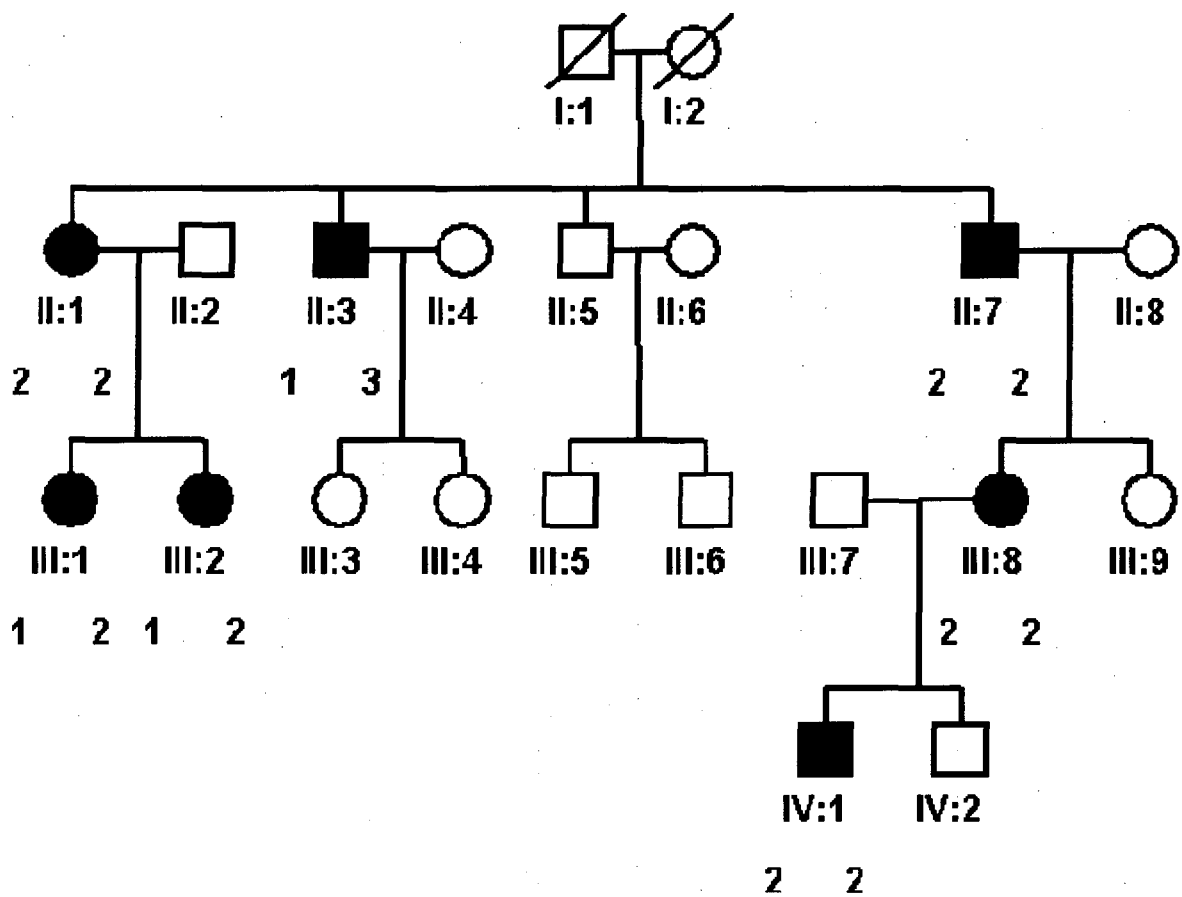


Figure 31 Segregation analysis of LQT3 marker in family A

The allele sizes obtained for the marker SCN5AGTExon16 are shown. The locus was excluded as containing the mutation responsible for the phenotype in family A, since there was no commonly inherited allele among the affected subjects (assuming no recombination event has taken place).

3.1.2.4 LQT4

ANKB is located at base pairs 114,429,690-114,762,091 on chromosome 4. Microsatellite marker D4S1611 was located at 114,906,243-114,906,519 base pairs. Microsatellite markers TG129ANK2 and TA226ANK2 were also chosen within 1 Mb of the gene. The positions of the gene and markers are obtained from the Human Genome NCBI Build 35.1. Genescan analysis did not show commonly inherited allele among the affected members (figure 33). Since the markers were very close to the gene, recombination was unlikely to occur and therefore the locus was considered excluded as containing the mutation causing the phenotype in family A.

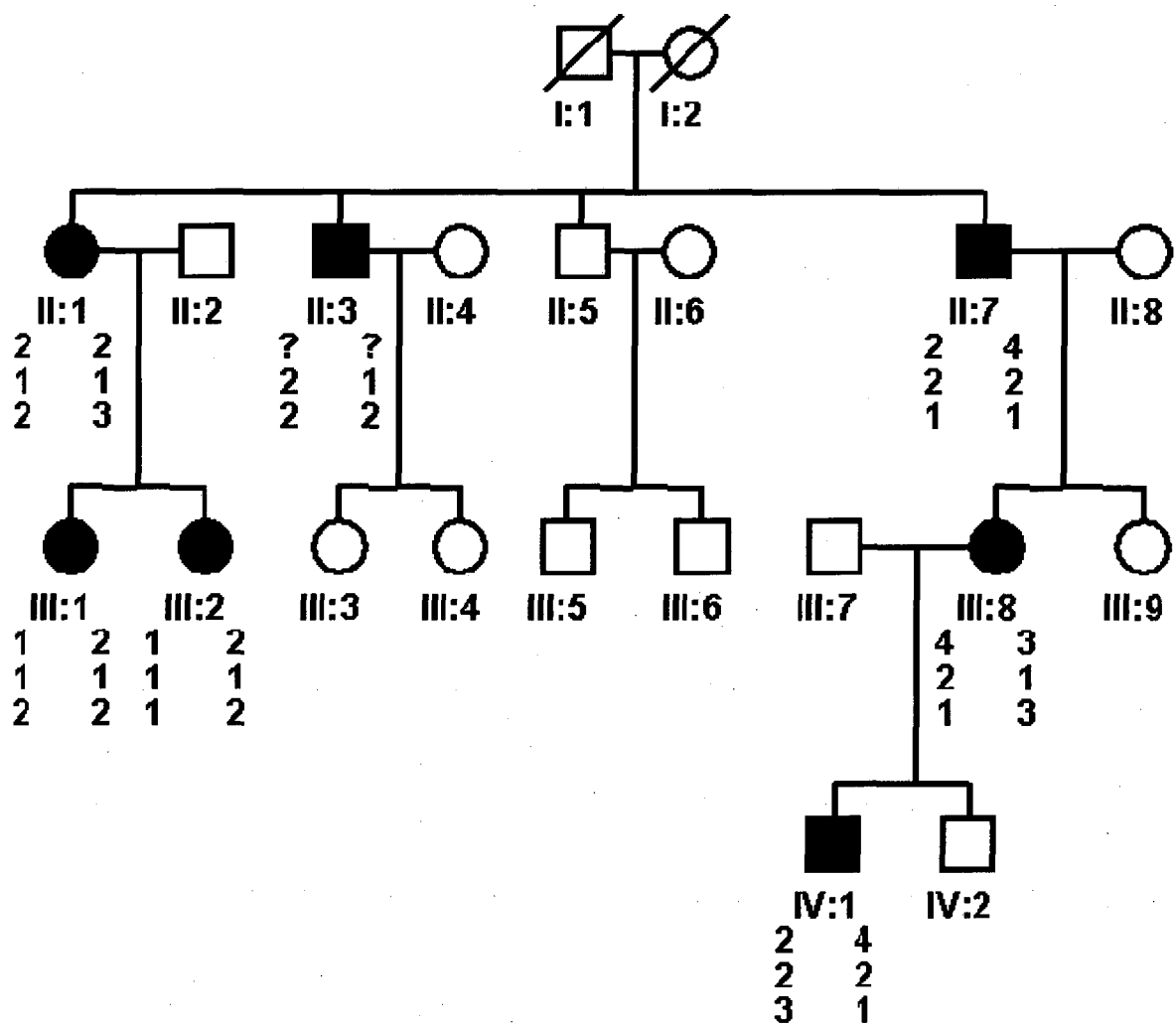


Figure 32 Segregation analysis of LQT4 markers in family A

The allele sizes obtained for the markers TG129ANK2, TA226ANK2 and D4S1611 are shown. Absence of commonly inherited allele among the affected subjects excluded the locus as containing the mutation of interest in family A (assuming no recombination event has taken place).

3.1.2.5 LQT5 & LQT6

KCNE1 and *KCNE2*, mutations in which lead to LQT5 and LQT6 are located very close to each other. The location of *KCNE1* is at 34,739,384-34,804,968 base pairs and *KCNE2* is at 34,658,193-34,665,310 base pairs on chromosome 21. The microsatellite marker AC926KCNE1&2 is located at 35,187,312 base pairs. The marker D21S1920, located at base pairs 34,617,588-34,617,811 did not work, despite altering the annealing temperature and magnesium concentrations during PCR. The positions of the gene and markers are obtained from the Human Genome NCBI Build 35.1. Pedigree analysis showed no commonly inherited allele among the affected family members (figure 34). Since the markers were very close to the loci, recombination was unlikely and therefore the locus was ruled out as having the mutation of interest in family A.

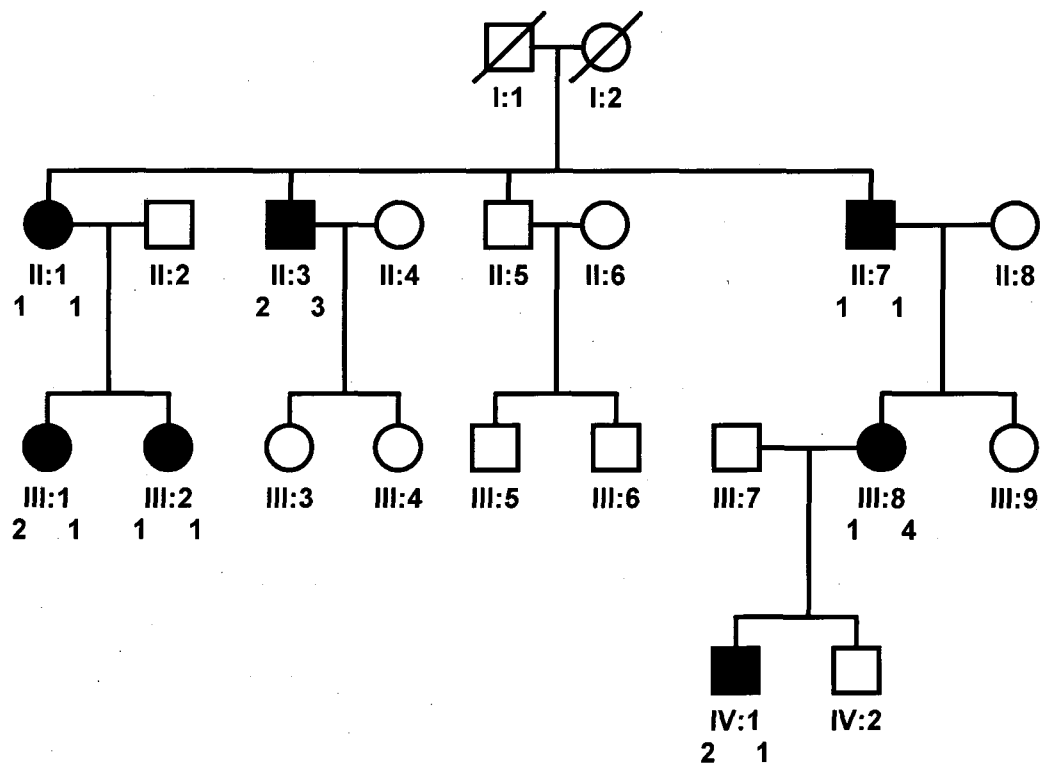


Figure 33 Segregation analysis of LQT5 & LQT6 loci in family A

The allele sizes obtained for the marker AC926KCNE1&2 is shown. The absence of common allele inheritance among the affected subjects ruled out this locus as having the mutation causing the phenotype in family A (assuming no recombination event has taken place).

3.1.2.6 RyR2

RyR2 is located at 233,502,289-234,293,240 base pairs. Three microsatellite markers were used. The marker B44 was located within the gene (233,665,539-233,774,163 bp). The marker D1S2850 (232,927,257-232,927,403 bp) was located close to the gene and telomeric to it. Marker B940 was located further telomeric and still very close to the gene (232,385,621-232,489,228 bp). The positions of the gene and markers are obtained from the Human Genome NCBI Build 35.1.

Commonly inherited alleles among the affected members in family suggest that linkage to the locus cannot be excluded (figure 35).

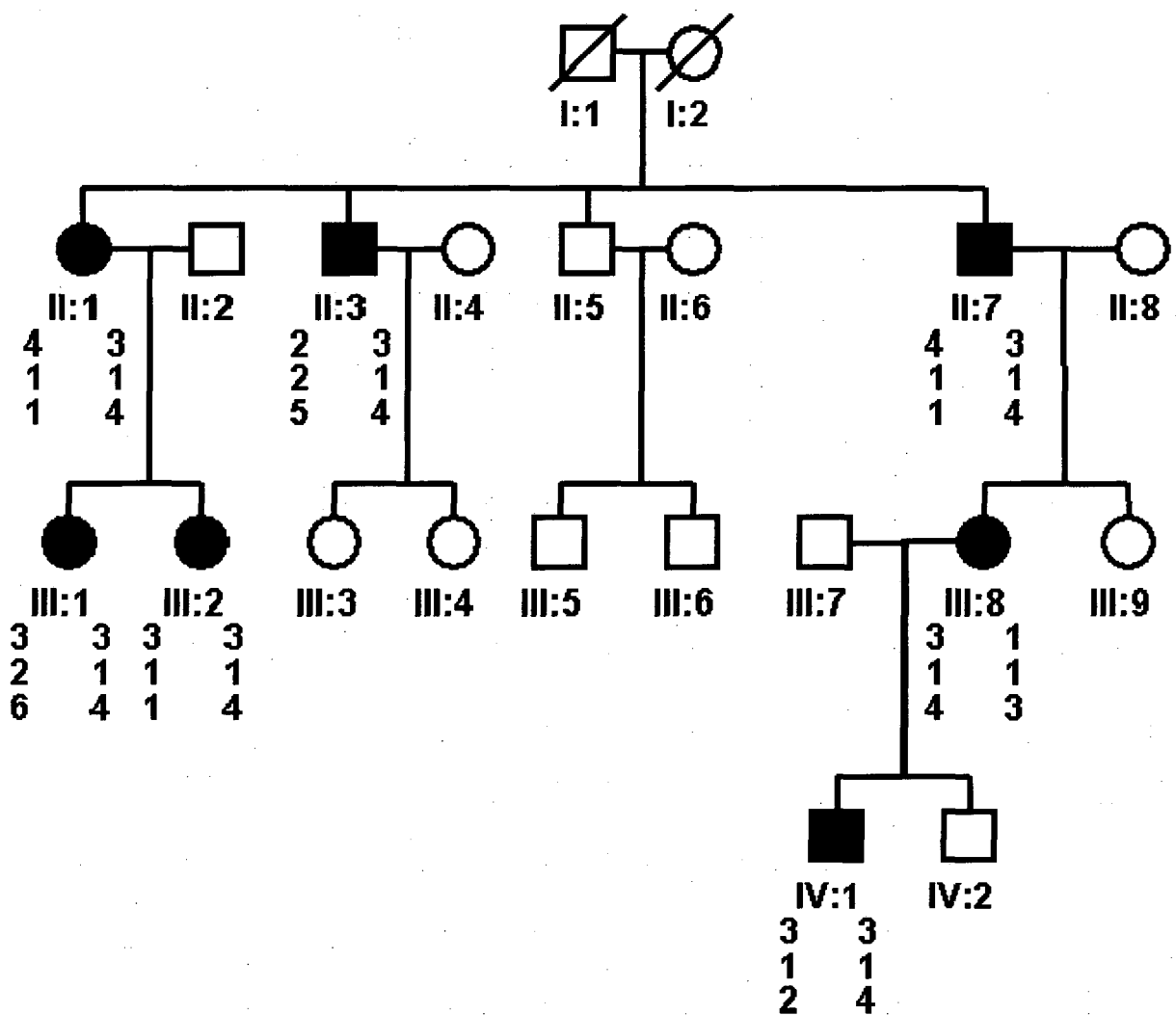


Figure 34 Segregation analysis of RyR2 markers in family A.

The allele sizes obtained for markers D1S2850, B940 and B44 are shown in the same order. The commonly inherited alleles among the affected subjects suggest that linkage to this locus in family A could not be excluded.

3.1.2.7 TNNT2

Microsatellite markers D1S2764 and D1S306 were within 1Mb of the TNNT2 locus. D1S2764 was located at 199,852,930-199,853,074 bp and D1S306 was located at 199,671,611-199,671,877 bp on chromosome 1. The positions of the gene and markers are obtained from the Human Genome NCBI Build 35.1. Following gene-scan analysis, the genotyping data suggested common allele inheritance among the affected subjects (figure 36). Therefore this locus cannot be excluded in this family.

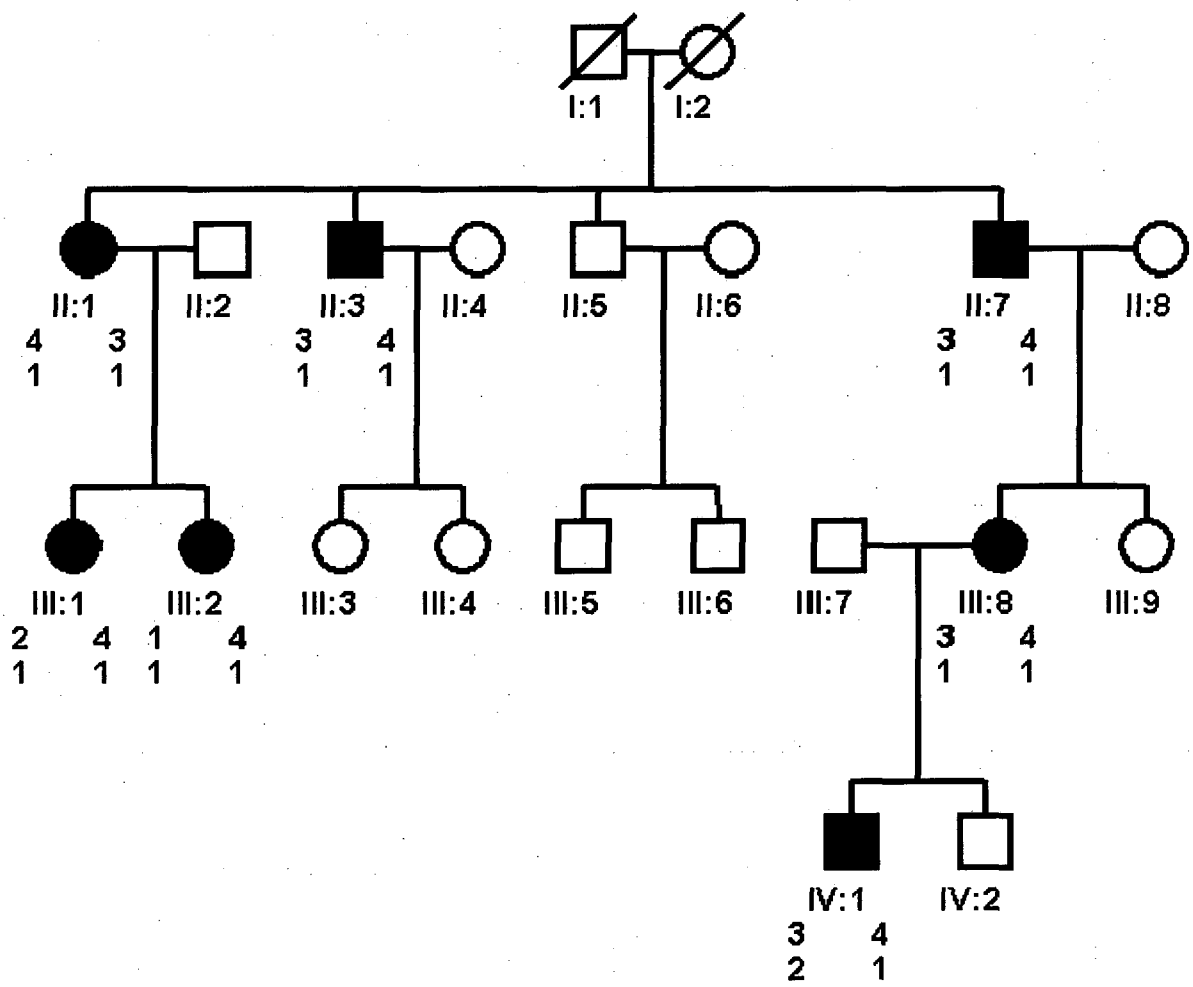


Figure 35 Segregation analysis of TNNT2 markers in family A

The allele sizes obtained with microsatellite markers D1S2764 and D1S306 are shown. A common allele segregates with the disease. Therefore, linkage to this locus in family A could not be excluded.

3.1.3 Direct sequencing of TNNT2

TNNT2 and *RyR2* could not be excluded after genotyping. Mutations in *TNNT2* can cause cardiomyopathy with minimal or absent hypertrophy on echocardiography and can manifest with similar ECGs as in family A. *RyR2* mutations were less likely to present with the ECG changes found in family A, and therefore *TNNT2* was prioritized for mutation screening.

3.1.3.1 Genomic structure of TNNT2

TNNT2 is composed of 17 exons (figure 37) over 17 kb and gives rise to 4 isoforms (cTnT1-4). These isoforms are expressed in the fetal, adult and diseased heart in varying proportions¹⁵⁶. The cDNAs which correspond to the 4 isoforms differ by the variable inclusion of a 15- and a 30-nucleotide exon at the 5' end of the coding region. cTnT1 contain both peptides encoded by the 30- and 15-nucleotide exons, cTnT2 contains the peptide coded by the 30 nucleotide exon alone, cTnT3 contains a 5-residue peptide and is the major isoform in the human adult heart. cTnT4 lacks both the 15- and 30-nucleotide sequences⁹⁵.

The first exon of *TNNT2* is the 5' untranslated region (UTR). The UTR was not sequenced since the presence of a mutation in it was thought to be less likely than a mutation in the coding exons or intron-exon boundaries. Exons 2 to 17 of subject II: 1 was sequenced. The exons of other affected family members were sequenced when variations were observed in the sequences of II: 1. This was based on the prediction that the pathologic mutation should be present in all affected individuals in the family.

Oligonucleotide primers were designed that crossed the intron exon boundaries of each of the 16 transcribed exons of *TNNT2*. Exons 3 and 4 were small and the intervening intron 3 only had 98 nucleotides. Therefore exons 3 & 4 were co-amplified as a single product. The PCR products were screened by automated cycle sequencing using ABI 377 sequencer and corresponding forward or reverse primers were used.

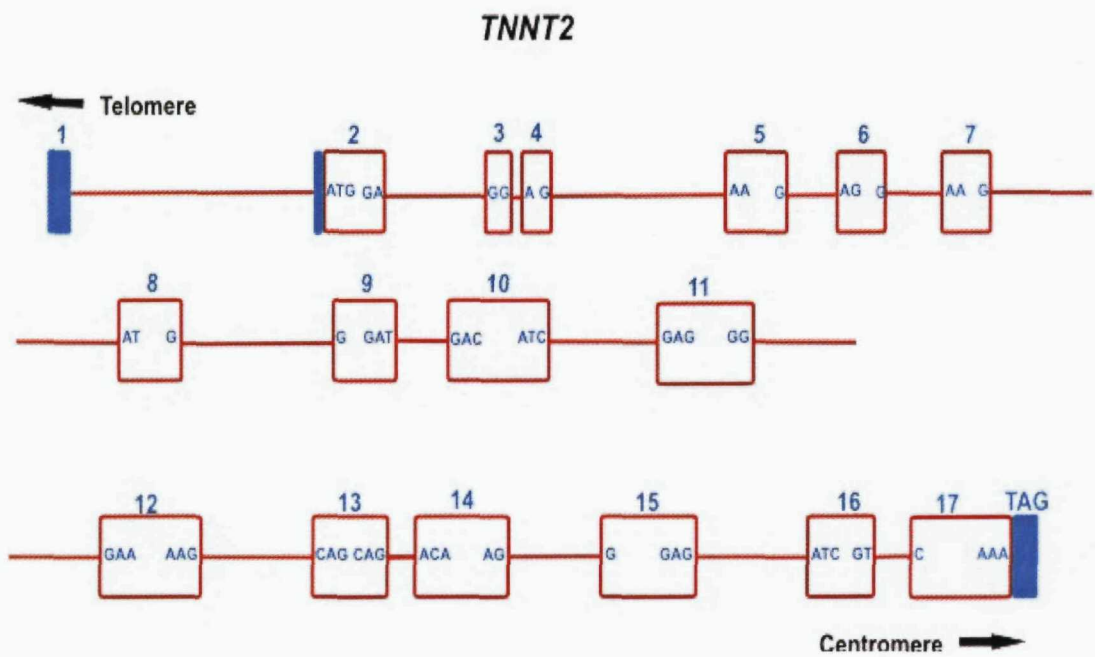


Figure 36 Genomic structure of *TNNT2*

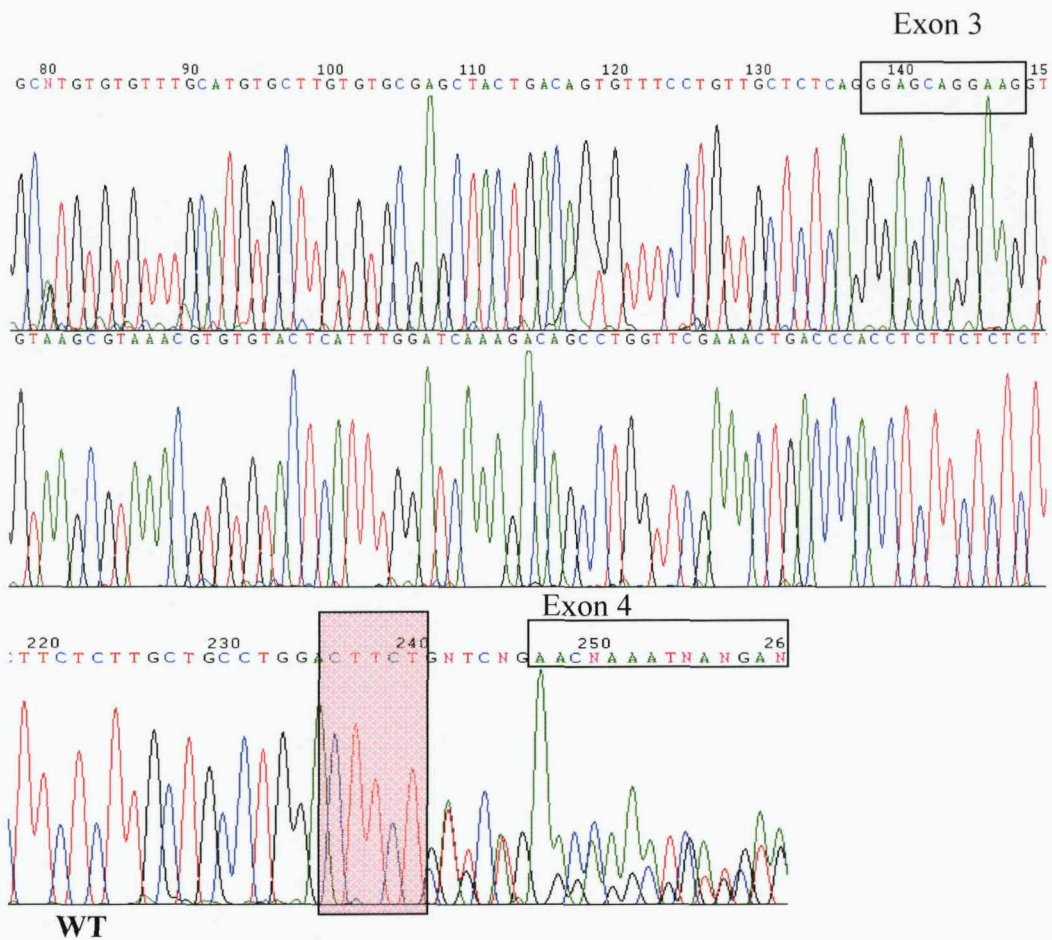
Figure shows genomic structure of troponin T with 17 exons and the intron-exon boundaries. The exon and intron sizes have been drawn to proportion. Non- coding regions are shaded in blue. Exon 1 is the 5' UTR and codons 2-17 are the coding exons.

3.1.3.2 Results of direct sequencing

A 5-base pair Insertion in intron 3

The analysis of sequence traces of exons 3 and 4 showed a 5 bp insertion in intron 3, in subject IV: 1 (figure 38).

The analysis of sequence traces of exons 3 and 4, in subjects II: 1, II: 7 and III: 8 did not reveal this 5 bp insertion, and therefore the change seen in IV: 1 is unlikely to be the genetic cause for the phenotype in this family.



GGAGCAGGAAGgttaagcgtaaacgtgtactcattggatcaaagacagcctgggtcgaaa
ctgaccacccacccctttctctttctgtgcctggagagcagAAGCAGCTGTTGAgt

Subject IV: 1

GGAGCAGGAAGgttaagcgtaaacgtgtactcattggatcaaagacagcctgggtcgaaa
ctgaccacccacccctttctctttctgtgcctggacttctgagcagAAGCAGCTGTTGAgt

Figure 37 CTTCT insertion in intron 3 of *TNNT2*

The sequence trace of exon 3, intron 3 and exon 4 in subject IV: 1 is shown at the top and the CTTCT insertion polymorphism is boxed and highlighted. The sequence of the wild type (WT) and subject IV: 1 are also shown. Exonic sequences are written in capital letters. The full sequence of the exons with the intron-exon boundaries are shown in Appendix J.

Single base substitution in exon 9

Figures 39 and 40 show the results from the analysis of sequence trace of exon 9 in subject II: 1. A single nucleotide substitution within exon 9 is shown. This resulted in a change in the nucleotide sequence A/G which did not cause a change in the coded aminoacid. Because of the A/G change, the resulting codon becomes TCA or TCG and both code for serine. This SNP was not identified in two other affected subjects of the same family (III: 8 and IV: 1) excluding it as the cause of the phenotype in this family.

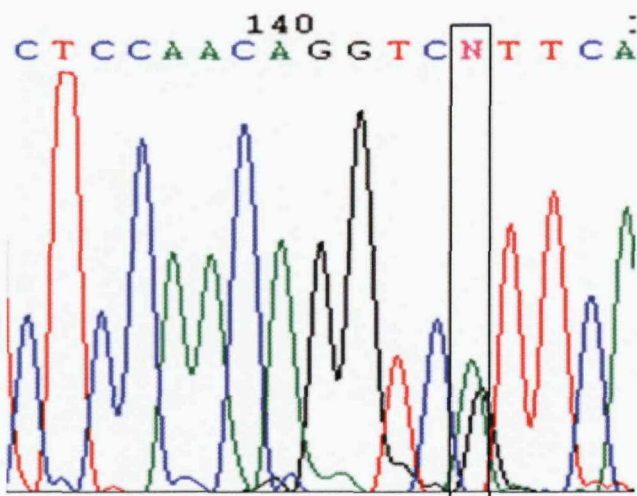


Figure 38 Forward sequence of exon 9 of *TNNT2* in subject II: 1

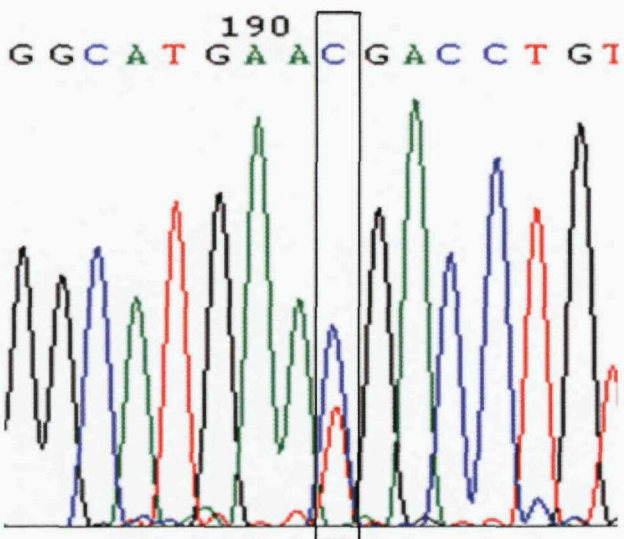


Figure 39 Reverse sequence of exon 9 of *TNNT2* in subject II: 1

Figure 33 shows forward sequence of exon 9F showing single base substitution at position 144 (A/G polymorphism) in subject II: 1. Figure 34 shows reverse sequence of exon 9 in subject II: 1, with the same change.

3.2 INVESTIGATION AND RESULTS OF FAMILY B

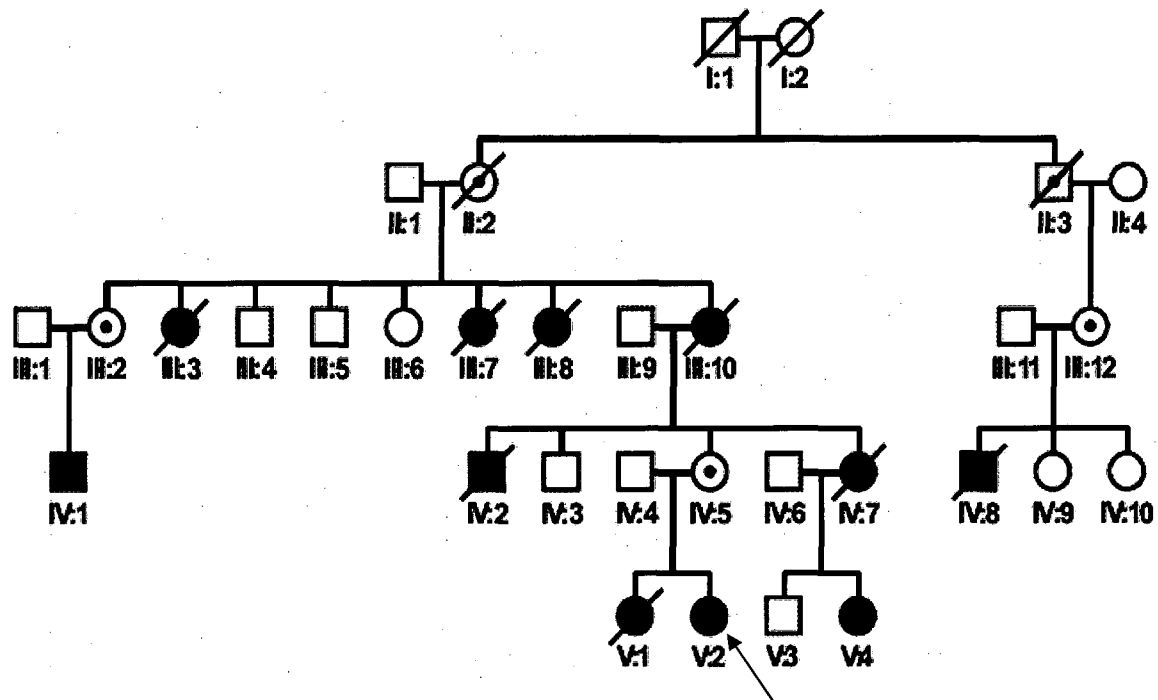
3.2.1 Family B ascertainment

Family B was ascertained via the Regional Clinical Genetics Service. A pedigree of family B is shown in figure 41. Eight members of the family had sudden cardiac death. The proband was V: 2, who presented at the age of 18 following a blackout. Her sister had sudden cardiac death at 19 years of age and her maternal aunt and uncle had sudden cardiac death at a similar age. Subjects III: 3, III: 7, III: 8, III: 10, IV: 2, IV: 7 and V: 1 also had sudden cardiac death. Subjects IV: 2 and IV: 7 died suddenly while swimming. Subjects IV: 1 and V: 4 suffered from blackouts, suggestive of cardiac syncope.

III: 2 is a carrier since her son is affected. III: 12 is a carrier since her son had sudden cardiac death. IV: 5 is a carrier since her daughter is affected and her mother had sudden cardiac death. II: 2 is a carrier since four of her daughters had sudden cardiac death and one grandson is affected. II: 3 is a carrier since her daughter is a carrier and her grandson had a sudden cardiac death.

Resting ECGs of the affected family members were normal (figure 42). Ambulatory ECG monitoring of IV: 1, V: 2 and V: 4 revealed episodes of nonsustained VT correlating with patient reported symptoms of palpitations. These individuals were classified as having a high risk of sudden cardiac death and therefore had implantable cardioverter defibrillators.

Exercise ECG testing done on subjects IV: 1 and V: 2 did not reveal exercise induced arrhythmias or underlying ischaemia. Subjects IV: 1, V: 2 and V: 4 had echocardiograms that showed a structurally normal heart (data not shown).



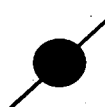
unaffected male



carrier female



affected male



affected dead female

Figure 40 Pedigree of family B

The figure shows the pedigree of family B. The symbols used are shown below the pedigree. The family members are identified by the numberings below the symbols. The proband V: 2 is arrowed.

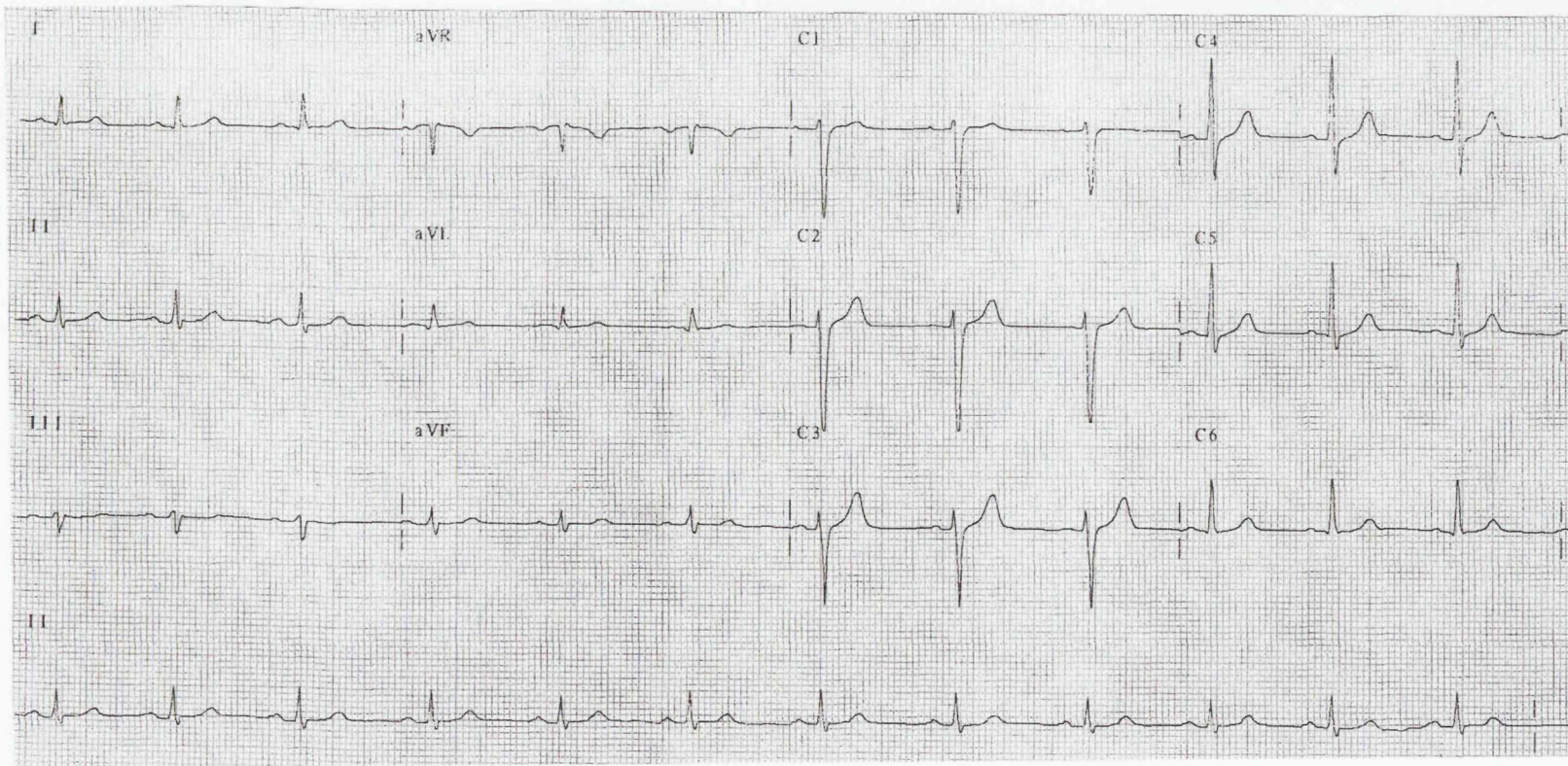


Figure 41 Resting ECG on family member IV: 1

12 lead ECG of the affected subject IV: 1 shows no abnormalities. Corrected QT interval in this ECG is 420 ms, which is within normal limits.



Figure 42 Exercise ECG on family member V: 2

Exercise ECG in V: 2, showing a QTc of 500ms early in the test. There were no significant ST- T wave changes or arrhythmias. Measurement of QTc at fast heart rate is unreliable and the QT measurement of 500 ms is not significant.

3.2.2 Genotyping

The DNA samples of 5 affected individuals (III: 2, III: 12, IV: 5, V: 2 and V: 4) in the family were available. Exercise testing in individual V: 2 showed QT prolongation (QTc of 500 ms) early on in the exercise. Therefore *KCNQ1*, *KCNH2*, *SCN5A*, *ANKB*, *KCNE1* and *KCNE2* were candidate genes. *RyR2* mutations which lead to catecholaminergic polymorphic ventricular tachycardia is also known to produce sudden death in families, especially with exertion and often with a normal ECG and structurally normal heart. Thus *RyR2* was a strong candidate gene. *TNNT2* mutations can lead to minimal or no hypertrophy of the heart on investigations, but produce ventricular arrhythmias. Therefore *TNNT2* was included as a candidate gene.

Microsatellite markers were chosen within 1 Mb of the candidate gene. Where possible, markers from Genome Database (GDB) and Genethon were used. When suitable published markers were not available, markers were designed using Primer Select software (see 2.2.5). Markers were labelled with fluorescent dyes. PCR was performed according to standard procedures (see 2.2.3) using the markers and the DNA samples followed by agarose gel electrophoresis (see 2.2.4). The appearance of bands at the expected size range confirmed whether the PCR had worked. Once confirmed, the PCR product was run on polyacrylamide gel (see 2.1.2.2) and gene-scan analysis was performed using ABI 377 and Genescan analysis software (Applied Biosystems Inc, see 2.2.6). The allele sizes obtained were plotted on the pedigree. Some markers did not work despite changing the PCR conditions. It was sometimes possible to work out which allele was obtained from the mother and the father. In situations where more than one marker gave allele sizes, thus it was sometimes possible to work out the haplotypes. Where possible, the paternal allele was written first, then the maternal allele. The allele sizes obtained for family B are shown in appendix K.

3.2.2.1 LQT1

Swimming appears to be a *KCNQ1* specific arrhythmogenic trigger²⁸ Since cardiac death occurred to two subjects in family B, while swimming, *KCNQ1* was a likely candidate.

KCNQ1 (*KvLQT1*) is located at 2,430,350-2,834,048 bp on chromosome 11. Polymorphic microsatellite markers KvLQT1CA86 (located at 2,224,259-2,224,334bp) and D11S4088 (located at 2,719,260-2,719,466 bp) were chosen. The marker D11S4088 was intra-genic and the marker KvLQT1CA86 was located within 2 Mb of the gene *KCNQ1*. The positions of the gene and markers are obtained from the Human Genome NCBI Build 35.1. D11S4088 did not work despite altering the PCR conditions. Genotyping and pedigree analysis showed that no common allele segregated with the disease and therefore the *KCNQ1* locus was excluded as having the mutation responsible for the phenotype in family B (figure 44).

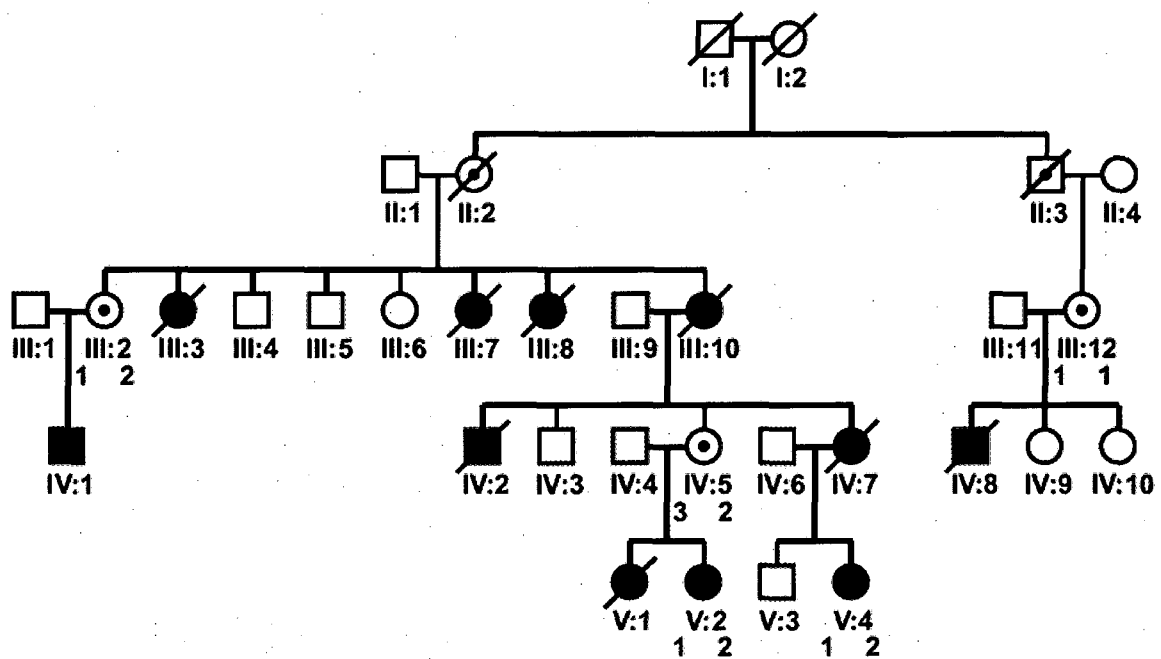


Figure 43 Segregation analysis of LQT1 marker in family B

Figure shows that the affected subjects have inherited a common allele except for subject IV: 5, ruling out this locus as having the mutation responsible for the phenotype in family B (assuming no recombination event has taken place).

3.2.2.2 LQT2

KCNH2 is located at 149,956,934 - 149,989,899 bp on chromosome7. D7S642 (located 150,271,345-150,271,535 bp) is centromeric to the gene and within 1Mb and D7S2439 (located 148,634,628-148,634,782 bp) is telomeric to the gene and within 1Mb. The positions of the gene and markers are obtained from the Human Genome NCBI Build 35.1.

Pedigree analysis did not show segregation of a common allele among the affected members of the family. Since the markers were close to the gene, recombination was unlikely and therefore the locus was considered excluded (figure 45).

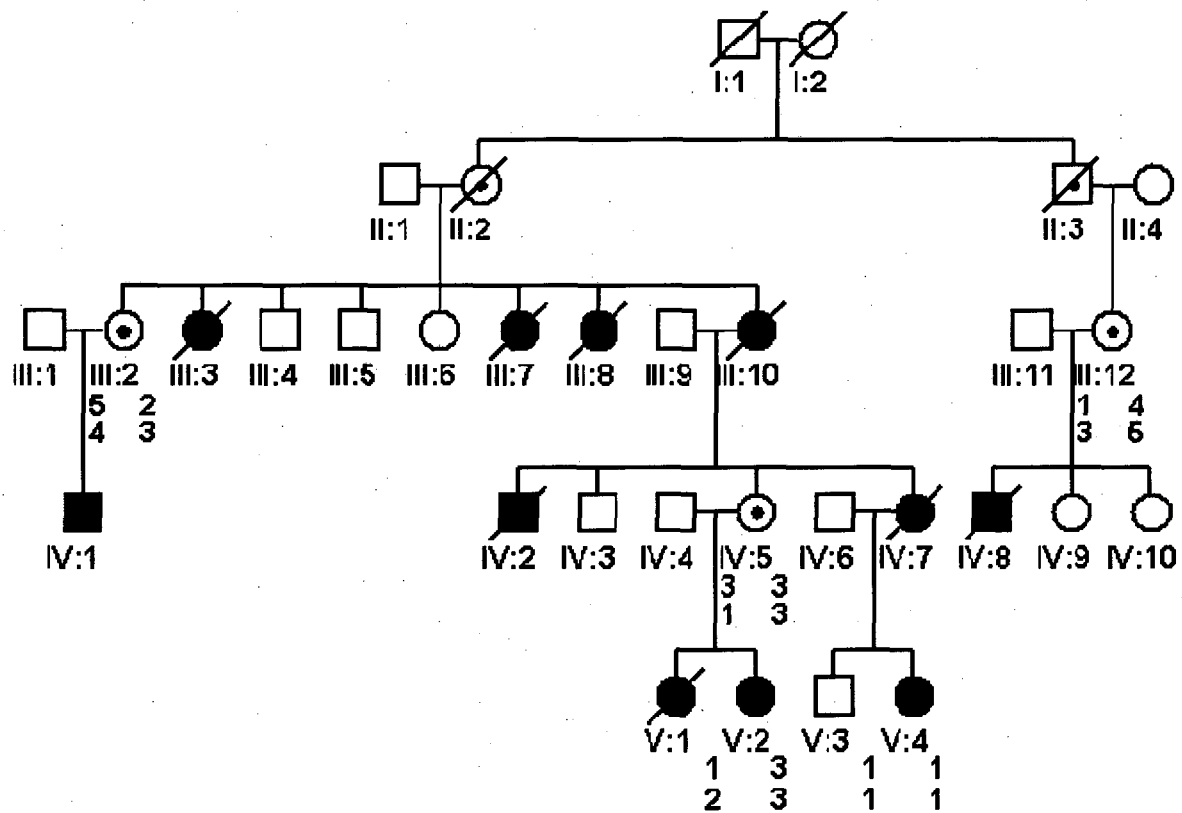


Figure 44 Segregation analysis of LQT2 markers in family B

The alleles obtained for D7S642 and D7S2439 are shown in the same order on the pedigree. There is no segregation of allele with the disease in the family and the locus was thus excluded as having the mutation causing the phenotype in this family (assuming no recombination event has taken place).

3.2.2.3 LQT3

SCN5A is located at 38,564,556-38,666,166 bp on chromosome 3. The markers SCN5ACA132660120 (location 38,626,216 bp) and SCN5AGTExon16 (location 38,587,884 bp) were intragenic. The positions of the gene and markers are obtained from the Human Genome NCBI Build 35.1. PCR with marker SCN5AGTExon16 did not work, despite changing the annealing temperature and magnesium concentration.

A common allele did not segregate with the disease in family B for marker SCN5ACA132660120 (figure 46). Since a recombinant event is very unlikely, this locus was considered excluded as having the mutation causing the phenotype in family B.

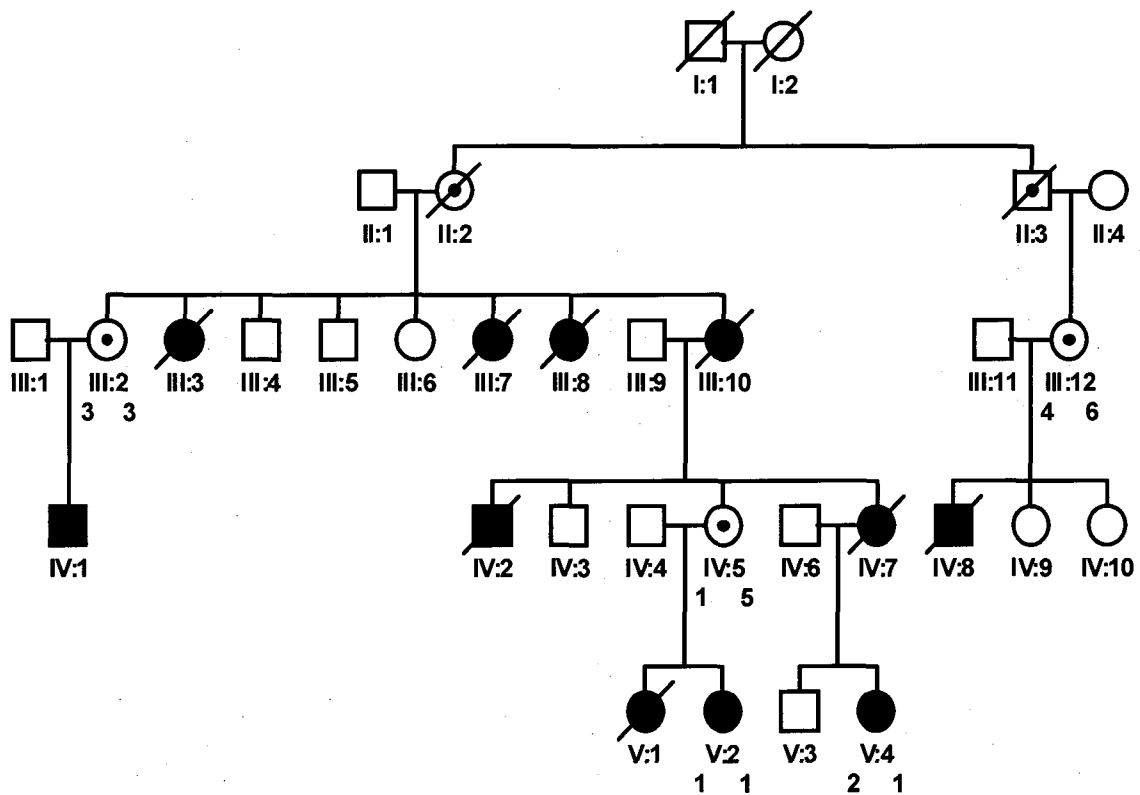


Figure 45 Segregation analysis of LQT3 locus in family B

The alleles obtained with the marker SCN5ACA132660120 are shown. Since there are no common alleles among the affected subjects, the locus was considered excluded (assuming no recombination event has taken place).

3.2.2.4 LQT4

ANKB is located at 114,429,690-114,762,091 bp on chromosome 4. Microsatellite markers TG129ANK2, TA226ANK2 were chosen within 1 Mb of the gene. The positions of the gene and markers are obtained from the Human Genome NCBI Build 35.1. Genescan analysis and pedigree charting showed non-informative allele sizes (figure 47). Further markers were not typed for this locus. Therefore, this locus has not been excluded in family B.

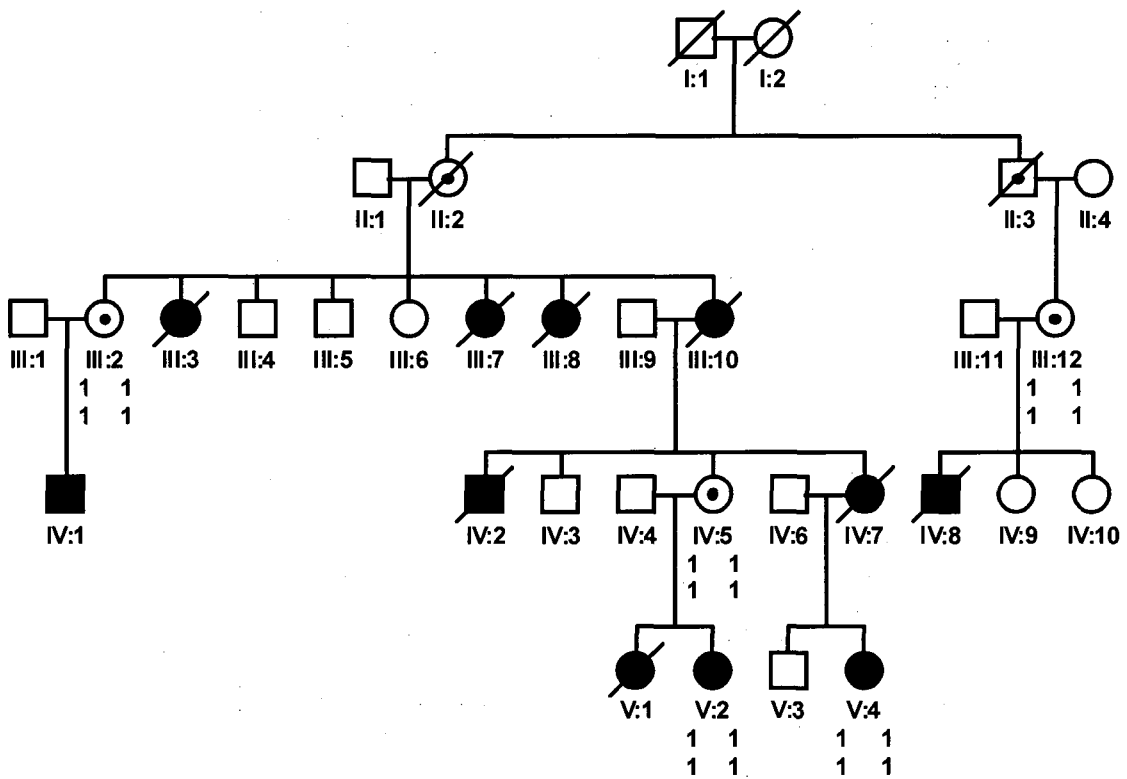


Figure 46 Segregation analysis of LQT4 locus in family B

The allele sizes obtained with the microsatellite markers TG129ANK2 and TA226ANK2 are shown. Non informative data was obtained and therefore this locus has not been excluded in this family.

3.2.2.5 LQT 5&6

KCNE1 and *KCNE2*, mutations in which lead to LQT5 and LQT6 are located very close to each other. *KCNE1* is located at 34,739,384-34,804,968 bp and *KCNE2* is at 34,658,193-34,665,310 bp on chromosome 21. The microsatellite marker D21S1895 is located at 35,272,929-35,273,190 bp, within 1 Mb of the gene. The positions of the gene and markers are obtained from the Human Genome NCBI Build 35.1.

Pedigree analysis did not show common allele inheritance among affected subjects (figure 48). Since the markers were very close to the loci, recombination was unlikely and therefore the locus was ruled out as having the mutation of interest in family B.

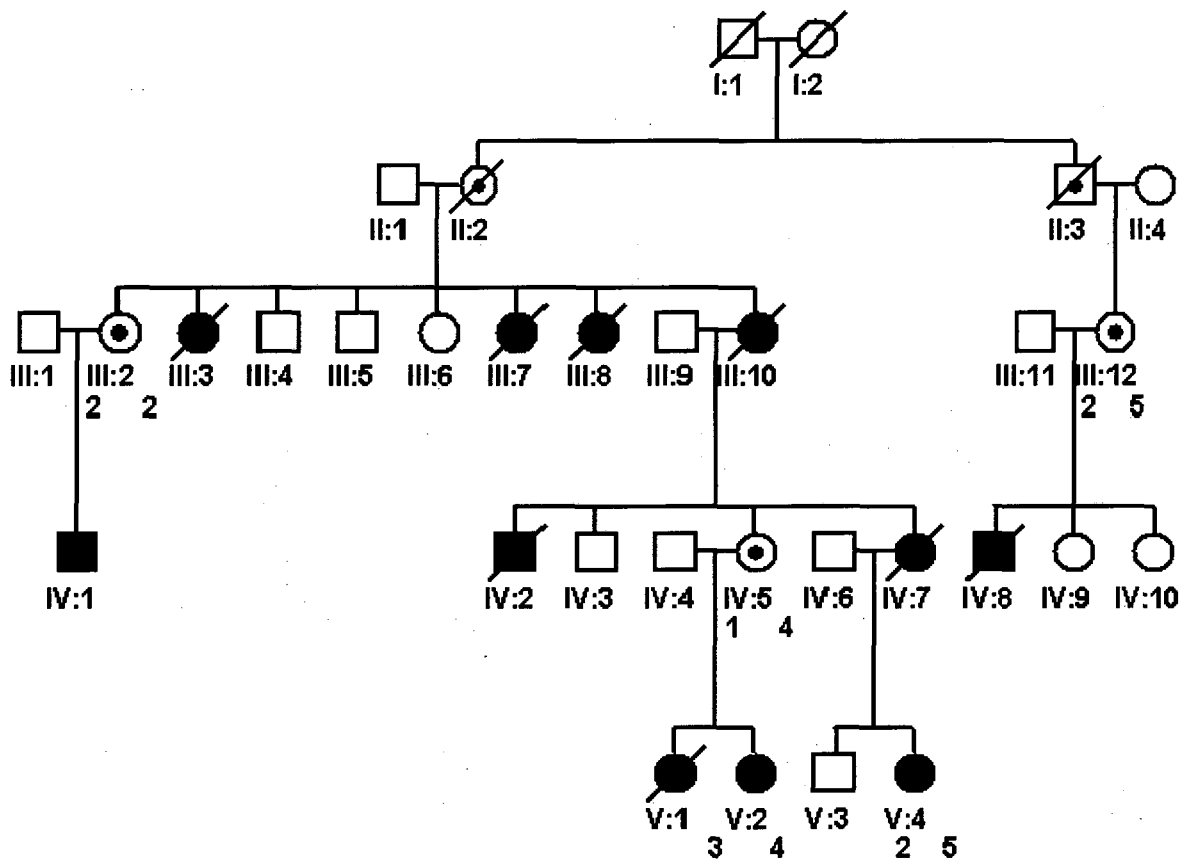


Figure 47 Segregation analysis of D21S1895 marker in family B

Pedigree analysis shows that there are no commonly inherited alleles among the affected subjects, and thus excludes this locus in family B (assuming no recombination event has taken place).

3.2.2.6 RyR2

Three microsatellite markers were used. *RyR2* is located at 233,502,289-234,293,240 bp on chromosome1. Marker B44 was located within the gene (233,665,539-233,774,163 bp). D1S2850 located at 232,927,257-232,927,403 bp was very close to the gene and telomeric to it. Further telomeric and still close to the gene, marker B940 was located (232,385,621-232,489,228 bp). The positions of the gene and markers are obtained from the Human Genome NCBI Build 35.1.

The markers yielded data showing common allele inheritance among the affected subjects (figure 49).The data could not exclude linkage to the *RyR2* locus in this family.

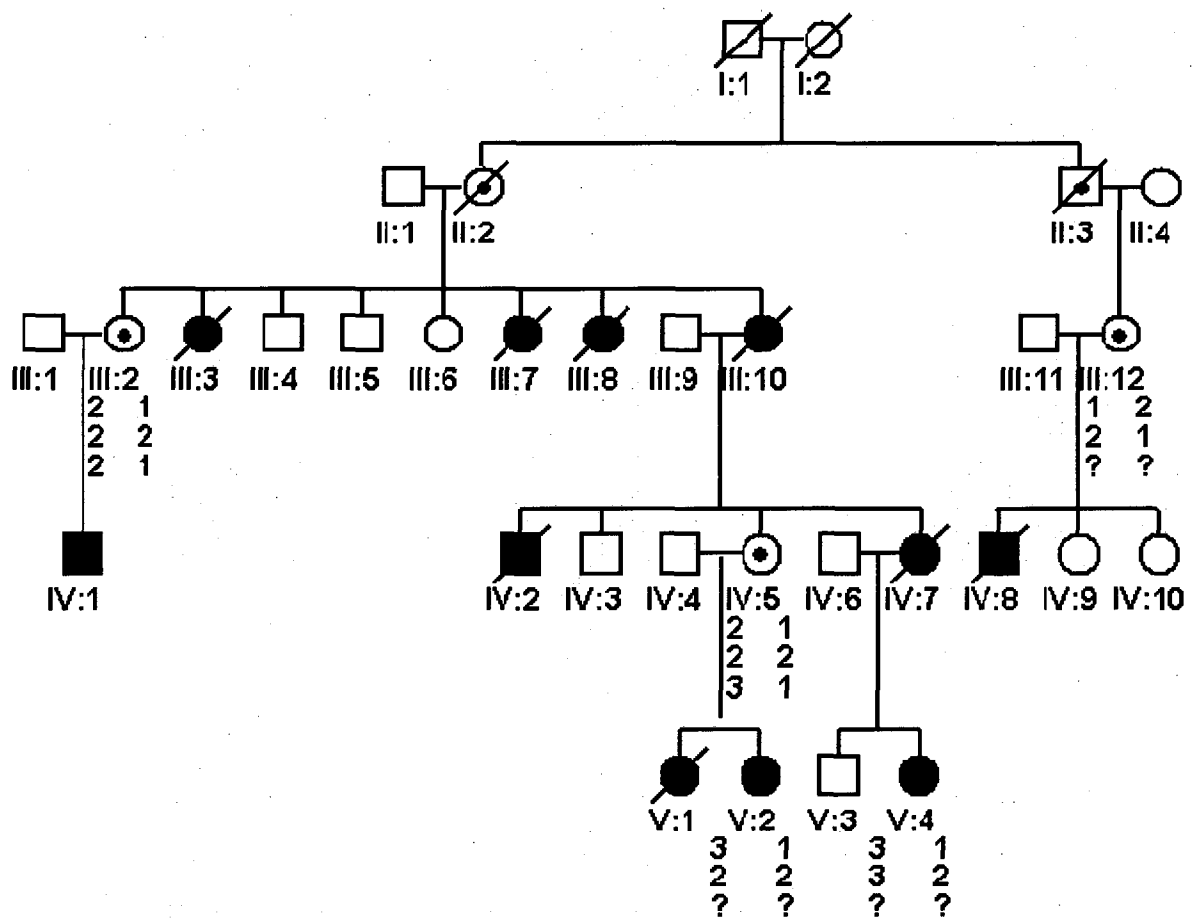


Figure 48 Segregation analysis of markers near RyR2 locus in family B

The allele sizes obtained with markers B44, B940 and D1S2850 are shown in the same order. '?' denotes allele sizes not obtained. Due to the common allele sharing among the affected subjects, linkage to this locus could not be excluded in this family.

3.2.2.7 TNNT2

Microsatellite marker D1S306 was within 1Mb of the TNNT2 locus. D1S306 was located at 199,671,611-199,671,877 bp on chromosome 1. Following gene-scan analysis, the genotyping data did not show common allele inheritance among the affected subjects thus excluding this locus in this family (figure 50).

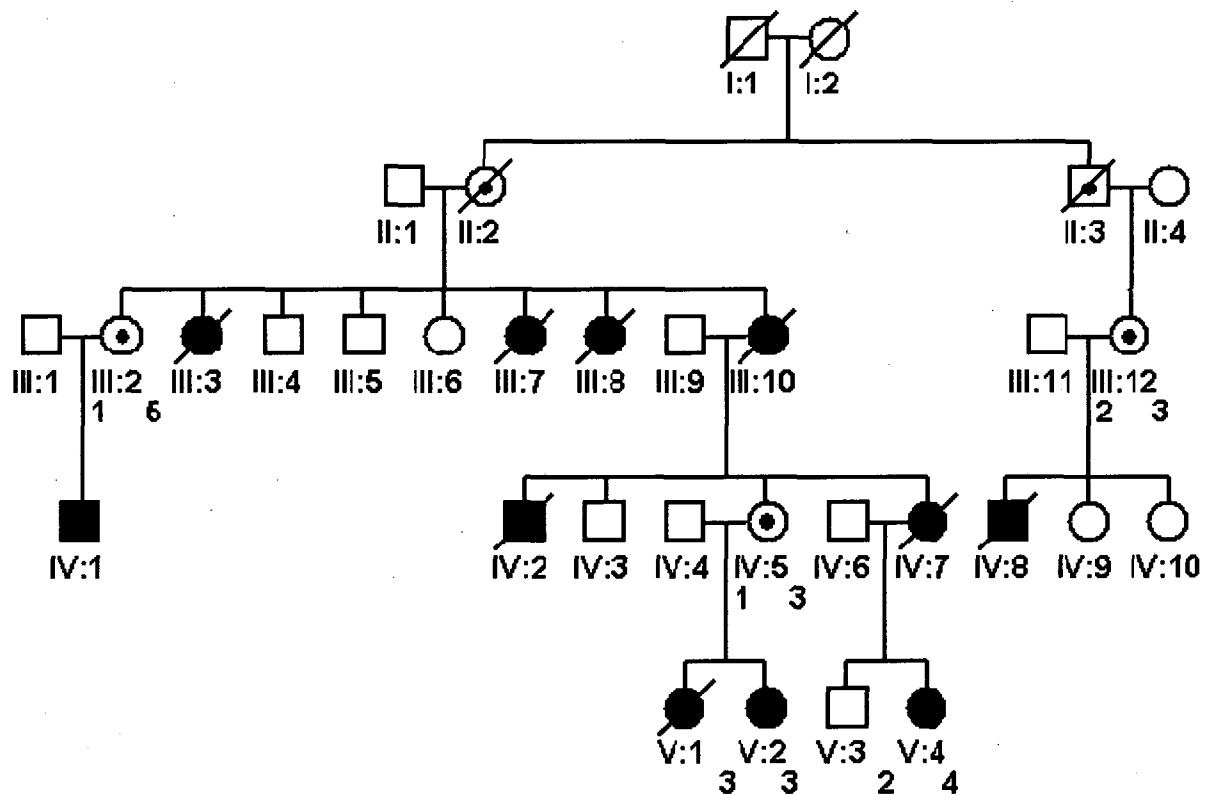


Figure 49 Segregation analysis of TNNT2 locus in family B

The allele sizes obtained with the marker D1S306 are shown. The absence of a commonly inherited allele among the affected subjects, excludes this locus in this family (assuming no recombination event has taken place).

3.3 SUMMARY OF THE RESULTS

With family A, the genotyping data excluded linkage to LQT1, LQT2, LQT3, LQT4, LQT5 and LQT6 loci. The data could not exclude linkage to two loci. The first locus was RyR2 at 1q42 and the other was the TNNT2 locus at 1q32. Mutations in *TNNT2* lead to similar ECG and clinical features as in family A. Therefore *TNNT2* was prioritised and directly sequenced for mutations. A 5-basepair insertion was identified in intron 3 and a single base substitution was identified in exon 9, which were not shared by other tested, affected, family members. Therefore these genetic variations were excluded as being responsible for the disease phenotype in the family.

With family B, the genotyping data excluded linkage to LQT1, LQT2, LQT3, LQT5, LQT6 and TNNT2 loci. The data was not informative to rule out LQT4 locus and the data could not exclude linkage to the RyR2 locus at 1q42.

4.0 CHAPTER 4: DISCUSSION

In this study, two families affected by ventricular tachyarrhythmias were investigated. The results of the investigations for the two families, the possible alternative approaches and limitations of these investigations are discussed.

4.1 FAMILY A

4.1.1 The clinical phenotype

The proband in Family A presented with cardiac arrest secondary to ventricular tachyarrhythmias. She had an abnormal ECG and 6 other members of the family had similar abnormal ECGs. The abnormal ECG changes in family A were ST segment and T wave changes in leads representing multiple vascular territories (table 12). Standard investigations showed affected members to have structurally normal hearts. There was no evidence of coronary artery disease or hypertrophic cardiomyopathy in the affected members to explain the ECG findings. Therefore, this pattern appeared distinct from known ECG patterns in conditions predisposing to sudden cardiac death in structurally normal hearts and was considered a novel phenotype. It was hypothesised that the condition affecting family A resulted from mutations in a novel gene or novel mutations in a known gene.

	ECG features
Family A	Normal QTc ST depression & T wave inversion
LQTS	Prolonged QTc (>440 ms in males & 460 ms in females). Early onset of broad based T wave in LQT1, low amplitude & often notched T wave in LQT2, late onset T wave with normal duration & amplitude in LQT3. ST segment depression & T wave inversion can occur. ECG can be normal.
SQTS	Short QTc (<300 ms) Peaked T waves
Brugada syndrome	Right bundle branch block ST segment elevation in leads V1- V3 T wave inversion & biphasic T wave can occur Normal QTc. Random ECG can be normal.
CPVT	RBBB morphology VT Bidirectional VT Normal resting ECG Normal QTc
HCM	Can show varying degrees of conduction delays Tall R waves and deep S waves often present ST depression- T wave inversion often present Normal QTc
ARVC	Non specific T wave inversion Epsilon wave Normal QTc

Table 12 Comparison table of ECG changes

Table 12 compares the ECG changes in family A compared to ECGs seen in candidate gene syndromes.

4.1.2 Flecainide challenge test

Administration of flecainide in family A exaggerated the ST segment depression in the ECGs. Since flecainide is a sodium channel blocker the possibility of mutations in a gene encoding a sodium channel subunit (eg, *SCN5A*) was raised. *SCN5A* mutations lead to LQT3 and Brugada syndrome which are conditions associated with ventricular arrhythmias. Therefore *SCN5A* was a candidate gene. Flecainide challenge test helps to unmask latent cases of Brugada syndrome by bringing out new ST elevation or exaggerating existing but subtle ST changes in the right precordial ECG leads V1-V3. These changes are not specific to Brugada syndrome¹⁵⁷. Moreover the effects of Flecainide on normal ECGs or on ST segments in various conditions have not been systematically studied. It is therefore not possible to exclude the possibility that the worsening ST segment changes observed in family A were non specific.

4.1.3 Candidate genes in family A

After studying the clinical presentation of the family (including ECG findings) and performing a literature review, 8 possible candidate genes were identified.

At the start of the project, mutations in 6 genes were known to cause LQTS. The corrected QT intervals in our subjects were normal. However it is known that prolonged QT interval on the ECG may manifest only occasionally and having a normal QT interval on the ECG does not rule out LQTS. The six LQTS genes were therefore included as candidate genes.

SCN5A mutations lead to LQT3 and Brugada syndrome, both of which can cause ventricular tachyarrhythmias and sudden cardiac death. Since flecainide exaggerated the ECG changes, *SCN5A* was an important candidate gene.

Catecholaminergic polymorphic ventricular tachycardia is an inherited condition associated with high risk of ventricular arrhythmias and normal ECG, often secondary to mutations in the *RyR2* gene, which codes for a calcium release channel. Therefore, *RyR2* was included as a candidate gene.

Hypertrophic cardiomyopathy secondary to *TNNT2* mutations can present with abnormal ECG changes similar to the ECG changes in family A. These mutations often produce little or no hypertrophy on echocardiography, but confer a high risk for ventricular arrhythmias. *TNNT2* was therefore included as a candidate gene.

4.1.4 Genotyping

Following genotyping in family A, common alleles segregated with the disease for genetic markers near *RyR2* and *TNNT2*.

RyR2 is located at 1q42.1-q43 at 233.5-234 Mb. Three microsatellite markers gave genotyping data. The marker B44 was located within the gene. Markers D1S2850 and B940 were located close to the gene (figure 51). Because of the proximity of the markers to the gene, recombination events between a marker and the gene are extremely unlikely. The disease locus is therefore potentially linked to the alleles.

TNNT2 locus is at 1q32. The markers used for *TNNT2* locus in family A were D1S2764 & D1S306. They are located as shown in figure 51.

Linkage to markers near the *RyR2* and *TNNT2* genes on chromosome 1q could not be excluded, suggesting that the mutated gene in this family could be either of these genes or another gene located closely.

Ideally, both *RyR2* and *TNNT2* had to be screened for mutations, but due to limitations on time, one of the genes was prioritised for mutation screening. *RyR2* mutations cause Arrhythmogenic Right Ventricular Cardiomyopathy (ARVC) and Catecholaminergic Polymorphic Ventricular Tachycardia (CPVT). Clinically family A did not have features to suggest either of these conditions. It was known that *TNNT2* mutations can cause cardiomyopathy and manifest ventricular arrhythmias, with no cardiac hypertrophy on imaging, and yet present with ECG changes not dissimilar to family A. Therefore, *TNNT2* was screened for mutations in preference to *RyR2*.



Figure 50 Genotyping results summary in family A

Figure shows the location of the *TNNT2* and *RyR2* loci on chromosome 1q, and the location of the microsatellite markers used for genotyping. *TNNT2* is located on chromosome 1 between positions 198,606,400-198,650,683 bp. *RyR2* is telomeric and nearly 35 Mb from *TNNT2* at 233,502,289-234,293,240 bp. The positions are based on Human Genome NCBI Build 35.1.

4.1.5 Mutation screening of TNNT2

Direct sequencing of *TNNT2* was performed to identify any sequence variations. Two variations were identified in two different individuals.

4.1.5.1 Insertion of a CTCTT sequence in intron 3

A 5 base pair insertion was identified in intron 3 of individual IV: 1 in family A. This variation was not seen in individuals II: 1, II: 7 and III: 8. Since this variation is present in only 1 out of 4 affected members of the same family, it cannot be the cause of the disease phenotype in this family.

If, however, this variation was identified in all the affected family members, further investigations would have been needed to find out, for instance, whether this insertion could affect exon 4 skipping and alter *TNNT2* gene expression.

The variation has been previously reported as a benign polymorphism¹⁵⁸, making it an unlikely cause for the phenotype in this family.

4.1.5.2 Single base substitution in exon 9

The A/G sequence variation (TCA>TCG) was seen in exon 9 in subject II: 1 in family A. This change was not seen in III: 8 and IV: 1. Since the variation was identified in only 1 out of 3 affected members of the same family, it has not co-segregated with the disease and it cannot be the cause of the disease phenotype in this family.

If this variation was identified in all the affected family members in this study, the variation would have been investigated further, to find out whether it is located within an exonic splicing regulatory sequence and whether it can interfere with the splicing of the upstream intron.

Investigators have previously identified this single base substitution (TCA>TCG) within exon 9 as a benign polymorphism¹⁵⁸, making it an unlikely cause for the phenotype in this family.

4.1.6 Limitations of the direct sequencing approach

Although all the coding exons and the intron - exon boundaries were sequenced, the whole of intronic sequence was not sequenced. It is possible that mutations in non-exonic regulatory regions will not be identified. Also the UTR was not sequenced as a significant mutation in the UTR was felt less likely than in the coding exons. However, it is known that UTR can contain regulatory sequences that play a role in gene expression and therefore it is possible that potentially significant variations in the UTR could have been missed. Lastly, it is also possible to miss large deletions or insertions comprising a whole or several exons by direct sequencing¹⁵⁹. Additional methods like FISH (Fluorescent in situ Hybridisation) or MLPA (Multiplex ligation-dependent probe amplification)¹⁶⁰ may need to be considered if large deletions or insertions in TNNT2 are thought to be the underlying genetic cause in this family. These investigations were not performed due to limited time remaining in the project.

4.2 FAMILY B

Family B was known to the Clinical Genetics Service with a familial history of sudden cardiac death and cardiac syncope. Resting ECGs were normal. The DNA of 5 affected family members was available for investigation.

Standard investigations showed affected members to have structurally normal hearts. Since the clinical characteristics did not fit with known conditions causing sudden death in structurally normal hearts, such as ion channelopathies and some subtle forms of cardiomyopathy, it was hypothesised that the condition affecting family B was novel, resulting from mutations in a novel gene or novel mutations in a known gene.

4.2.1 Candidate genes in family B

In long QT syndrome, 6 genes had been identified at the start of the project, mutations in which lead to prolongation of the QT interval and increase the risk of ventricular arrhythmias. There was no documented prolongation of QT interval on the resting ECG of our family members. However there was evidence of prolonged QT interval during exercise testing in individual V2. In addition, two members of the family had sudden death when swimming. Since swimming is known to be a specific trigger for ventricular arrhythmias in LQT1, the LQTS genes were important candidate genes. In addition to LQT1, we included LQT 2, 3, 4, 5 and 6 as candidate loci, since it is known that affected subjects may not always demonstrate QT prolongation on their resting ECGs.

Catecholaminergic polymorphic ventricular tachycardia is an inherited condition associated with high risk of ventricular arrhythmias, often secondary to mutations in the *RyR2* gene, which codes for a calcium release channel. The ECG is often normal and the heart is structurally normal. Therefore, *RyR2* was included as a candidate gene. Hypertrophic cardiomyopathy secondary to *TNNT2* mutations can present with little or no hypertrophy on echocardiography, but with a high risk for ventricular arrhythmias. *TNNT2* was therefore included as a candidate gene.

4.2.2 Genotyping

Genotyping excluded linkage to LQT1, LQT2, LQT3, LQT5, LQT6 and *TNNT2* loci in family B. Non informative genotyping data was obtained for LQT4 locus and therefore this locus has not been excluded. However, more markers were not typed for the LQT4 locus. Although LQT4 was an initial candidate locus, it was felt at this time that it was an unlikely candidate because a) LQT4 forms only a very small proportion of LQTS b) LQT4 patients often had sinus bradycardia or features of sinus node dysfunction which was absent in the family. If in the rare chance that it was the gene with the mutation in the family, it was felt that it would still be picked up once the family was investigated with genome wide scan.

Further investigations were not performed on the LQT4 locus because of all these reasons coupled with the fact that there was limited time. Genotyping with markers close to *RyR2* gene showed common alleles segregating with the disease in family B. Thus the data could not exclude linkage to this locus. Mutation screening of the *RyR2* gene was not performed due to time constraints.

4.3 DISCUSSION ON THE APPROACH FOR GENE MAPPING

4.3.1 Candidate gene approach

The candidate gene approach is an effective method for gene identification when the number of available subjects are small and when there is restriction on time and funding. The disadvantage is that the process of selecting specific candidates among many reasonable possibilities is subjective.

The number of available DNA in the families (n=7 in family A and n=5 in family B) were not large enough for statistical confirmation of linkage using the genotyping data, but enough to exclude candidate genes. The identification of candidate genes was possible because of the clues to the underlying genetic cause. The ECG changes in family indicated that abnormalities in the gene caused changes in the repolarisation phase of the cardiac cycle. Previous studies have shown that mutations in the genes encoding ion channel components, such as potassium, sodium and calcium channel components can lead to abnormalities in the repolarisation phase of the cardiac cycle and cause ventricular arrhythmias (Long QT syndromes, Brugada syndrome and CPVT). Therefore the genes, which are mutated in these conditions, became candidate genes for the family. Hypertrophic cardiomyopathy secondary to *TNNT2* mutation can present in a similar manner as family A with ECG changes and no evidence of cardiac hypertrophy but with significant risk of sudden death. Therefore *TNNT2* was included as a candidate gene as well. For family B, there was prolonged QT interval during exercise stress testing of one individual. Also, two individuals had sudden death while swimming. Therefore

the LQT 1, 2, 3, 4, 5 and 6 loci were included as candidate loci in family B. *TNNT2* was also included as a candidate gene in family B, since mutations in this gene is known to cause sudden death in subjects with a structurally normal heart.

The strategy was to look at the above candidate genes systematically using microsatellite markers for genotyping. The methods used were powered to exclude linkage to the candidate genes.

4.3.2 Possible alternative approach

The other possible approach for identifying the genetic cause in these families would have been genome-wide scanning. The principal advantage of genome-wide scanning is that it is objective and makes no assumptions regarding the importance of specific features of the disease. The principal disadvantages are that it is expensive, resource intensive and more subjects are usually required.

A genome wide association approach without *a priori* assumptions may have identified the region in the genome, which is likely to harbour the gene of interest, in the families. This region could then be looked at, more closely with a view to identifying candidate genes, mutations in which could explain the phenotype in the families. The genes could then be screened for mutations and the function of the gene in more detail could be studied.

If a genome wide approach was used, more subjects would need to have been investigated. This would have been our approach if we had no suitable candidate genes to start with.

4.4 IMPORTANCE OF THE STUDY FINDINGS

KCNQ1, KCNH2, SCN5A, ANKB, KCNE1 and *KCNE2* have been excluded as the source of mutation in family A. In addition, a locus in the genome which is likely to harbour the gene of interest in family A has been identified. This region is in the long arm of chromosome 1. It remains to be determined if the disease gene is localized to chromosome 1. A genome wide scan may identify other potential regions in the genome where the mutated gene may be located, that may warrant further investigation.

For family B, the data obtained excludes *KCNQ1, KCNH2, SCN5A, KCNE1, KCNE2* and *TNNT2*. Segregation of alleles near *RyR2* with the disease in family B suggests that this locus could not be excluded as having the genetic mutation in this family.

4.5 LIMITATIONS OF THE STUDY

The study design was limited by the number of DNA samples available for genotyping. Since only the DNA of the 7 affected subjects in family A and 5 affected subjects in family B were available, the study was designed to exclude potential candidate genes. Genes which could not be excluded were planned to be screened for mutations. Due to restrictions on time, *TNNT2* was screened for mutations and not *RyR2*. No pathogenic mutations were found, and therefore the genetic mechanisms remain unclear.

4.6 FUTURE WORK

Future work would involve typing more markers in 1q in all possible members of the families. Haplotyping could then help to narrow down the region of interest. The genes located in this region could be prioritised and mutation screened to identify the mutations in this family. Once the mutations are identified, it could be confirmed and the functional effects of the mutation can be studied.

If gene identification is not possible by this method, genome wide scanning would be the way forward to identify the region of the genome likely to harbour the gene of interest. For this to happen, careful phenotyping of extended family members would be needed. Also a search for other families with the same phenotype would be important. Since the start of this research project, further affected members have been identified.

This project has done important groundwork for future studies. The findings from these studies will increase our knowledge on inherited ventricular arrhythmias which in turn will help in better management of these conditions.

Appendix A

SOURCES OF MATERIALS

Product	Company	Address	Product no:
Taq DNA polymerase	Promega	MADISON, USA	M1665
Deoxynucleotide triphosphates - dNTPs	Promega	MADISON, USA	U1240
Magnesium chloride, 50 mM	Promega	MADISON, USA	Provided with Taq
10× PCR Buffer (minus Magnesium)	Invitrogen	Paisley, UK	Provided with Taq
Acrylamide	Severn	UK	003661
Agarose (pure)	Life	Paisley, Scotland	15510-027
TEMED(N,N,N',N'-Tetramethylethylenediamine)	Sigma	USA	EC 203-744
10×TBE	BDH	Poole, UK	10315
Ethidium bromide 10mg/ml	Sigma	USA	EEC 214-984-6
100 basepair DNA Ladder	Promega	Madison, USA	G2101

Appendix B

SOURCES OF INSTRUMENTS

Fluorimager: Model F1595	Molecular Dynamics, Sunnyvale, CA
Thermal cycler: DNA Engine Tetrad.	M J Research Inc, USA
Centrifuge	International Equipment Company Inc, Centra MP4, Model PTC-225; Watertown, Massachusetts, USA
Microcentrifuge: 1.5mL tube	International Equipment Company (IEC), centra MP4, Model 230, USA
Output power supply: 250 V/A	HOWE (Power Pac Junior)
Output power supply: 200 V/A, 50- 60 Hz	BIO-RAD laboratories Inc, CA,USA
Pipette: pipetman (2 µl, 10µl, 20 µl, 200µl, 1000µl)	GILSON S.A. Villiers-le-Bel, France
Disposable lab tips: 5-200µl, Cat No 94300120; 200-1000µl, catalogue number: 94300220;	Life Science International Ltd, Hampshire, UK. 0.1-10µl was provided by Thermolife Sciences, 012560817282, product code tp46.
Microtubes (0.5ml)	Alpha Laboratories Ltd. Catalogue number: LW2372 and 1,5ml, catalogue number: LW 2375, Hampshire, UK

Appendix C

PRIMER INFORMATION

Marker	Forward sequence	Reverse sequence	Product size (bp)	Position NCBI (bp)	PCR annealing temperature
KVLQT1CA86	ACATATGTGCACTGGTTAGGG	GGCTCCAGTCTGCCACTTAC	161	2,224,259-2,224,334	56
D11S4088	GGGCAGAGGCAGTGGAG	GCATGTTCGGGGGTG	204-252	2,815,660-2,815,875	54
D7S642	GTGCTGAAGATCCTGAACGG	AGCTCCAAAAGGTAGGGC	191-207	149,203,097-149,203,287	56
D7S2439	CAGCAAAAGGTACAGCAATTTC	AAAGTCTACGCCGCATTC	195-211	149,385,603-149,385,803	54
SCN5ACA132660I20	GTCCCTCCGTCAAGTTGGTA	GAGGAAAGCCTTGGCACATA	180-204	38,626,216	54
D4S1611	AGAGTAGTTCCATCTTGTTTTC	GGGCAAGGCTCATCAC	277-285	114,906,243-114,906,519	58-62
AC926KCNE1&2	GCAATGGGTGAAGTGCTTT	CTTACCATGCATGTGGACCT	233	35,187,312	54
D21S1920	TGAGCCGAGATTGCACC	CGTTCCAAAAGATTAGAGCC	220-234	34,619,062-34,619,285	54

D21S1895	AGTCCTACTGATAAACTGTGGC	CTGTCTCATAAGAACCTACCTGG	224-282	35,272,929-35,273,190	54
D1S2850	CGAAGGTGTACTGGGACTGG	AATCAGGATCATGCTACAGGG	145-153	232,927,257-232,927,403	58-62
D1S2764	GATCTGATAAGATTCCCCAA	GAGCTGGAGGTGCAAG	125-149	199,852,930-199,853,074	54
D1S306	CTGGGACTGGAAACACTTTGAT	CCAGAGGGAGCATTGGTG	261-281	199,671,611-199,671,877	54

Appendix D

ALLELLE SIZES FOR MARKERS IN FAMILY A

Subject	Marker	alleles		allele size (bp)	
II: 1	KVLQT1CA86	1	3	165	177
II: 3	KVLQT1CA86	1	2	165	167
II: 7	KVLQT1CA86	1	3	165	177
III: 1	KVLQT1CA86	3	3	177	177
III: 2	KVLQT1CA86	3	3	177	177
III: 8	KVLQT1CA86	1	3	165	177
IV: 1	KVLQT1CA86	1	3	165	177
II: 1	D7S2439	2	4	197	201
II: 3	D7S2439	1	4	193	201
II: 7	D7S2439	2	3	197	199
III: 1	D7S2439	2	5	197	205
III: 2	D7S2439	2	6	197	211
III: 8	D7S2439	1	3	193	199
IV: 1	D7S2439	1	4	193	201
II: 1	SCN5AGTEXON16	2	2	169	169
II: 3	SCN5AGTEXON16	1	3	167	171
II: 7	SCN5AGTEXON16	2	2	169	169
III: 1	SCN5AGTEXON16	1	2	167	169
III: 2	SCN5AGTEXON16	1	2	167	169
III: 8	SCN5AGTEXON16	2	2	169	169
IV: 1	SCN5AGTEXON16	2	2	169	169

II: 1	TG129ANK2	2	2	208	208
II: 3	TG129ANK2	-	-	-	-
II: 7	TG129ANK2	2	4	208	216
III: 1	TG129ANK2	1	2	194	208
III: 2	TG129ANK2	1	2	194	208
III: 8	TG129ANK2	3	4	212	216
IV: 1	TG129ANK2	2	4	208	216
II: 1	TA226ANK2	1	1	228	228
II: 3	TA226ANK2	1	2	228	230
II: 7	TA226ANK2	2	2	230	230
III: 1	TA226ANK2	1	1	228	228
III: 2	TA226ANK2	1	1	228	228
III: 8	TA226ANK2	1	2	228	230
IV: 1	TA226ANK2	2	2	230	230
II: 1	D4S1611	2	3	280	282
II: 3	D4S1611	2	2	280	280
II: 7	D4S1611	1	1	278	278
III: 1	D4S1611	2	2	280	280
III: 2	D4S1611	1	2	278	280
III: 8	D4S1611	1	3	278	282
IV: 1	D4S1611	1	3	278	282
II: 1	AC926KCNE1&2	1	1	228	228
II: 3	AC926KCNE1&2	2	3	232	234
II: 7	AC926KCNE1&2	1	1	228	228
III: 1	AC926KCNE1&2	1	2	228	232
III: 2	AC926KCNE1&2	1	1	228	228
III: 8	AC926KCNE1&2	1	4	228	238
IV: 1	AC926KCNE1&2	1	2	228	232
II: 1	D1S2850	3	4	150	152
II: 3	D1S2850	2	3	148	150

II: 7	D1S2850	3	4	150	152
III: 1	D1S2850	3	3	150	150
III: 2	D1S2850	3	3	150	150
III: 8	D1S2850	1	3	146	150
IV: 1	D1S2850	3	3	150	150
II: 1	B940	1	1	317	317
II: 3	B940	1	2	317	321
II: 7	B940	1	1	317	317
III: 1	B940	1	2	317	321
III: 2	B940	1	1	317	317
III: 8	B940	1	1	317	317
IV: 1	B940	1	1	317	317
II: 1	B44	1	4	189	201
II: 3	B44	4	5	201	203
II: 7	B44	1	4	189	201
III: 1	B44	4	6	201	205
III: 2	B44	1	4	189	201
III: 8	B44	3	4	193	201
IV: 1	B44	2	4	191	201
II: 1	D1S2764	3	4	143	145
II: 3	D1S2764	3	4	143	145
II: 7	D1S2764	3	4	143	145
III: 1	D1S2764	2	4	137	145
III: 2	D1S2764	1	4	135	145
III: 8	D1S2764	3	4	143	145
IV: 1	D1S2764	3	4	143	145
II: 1	D1S306	1	1	263	263
II: 3	D1S306	1	1	263	263
II: 7	D1S306	1	1	263	263
III: 1	D1S306	1	1	263	263

III: 2	D1S306	1	1	263	263
III: 8	D1S306	1	1	263	263
IV: 1	D1S306	1	2	263	275

Appendix E

12 LEAD ECGS OF FAMILY A

E.1 ECG OF II: 1

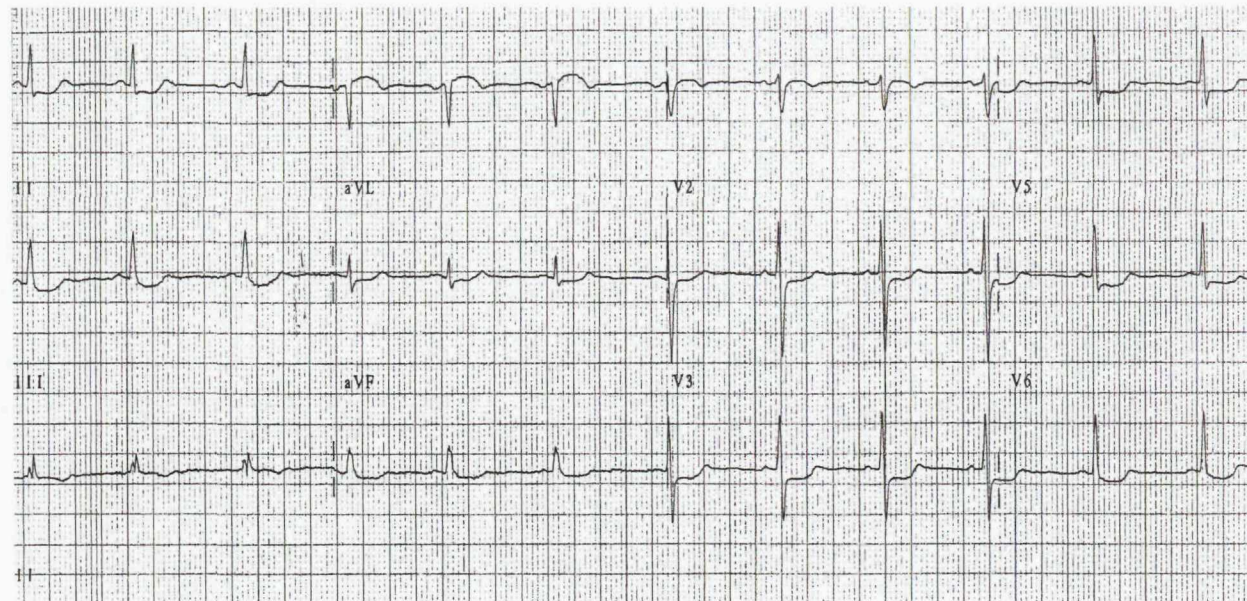


Figure 51 ECG of subject II: 1 in family A

ECG of II: 1 (paternal aunt of the index case) showing ST-T wave changes similar to the index case, suggesting affected status.

E.2 ECG OF IV: 1

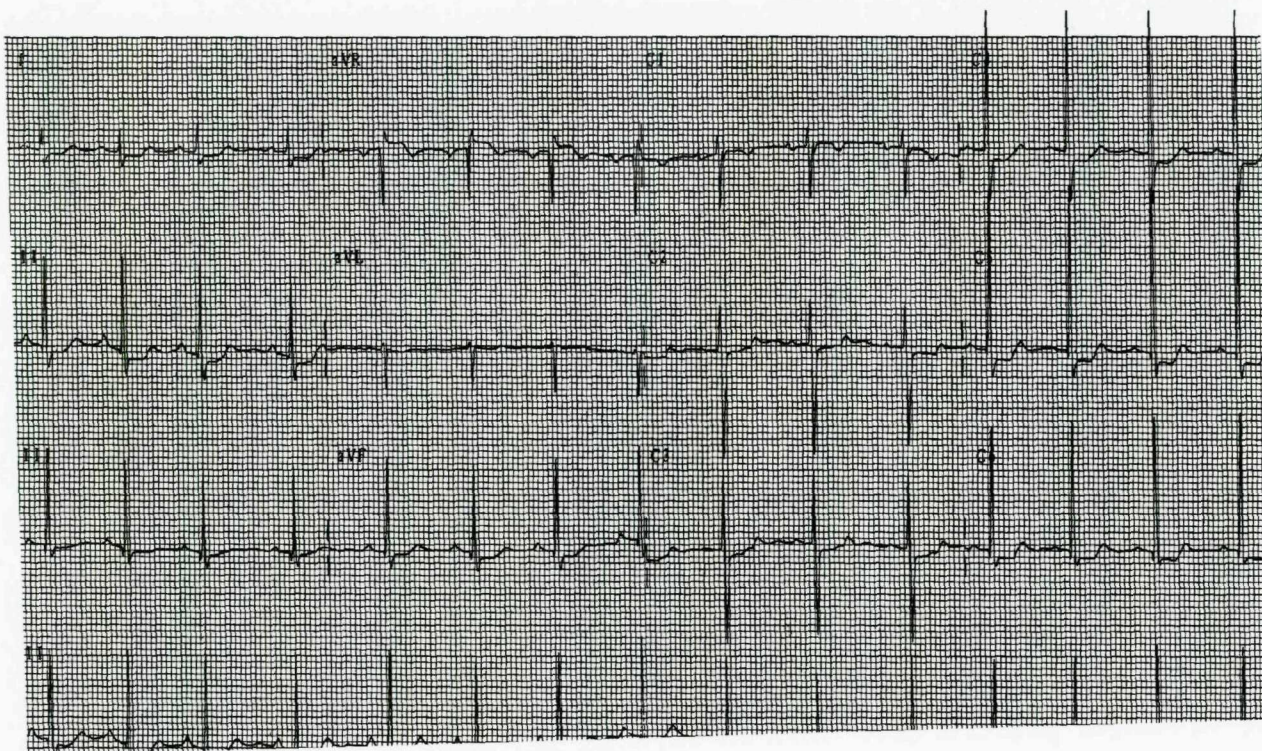


Figure 52 ECG of subject IV: 1 in family A

12 lead ECG of IV: 1 (son of the index case) shows resting ST- T wave changes similar to the index case, suggesting affected status.

E.3 ECG OF II: 3

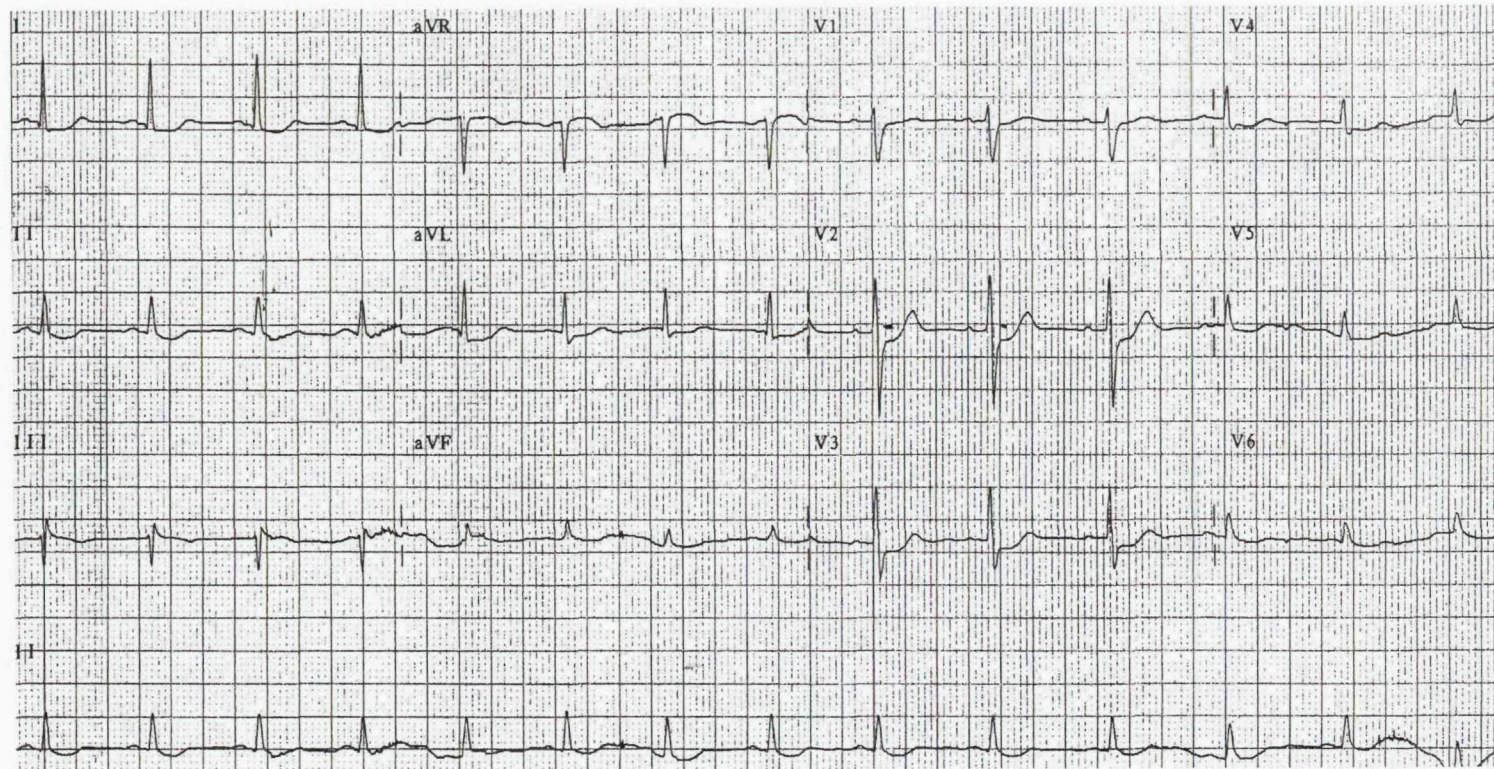


Figure 53 ECG of subject II: 3 in family A

12 lead ECG of II: 3 (paternal uncle of index case) shows ST-T wave changes similar to the index case, suggesting affected status.

E.4 ECG OF III: 3

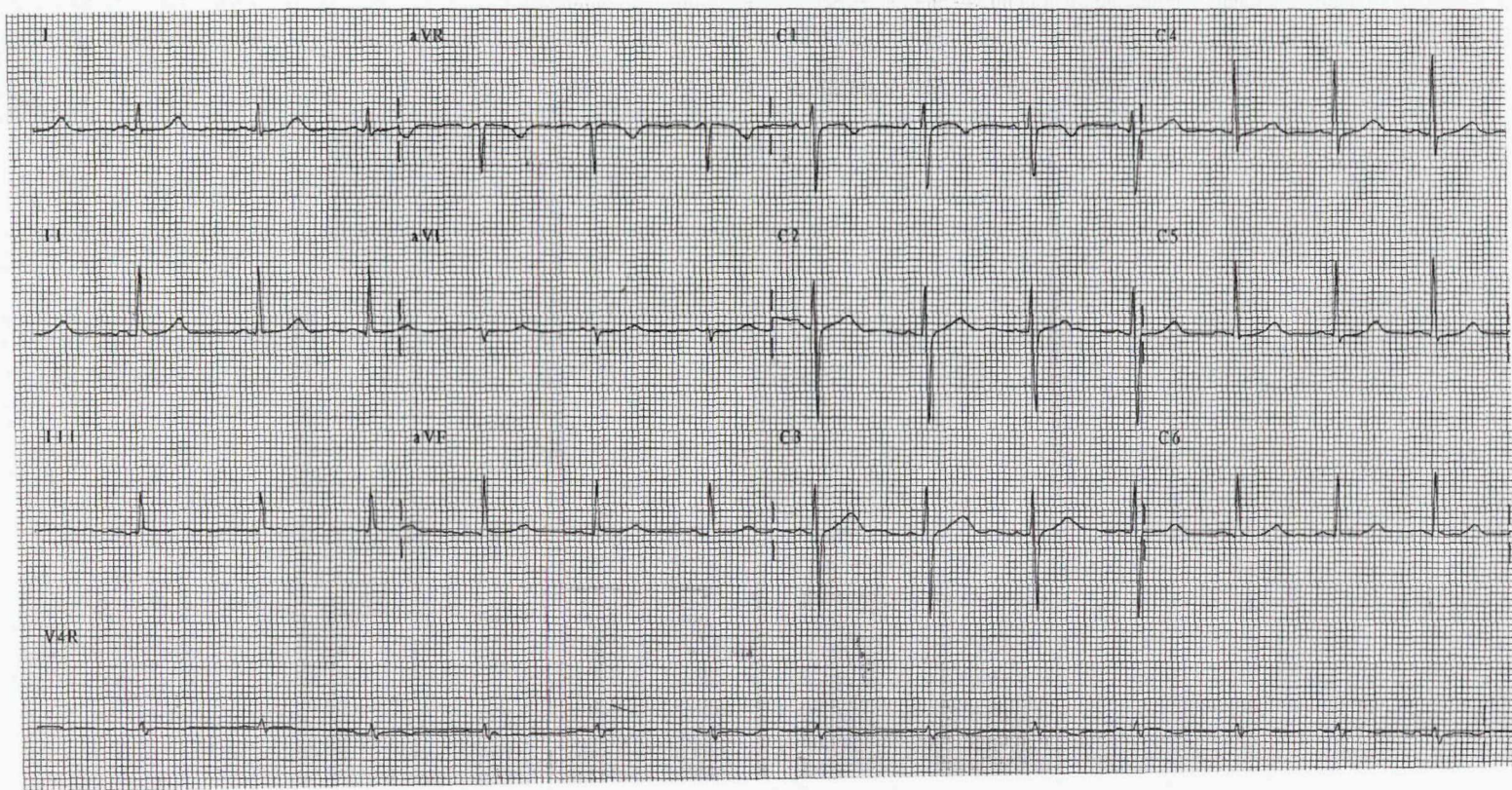


Figure 54 ECG of subject III: 3 in family A

ECG of III: 3 (daughter of affected individual II: 3) with a normal ECG suggesting non affected status.

E.5 ECG OF III: 5

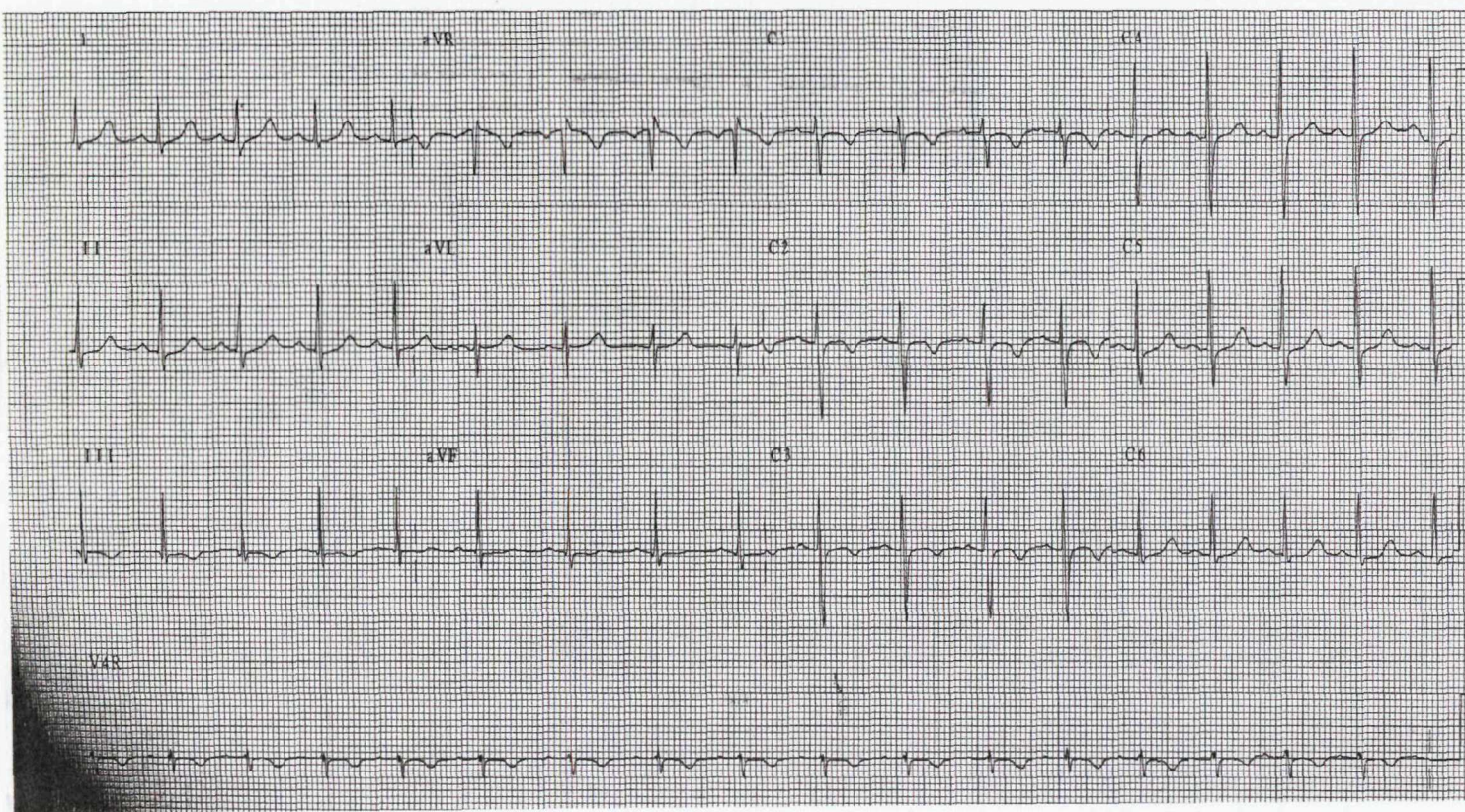


Figure 55 ECG of subject III: 5 in family A

ECG of III: 5 shows no ST changes but only T wave inversion in leads V1-V3, which is a normal variant in this age group. The subject was classified as unaffected.

E.6 ECG OF III: 1

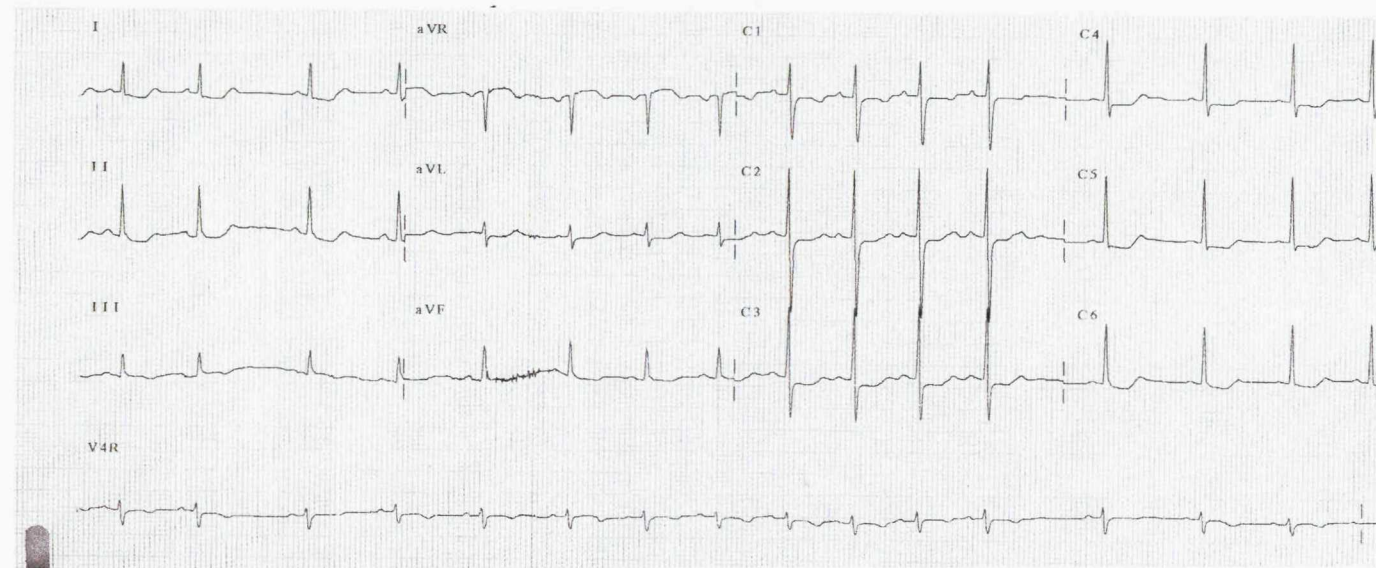


Figure 56 ECG of subject III: 1 in family A

ECG of III: 1 (daughter of II: 1), shows ST-T wave changes similar to the index case and classified as affected.

E.7 ECG OF III: 2

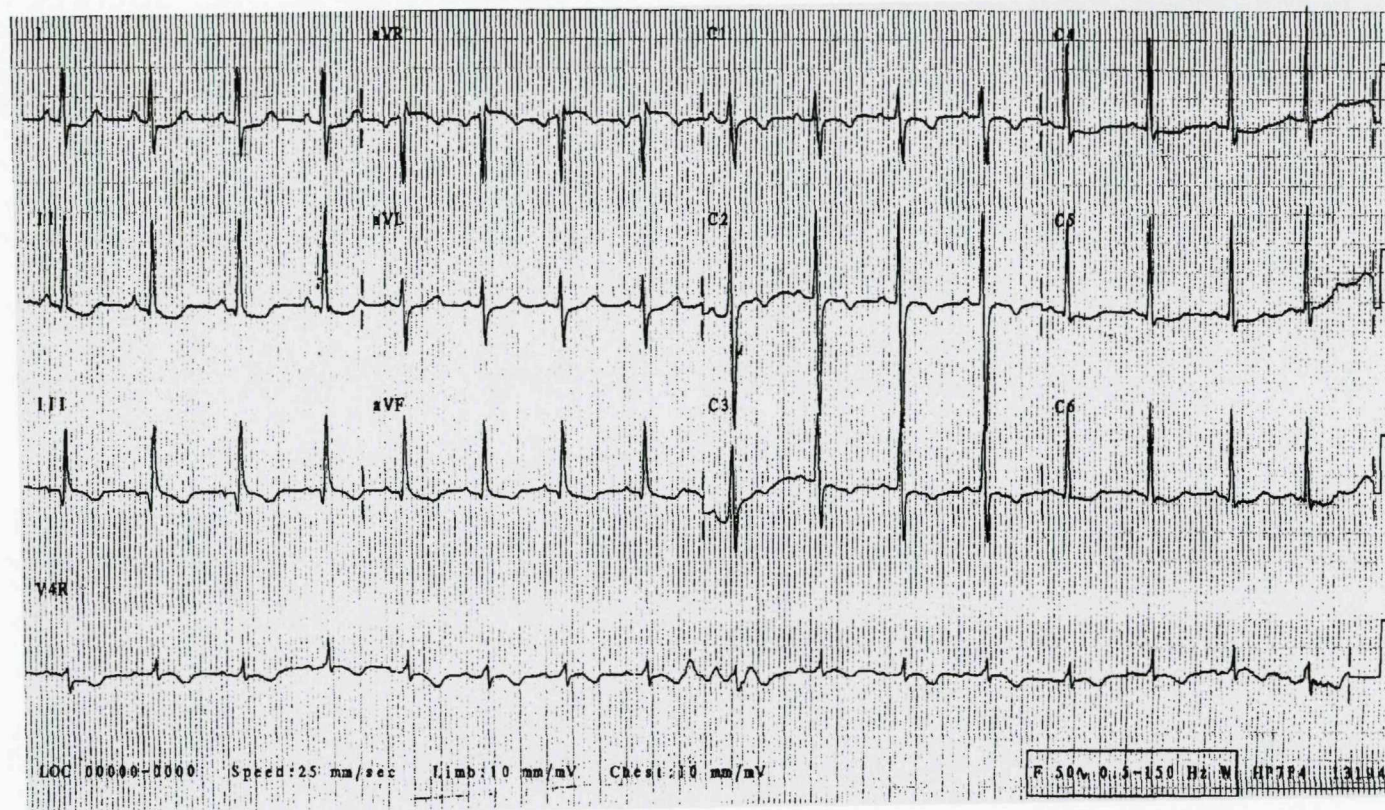


Figure 57 ECG of subject III: 2 in family A

ECG of III: 2 (daughter of II: 1) shows ST-T wave changes similar to the index case and classified as affected.

E.8 ECG OF III: 6

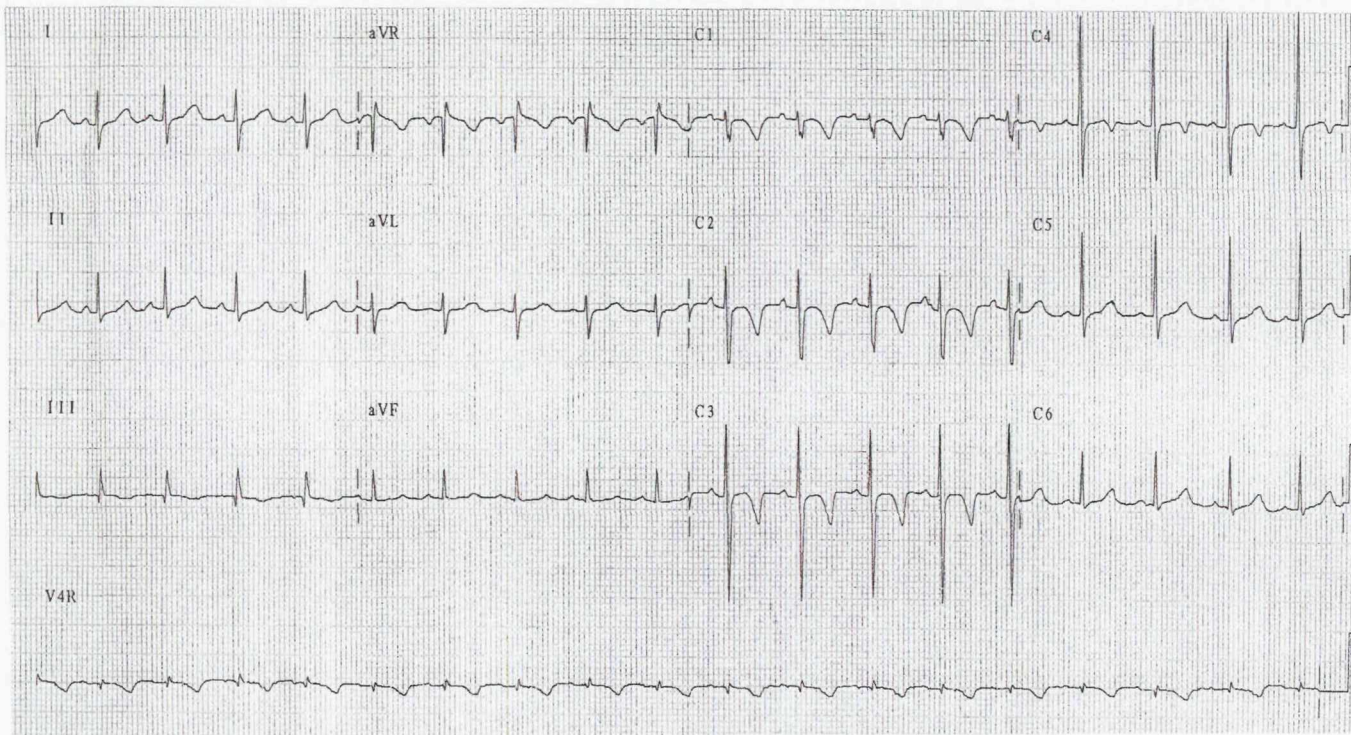


Figure 58 ECG of subject III: 6 in family A

ECG of III: 6 (a 4 year old boy) shows T wave inversion only, which is considered a normal feature in this age group. The subject was classed as unaffected.

Appendix F

ECHOCARDIOGRAPHIC ASSESSMENT OF FAMILY A

Subject	Age/sex	Ao root	LA	RV	IVSd	LVPWd	LVIDd	LVIDs	EF (>65%)
II: 1	40/F	2.8	3.2	2.1	1.0	0.8	4.6	2.9	70
II: 3	38/M	3.1	3.3	1.8	0.9	0.9	4.4	2.9	66
II: 7	49/M	2.1	2.8	2.2	0.9	0.8	3.8	2.7	68
III: 1	10/F	3.5	3.1	2.5	1.1	1.1	5.1	2.8	77
III: 2	12/F	3.2	4.0	2.0	0.8	1.0	4.7	3.1	72
III: 8	32/F	2.6	2.8	1.7	0.9	0.7	5.0	3.7	70
IV: 1	14/M	2.8	3.1	1.4	1.2	0.8	3.6	2.8	68

Table 13 Echocardiographic assessment of family A

Table shows cardiac dimensions of the subjects in centimetres (cm). Normal range in cm shown below the parameter. Ao root- aortic root, LA- left atrium, RV- right ventricle, IVSd- interventricular septum in diastole, LVPWd- left ventricular posterior wall in diastole, LVIDd- left ventricular internal dimension in diastole, LVIDs- left ventricular internal dimension in systole, EF- ejection fraction

Appendix G

VT STIMULATION PROTOCOL

The theory behind VT stimulation test was that by driving the ventricles at a high rate and introducing an early electrical stimulus which may fall in the excitable phase of cardiac repolarisation, VT may be induced. The ease with which VT can be induced serves as a marker for increased risk of VT in the future.

In the electrophysiology lab, a 6 French sheath was inserted in the right femoral vein. A quadripolar catheter was positioned in the right ventricular apex (RVA). Programmed electrical stimulation was given.

The first stimulus (S1) was emitted at a cycle length of 600 milliseconds. After 8 paced beats, the second stimulus (S2) was emitted at a shorter interval and reduced by 10 milliseconds, until failure to capture was seen. The third stimulus (S3) is emitted at shorter intervals until failure to capture is seen. The protocol was repeated at a faster Drive Cycle Length, if ventricular tachycardia was not seen with the earlier stimulation.

Ventricular tachycardia (VT) was called significant or the test was termed positive if VT lasted for more than 30 seconds or if it caused hemodynamic compromise to the patient. If ventricular stimulation in the RVA failed to stimulate VT, the catheter position was changed to right ventricular outflow tract and the programmed electrical stimulation repeated. If there was no evidence of significant VT from either of these sites, the test was deemed negative.

Appendix H

PROTOCOL FOR FLECAINIDE CHALLENGE TEST

The patient was admitted to the coronary care unit with full monitoring and resuscitative facilities. Baseline ECG was done. Continuous ECG monitoring was done while flecainide was administered in fractions of 10mg every two minutes intravenously up to a target dose of 2mg/kg.

The test was terminated when a type 1 ECG developed or if a type 2 or type 3 ECG changed to type 1 ECG or if ventricular arrhythmias developed.

Appendix I

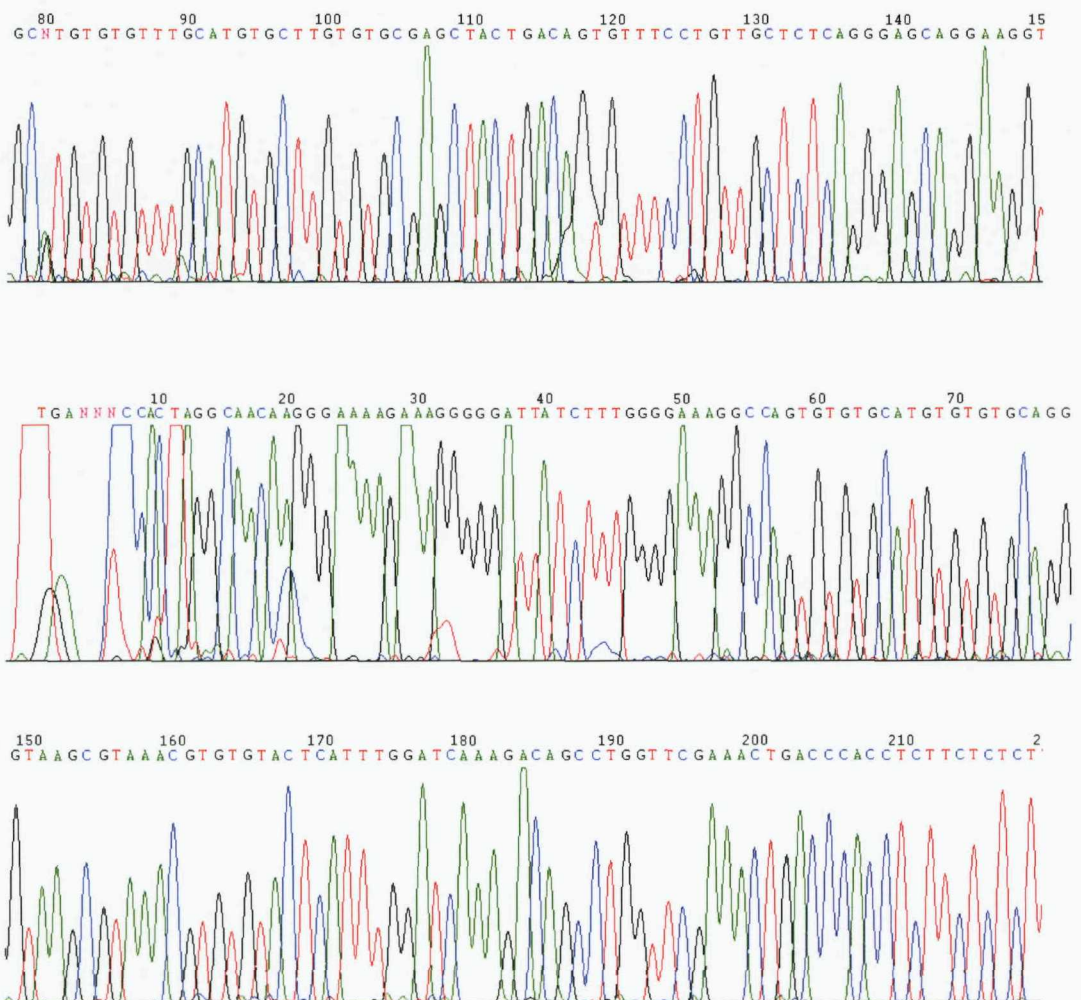
OLIGONUCLEOTIDES USED TO AMPLIFY THE VARIOUS EXONS OF *TNNT2*

Oligonucleotide	Sequence 5' to 3'	Pdt size
Exon 2F	GGCTTCCCTTTGTACCTGCACTG	241
Exon 2R	GGCTATATCTCTCCTCGGGGTGC	
Exon3&4F	GGAAAGGCCAGTGTGTGCATGT	284
Exon3&4R	GCTCCAGGATTCCACATTGC	
Exon5F	GCCTAACTCCAAAGCCCACACTC	225
Exon5R	CCTGGACAAGGAGGCTGCACT	
Exon6F	CGCTGCCATTCTCTGCTCT	207
Exon6R	GAATGGCTCCAGGGCTCTCG	
Exon7F	ACCCGAATGTGTGTGAGAGAGA	260
Exon7R	ATTCTCCTCCAAAGCTGCTGTGA	
Exon8F	ATCCACAGGGATCTAGCTCATCGA	249
Exon8R	GTACTGTGGTGCTCTGTGCCGAC	
Exon9F	CTATCATTGCTGTGGTGGTCGG	276
Exon9R	CCAGCCCAAGGTACAAAATCTC	
Exon10F	CCGCCAGAGGTCTTTGCAC	336
Exon10R	CTAGCTGGGTTGAGGCGCC	
Exon11F	GGAGGCCGGGCACCATTG	340
Exon11R	CACCGCACCCGGCCAATA	
Exon12F	GGTTTCCAATCCTTCCCTAA	234
Exon12R	GCTGCAGTGGACACCTCATTG	
Exon13F	GCTGTAACCCTCAGACCCACG	237
Exon13R	CTCCCAGGGAGCTCTCCAAA	
Exon14F	AGAAGAGCATAAGAGCCTGTCCC	350

Exon14R	ATGGGAAAATATGTGAGGCAGTC	
Exon15F	TGGAGGTGGGAAGGAGGGCT	240
Exon15R	GAGATGGAGATGCTGGCGG	
Exon16F	CTCCTTCTCCTCCTGCACTGC	227
Exon16R	ATGGGATAGCTGGAAGGTAGGG	
Exon17F	CCTTGGCACCCGAGTCCTAC	251
Exon17R	AGCTCCCCATTCCAAACAGG	

Appendix J

SEQUENCE TRACE OF EXON 3 & 4, SUBJECT IV: 1



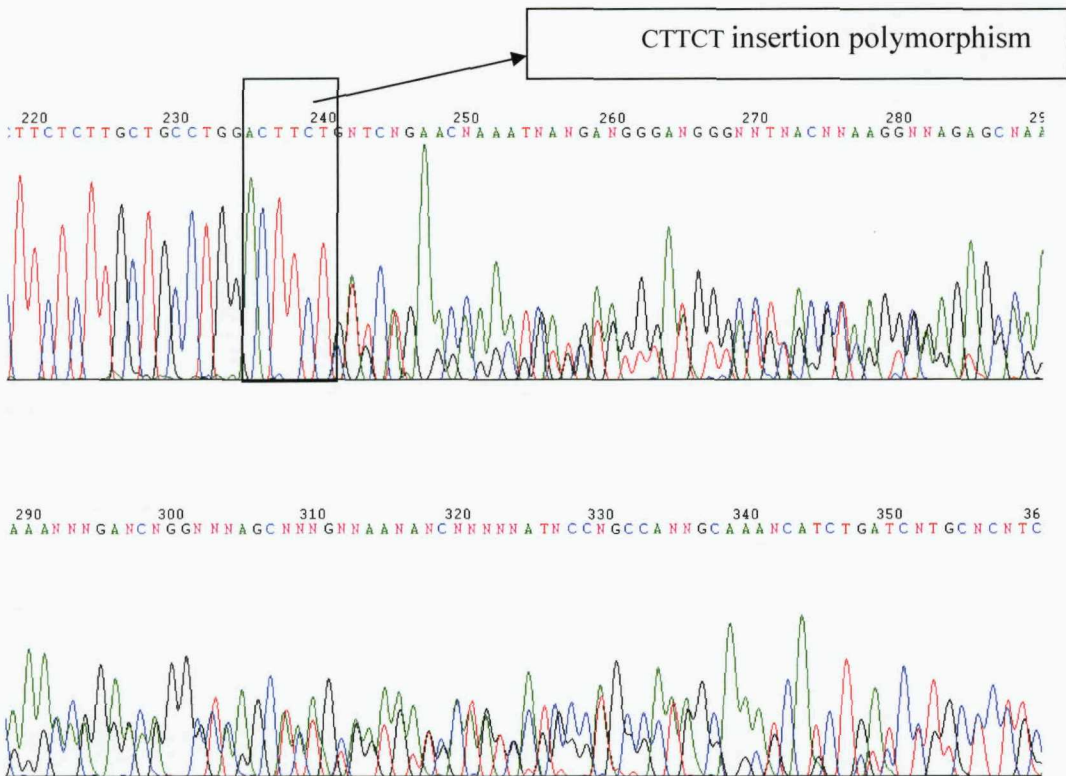
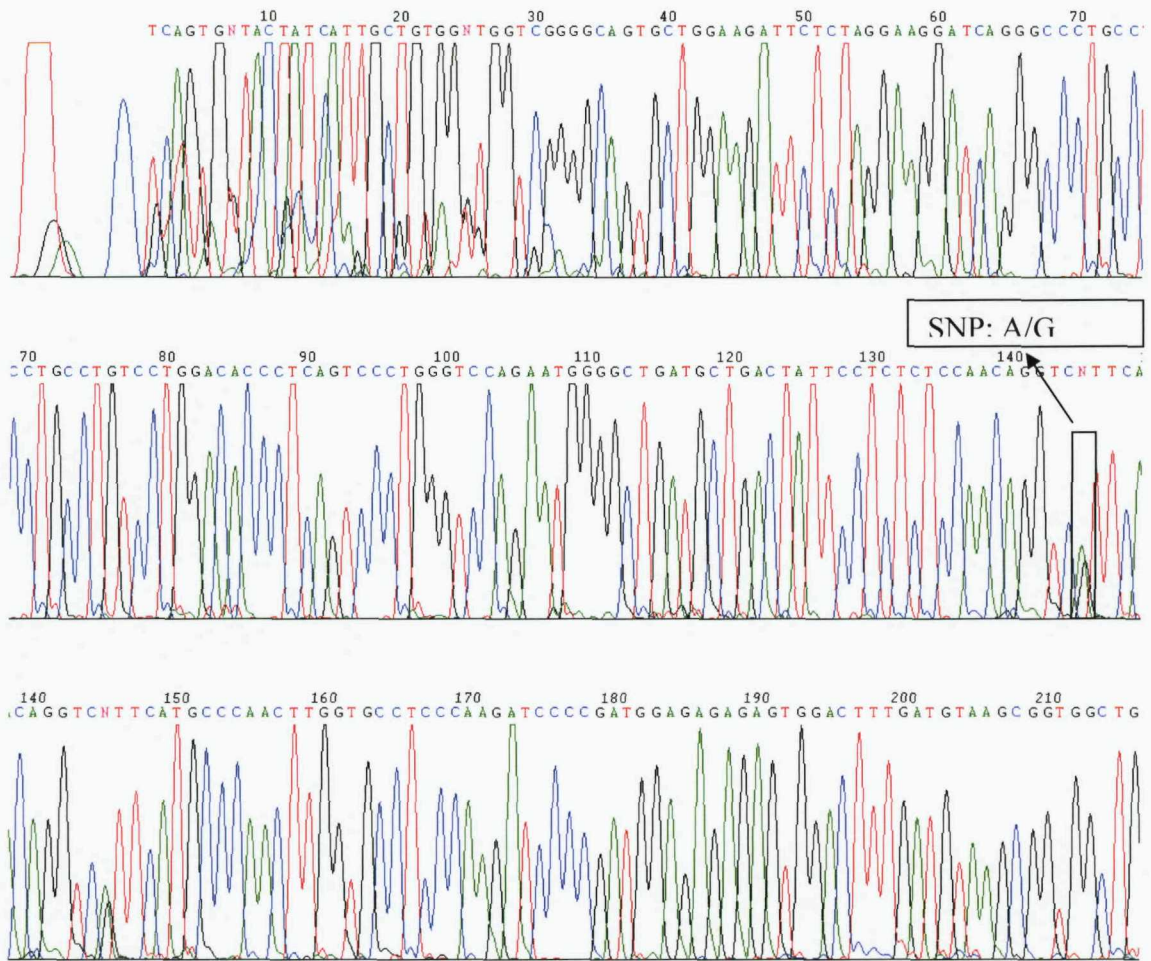


Figure 59 Sequence trace of exon 3 & 4, subject IV: 1

Figure shows sequence trace of exon 3 & 4 showing insertion polymorphism in intron 3 of subject IV: 1.

SEQUENCE TRACE OF EXON 9 F, SUBJECT II: 1



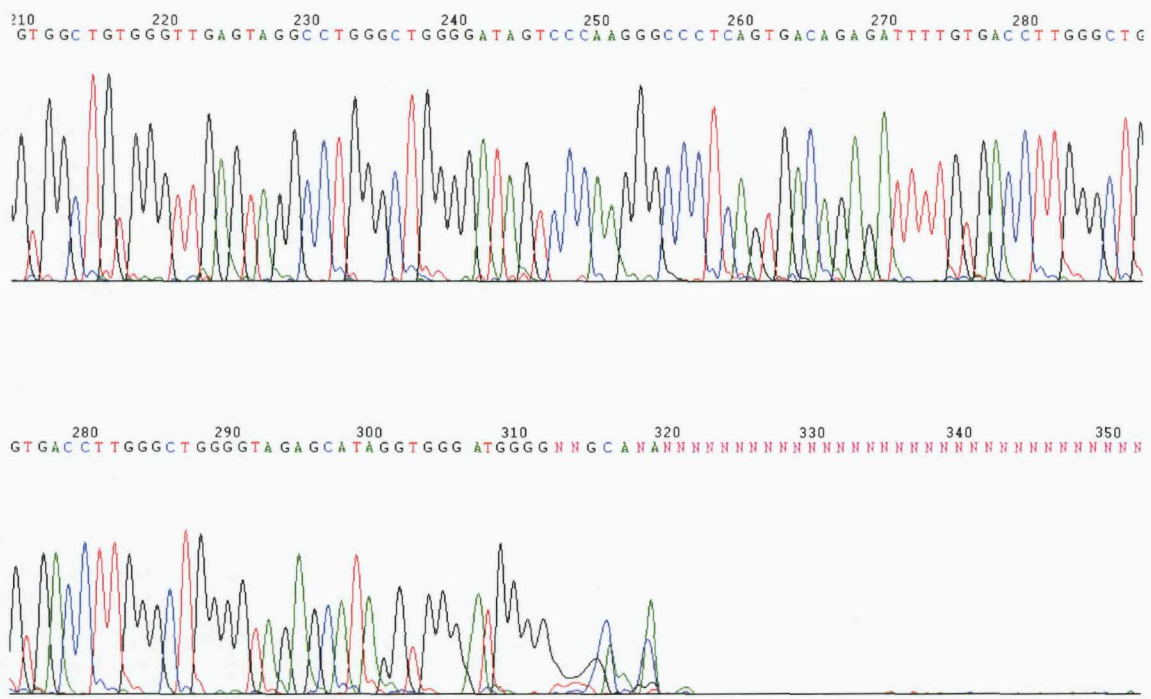
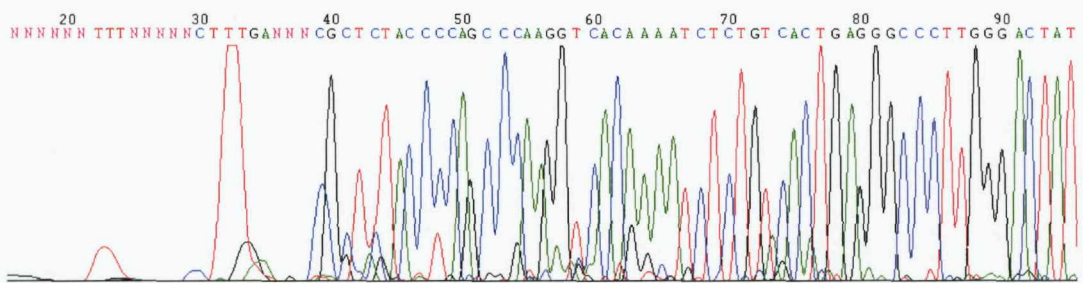


Figure 60 Forward sequence trace of exon 9, subject II: 1

Figure shows forward sequence trace of exon 9 showing A/G SNP in subject II: 1.



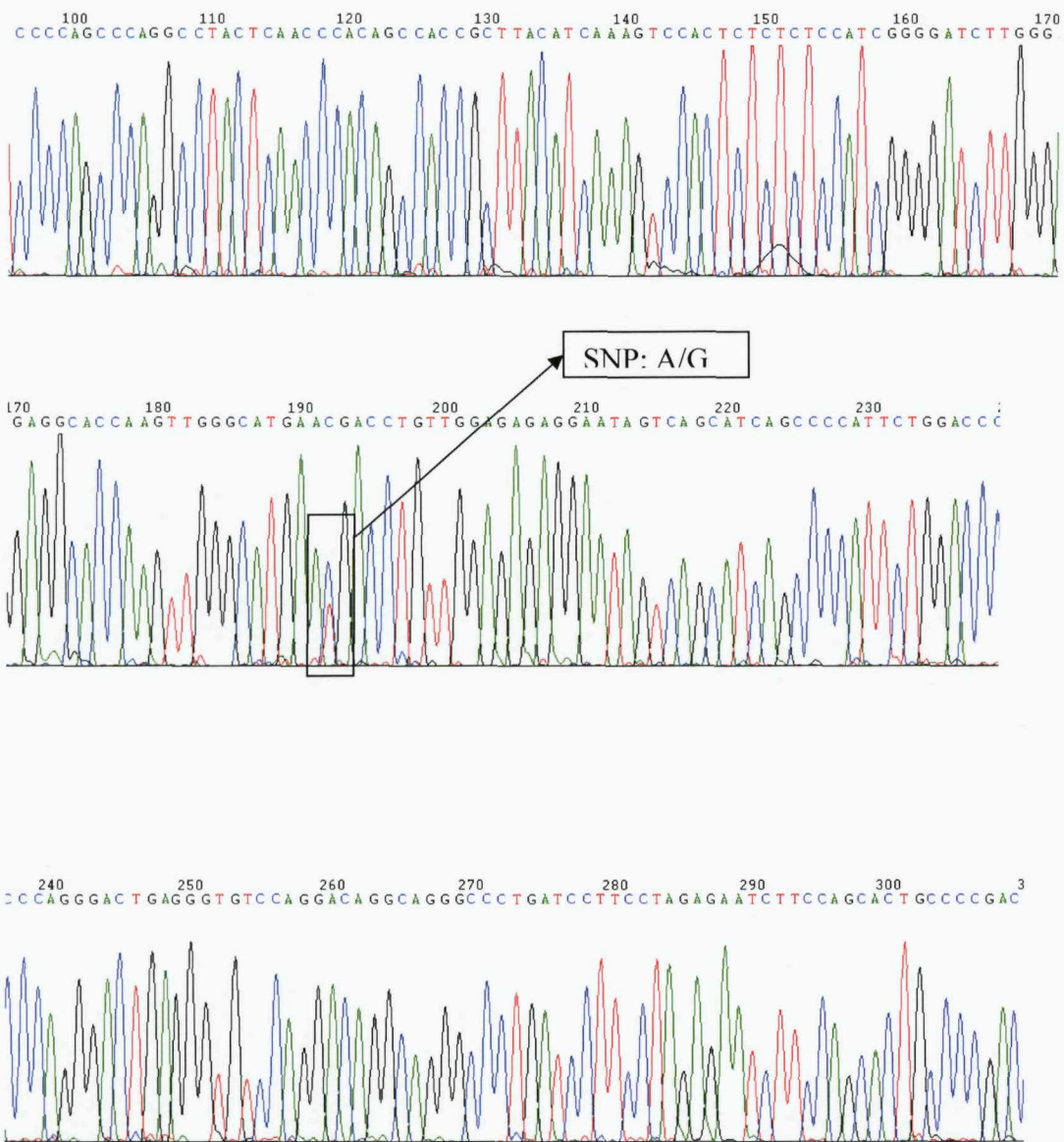


Figure 61 Reverse sequence of exon 9, subject II: 1

Figure shows reverse sequence of exon 9 in subject II: 1 with the A/G SNP.

Appendix K

ALLELLE SIZES OBTAINED FOR MARKERS IN FAMILY B

III: 2	KvLQT1Ca86	164	166	1	2
III: 12	KvLQT1Ca86	164	164	1	1
IV5	KvLQT1Ca86	166	174	2	3
V2	KvLQT1Ca86	164	166	1	2
V4	KvLQT1Ca86	164	166	1	2
III: 2	D7S642	193	203	2	5
III: 12	D7S642	191	199	1	4
IV5	D7S642	195	195	3	3
V2	D7S642	191	195	1	3
V4	D7S642	191	191	1	1
III: 2	D7S2439	197	201	3	4
III: 12	D7S2439	197	209	3	5
IV5	D7S2439	193	197	1	3
V2	D7S2439	195	197	2	3
V4	D7S2439	193	193	1	1
III: 2	SCN5ACA132660120	202	202	3	3
III: 12	SCN5ACA132660120	204	210	4	6
IV5	SCN5ACA132660120	196	206	1	5
V2	SCN5ACA132660120	196	196	1	1

V4	SCN5ACA132660120	196	200	1	2
III: 2	TA226ANK2	227	227	1	1
III: 12	TA226ANK2	227	227	1	1
IV5	TA226ANK2	227	227	1	1
V2	TA226ANK2	227	227	1	1
V4	TA226ANK2	227	227	1	1
III: 2	TG129ANK2	208	208	1	1
III: 12	TG129ANK2	208	208	1	1
IV5	TG129ANK2	208	208	1	1
V2	TG129ANK2	208	208	1	1
V4	TG129ANK2	208	208	1	1
III: 2	D21S1895	265	265	2	2
III: 12	D21S1895	265	275	2	5
IV5	D21S1895	263	273	1	4
V2	D21S1895	269	273	3	4
V4	D21S1895	265	275	2	5
III: 2	B44	185	191	1	2
III: 12	B44	185	191	1	2
IV5	B44	185	191	1	2
V2	B44	185	195	1	3
V4	B44	185	195	1	3
III: 2	B940	318	318	2	2
III: 12	B940	314	318	1	2
IV5	B940	318	318	2	2
V2	B940	318	318	2	2
V4	B940	318	320	2	3
III: 2	D1S2850	146	148	1	2
III: 12	D1S2850	-	-	-	-
IV5	D1S2850	146	150	1	3
V2	D1S2850	-	-	-	-

V4	D1S2850	-	-	-	-
III: 2	D1S306	1	5	262	272
III: 12	D1S306	2	3	264	268
IV5	D1S306	1	3	262	268
V2	D1S306	3	3	268	268
V4	D1S306	2	4	264	270

BIBLIOGRAPHY

1. Braunwald, E., Zipes, D.P. & Libby, P. Heart disease [electronic resource] : a textbook of cardiovascular medicine. 6th ed., editors Eugene Braunwald, Douglas P. Zipes, Peter Libby. edn (W.B. Saunders, [Great Britain], 2001).
2. Bayes de Luna, A., Coumel, P. & Leclercq, J.F. Ambulatory sudden cardiac death: mechanisms of production of fatal arrhythmia on the basis of data from 157 cases. *Am Heart J* **117**, 151-9 (1989).
3. Priori, S.G. et al. [Task Force on Sudden Cardiac Death, European Society of Cardiology. Summary of recommendations]. *Ital Heart J Suppl* **3**, 1051-65 (2002).
4. Maron, B.J., Epstein, S.E. & Roberts, W.C. Causes of sudden death in competitive athletes. *J Am Coll Cardiol* **7**, 204-14 (1986).
5. Zipes, D.P. & Wellens, H.J. Sudden cardiac death. *Circulation* **98**, 2334-51 (1998).
6. Bowker, T.J. et al. Sudden, unexpected cardiac or unexplained death in England: a national survey. *Qjm* **96**, 269-79 (2003).
7. Behr, E.R. et al. Sudden arrhythmic death syndrome: a national survey of sudden unexplained cardiac death. *Heart* **93**, 601-5 (2007).
8. Gilman, J.K., Jalal, S. & Naccarelli, G.V. Predicting and preventing sudden death from cardiac causes. *Circulation* **90**, 1083-92 (1994).
9. Burke, A.P. et al. Coronary risk factors and plaque morphology in men with coronary disease who died suddenly. *N Engl J Med* **336**, 1276-82 (1997).
10. Makikallio, T.H. et al. Frequency of sudden cardiac death among acute myocardial infarction survivors with optimized medical and revascularization therapy. *Am J Cardiol* **97**, 480-4 (2006).
11. Gillum, R.F. Coronary heart disease in black populations. I. Mortality and morbidity. *Am Heart J* **104**, 839-51 (1982).
12. Doval, H.C. et al. Nonsustained ventricular tachycardia in severe heart failure. Independent marker of increased mortality due to sudden death. GESICA-GEMA Investigators. *Circulation* **94**, 3198-203 (1996).
13. Belhassen, B. & Viskin, S. Idiopathic ventricular tachycardia and fibrillation. *J Cardiovasc Electrophysiol* **4**, 356-68 (1993).
14. Sarkozy, A. & Brugada, P. Sudden cardiac death and inherited arrhythmia syndromes. *J Cardiovasc Electrophysiol* **16 Suppl 1**, S8-20 (2005).
15. DeRose, J.J., Jr., Banas, J.S., Jr. & Winters, S.L. Current perspectives on sudden cardiac death in hypertrophic cardiomyopathy. *Prog Cardiovasc Dis* **36**, 475-84 (1994).
16. Tamburro, P. & Wilber, D. Sudden death in idiopathic dilated cardiomyopathy. *Am Heart J* **124**, 1035-45 (1992).

17. Bolger, A.P., Coats, A.J. & Gatzoulis, M.A. Congenital heart disease: the original heart failure syndrome. *Eur Heart J* **24**, 970-6 (2003).
18. Murdoch, J.L., Walker, B.A., Halpern, B.L., Kuzma, J.W. & McKusick, V.A. Life expectancy and causes of death in the Marfan syndrome. *N Engl J Med* **286**, 804-8 (1972).
19. Laso, F.J., Martin, C., Gonzalez-Buitrago, J.M. & de Castro, S. [Sudden death, exercise, and blood potassium]. *Med Clin (Barc)* **100**, 39 (1993).
20. Turkmen, N., Eren, B., Fedakar, R. & Durak, D. Sudden death related to anomalous origin of coronary artery and coexisting fenestrated membrane of the sinus coronarius. *Singapore Med J* **48**, 576-8 (2007).
21. Silingardi, E., Rivasi, F., Santunione, A.L. & Garagnani, L. Sudden death from tubercular myocarditis. *J Forensic Sci* **51**, 667-9 (2006).
22. Chizner, M.A., Pearle, D.L. & deLeon, A.C., Jr. The natural history of aortic stenosis in adults. *Am Heart J* **99**, 419-24 (1980).
23. Maron, B.J. et al. Task Force 4: HCM and other cardiomyopathies, mitral valve prolapse, myocarditis, and Marfan syndrome. *J Am Coll Cardiol* **45**, 1340-5 (2005).
24. Chang, S.T. & Chern, M.S. Sudden death in Wolff-Parkinson-White syndrome combined with syncope: a case report. *Int J Clin Pract Suppl*, 15-8 (2005).
25. Gupta, A., Lawrence, A.T., Krishnan, K., Kavinsky, C.J. & Trohman, R.G. Current concepts in the mechanisms and management of drug-induced QT prolongation and torsade de pointes. *Am Heart J* **153**, 891-9 (2007).
26. Habek, D., Janculjak, D., Cerkez Habek, J. & Jalsovec, D. Sudden death because of massive pulmonary thromboembolism and concomitant cerebrovascular trophoblastic embolism following artificial abortion. *Fetal Diagn Ther* **20**, 390-2 (2005).
27. Al-Khatib, S.M., LaPointe, N.M., Kramer, J.M. & Califf, R.M. What clinicians should know about the QT interval. *Jama* **289**, 2120-7 (2003).
28. Schwartz, P.J., Moss, A.J., Vincent, G.M. & Crampton, R.S. Diagnostic criteria for the long QT syndrome. An update. *Circulation* **88**, 782-4 (1993).
29. Priori, S.G., Napolitano, C. & Schwartz, P.J. Low penetrance in the long-QT syndrome: clinical impact. *Circulation* **99**, 529-33 (1999).
30. Brugada, P. & Brugada, J. Right bundle branch block, persistent ST segment elevation and sudden cardiac death: a distinct clinical and electrocardiographic syndrome. A multicenter report. *J Am Coll Cardiol* **20**, 1391-6 (1992).
31. Antzelevitch, C. et al. Brugada syndrome: report of the second consensus conference: endorsed by the Heart Rhythm Society and the European Heart Rhythm Association. *Circulation* **111**, 659-70 (2005).
32. Hopenfeld, B., Stinstra, J.G. & Macleod, R.S. Mechanism for ST depression associated with contiguous subendocardial ischemia. *J Cardiovasc Electrophysiol* **15**, 1200-6 (2004).
33. Hurst, J.W. Naming of the waves in the ECG, with a brief account of their genesis. *Circulation* **98**, 1937-42 (1998).
34. Shih, H.T. Anatomy of the action potential in the heart. *Tex Heart Inst J* **21**, 30-41 (1994).
35. Edwards, G. & Weston, A.H. Recent advances in potassium channel modulation. *Prog Drug Res* **49**, 93-121 (1997).

36. Lehnart, S.E. et al. Inherited arrhythmias: a National Heart, Lung, and Blood Institute and Office of Rare Diseases workshop consensus report about the diagnosis, phenotyping, molecular mechanisms, and therapeutic approaches for primary cardiomyopathies of gene mutations affecting ion channel function. *Circulation* **116**, 2325-45 (2007).
37. Trudeau, M.C., Warmke, J.W., Ganetzky, B. & Robertson, G.A. HERG, a human inward rectifier in the voltage-gated potassium channel family. *Science* **269**, 92-5 (1995).
38. Neyroud, N. et al. A novel mutation in the potassium channel gene KVLQT1 causes the Jervell and Lange-Nielsen cardioauditory syndrome. *Nat Genet* **15**, 186-9 (1997).
39. Splawski, I., Tristani-Firouzi, M., Lehmann, M.H., Sanguinetti, M.C. & Keating, M.T. Mutations in the hminK gene cause long QT syndrome and suppress IKs function. *Nat Genet* **17**, 338-40 (1997).
40. Splawski, I., Timothy, K.W., Vincent, G.M., Atkinson, D.L. & Keating, M.T. Molecular basis of the long-QT syndrome associated with deafness. *N Engl J Med* **336**, 1562-7 (1997).
41. Schwartz, P.J. et al. Genotype-phenotype correlation in the long-QT syndrome: gene-specific triggers for life-threatening arrhythmias. *Circulation* **103**, 89-95 (2001).
42. Curran, M.E. et al. A molecular basis for cardiac arrhythmia: HERG mutations cause long QT syndrome. *Cell* **80**, 795-803 (1995).
43. Priori, S.G. et al. Genetic and molecular basis of cardiac arrhythmias: impact on clinical management parts I and II. *Circulation* **99**, 518-28 (1999).
44. Yong, S., Tian, X. & Wang, Q. LQT4 gene: the "missing" ankyrin. *Mol Interv* **3**, 131-6 (2003).
45. Mohler, P.J. et al. Ankyrin-B mutation causes type 4 long-QT cardiac arrhythmia and sudden cardiac death. *Nature* **421**, 634-9 (2003).
46. Bianchi, L. et al. Cellular dysfunction of LQT5-minK mutants: abnormalities of IKs, IKr and trafficking in long QT syndrome. *Hum Mol Genet* **8**, 1499-507 (1999).
47. Abbott, G.W. et al. MiRP1 forms IKr potassium channels with HERG and is associated with cardiac arrhythmia. *Cell* **97**, 175-87 (1999).
48. Gaita, F. et al. Short QT Syndrome: a familial cause of sudden death. *Circulation* **108**, 965-70 (2003).
49. Brugada, R. et al. Sudden death associated with short-QT syndrome linked to mutations in HERG. *Circulation* **109**, 30-5 (2004).
50. Bellocq, C. et al. Mutation in the KCNQ1 gene leading to the short QT-interval syndrome. *Circulation* **109**, 2394-7 (2004).
51. Priori, S.G. et al. A novel form of short QT syndrome (SQT3) is caused by a mutation in the KCNJ2 gene. *Circ Res* **96**, 800-7 (2005).
52. Brugada, R., Hong, K., Cordeiro, J.M. & Dumaine, R. Short QT syndrome. *Cmaj* **173**, 1349-54 (2005).
53. Wang, Q. et al. Positional cloning of a novel potassium channel gene: KVLQT1 mutations cause cardiac arrhythmias. *Nat Genet* **12**, 17-23 (1996).
54. Sanguinetti, M.C., Jiang, C., Curran, M.E. & Keating, M.T. A mechanistic link between an inherited and an acquired cardiac arrhythmia: HERG encodes the IKr potassium channel. *Cell* **81**, 299-307 (1995).

55. Wang, Q. et al. SCN5A mutations associated with an inherited cardiac arrhythmia, long QT syndrome. *Cell* **80**, 805-11 (1995).

56. Rook, M.B. et al. Human SCN5A gene mutations alter cardiac sodium channel kinetics and are associated with the Brugada syndrome. *Cardiovasc Res* **44**, 507-17 (1999).

57. Chen, Q. et al. Genetic basis and molecular mechanism for idiopathic ventricular fibrillation. *Nature* **392**, 293-6 (1998).

58. Schott, J.J. et al. Cardiac conduction defects associate with mutations in SCN5A. *Nat Genet* **23**, 20-1 (1999).

59. Benson, D.W. et al. Congenital sick sinus syndrome caused by recessive mutations in the cardiac sodium channel gene (SCN5A). *J Clin Invest* **112**, 1019-28 (2003).

60. Groenewegen, W.A. et al. A cardiac sodium channel mutation cosegregates with a rare connexin40 genotype in familial atrial standstill. *Circ Res* **92**, 14-22 (2003).

61. Wang, Q. et al. Cardiac sodium channel mutations in patients with long QT syndrome, an inherited cardiac arrhythmia. *Hum Mol Genet* **4**, 1603-7 (1995).

62. Baroudi, G. & Chahine, M. Biophysical phenotypes of SCN5A mutations causing long QT and Brugada syndromes. *FEBS Lett* **487**, 224-8 (2000).

63. Zareba, W. et al. Influence of genotype on the clinical course of the long-QT syndrome. International Long-QT Syndrome Registry Research Group. *N Engl J Med* **339**, 960-5 (1998).

64. Fujiki, A. et al. ST segment elevation in the right precordial leads induced with class IC antiarrhythmic drugs: insight into the mechanism of Brugada syndrome. *J Cardiovasc Electrophysiol* **10**, 214-8 (1999).

65. Lehnart, S.E., Wehrens, X.H., Kushnir, A. & Marks, A.R. Cardiac ryanodine receptor function and regulation in heart disease. *Ann N Y Acad Sci* **1015**, 144-59 (2004).

66. Priori, S.G. et al. Mutations in the cardiac ryanodine receptor gene (hRyR2) underlie catecholaminergic polymorphic ventricular tachycardia. *Circulation* **103**, 196-200 (2001).

67. Priori, S.G. et al. Clinical and molecular characterization of patients with catecholaminergic polymorphic ventricular tachycardia. *Circulation* **106**, 69-74 (2002).

68. Lahat, H., Pras, E. & Eldar, M. A missense mutation in CASQ2 is associated with autosomal recessive catecholamine-induced polymorphic ventricular tachycardia in Bedouin families from Israel. *Ann Med* **36 Suppl 1**, 87-91 (2004).

69. Rosso, R. et al. Calcium channel blockers and beta-blockers versus beta-blockers alone for preventing exercise-induced arrhythmias in catecholaminergic polymorphic ventricular tachycardia. *Heart Rhythm* **4**, 1149-54 (2007).

70. Richardson, P. et al. Report of the 1995 World Health Organization/International Society and Federation of Cardiology Task Force on the Definition and Classification of cardiomyopathies. *Circulation* **93**, 841-2 (1996).

71. Geisterfer-Lowrance, A.A. et al. A molecular basis for familial hypertrophic cardiomyopathy: a beta cardiac myosin heavy chain gene missense mutation. *Cell* **62**, 999-1006 (1990).

72. Maron, B.J. et al. Prevalence of hypertrophic cardiomyopathy in a general population of young adults. Echocardiographic analysis of 4111 subjects in the CARDIA Study. Coronary Artery Risk Development in (Young) Adults. *Circulation* **92**, 785-9 (1995).

73. Poutanen, T. et al. Diastolic dysfunction without left ventricular hypertrophy is an early finding in children with hypertrophic cardiomyopathy-causing mutations in the beta-myosin heavy chain, alpha-tropomyosin, and myosin-binding protein C genes. *Am Heart J* **151**, 725 e1-725 e9 (2006).

74. Torricelli, F. et al. Prevalence and clinical profile of troponin T mutations among patients with hypertrophic cardiomyopathy in tuscany. *Am J Cardiol* **92**, 1358-62 (2003).

75. Richard, P. et al. Hypertrophic cardiomyopathy: distribution of disease genes, spectrum of mutations, and implications for a molecular diagnosis strategy. *Circulation* **107**, 2227-32 (2003).

76. Statement Development Group, H.R. et al. Clinical Indications for Genetic Testing in Familial Sudden Cardiac Death Syndromes: an HRUK Position Statement. *Heart* (2007).

77. Heitmancik, J.F. et al. Localization of gene for familial hypertrophic cardiomyopathy to chromosome 14q1 in a diverse US population. *Circulation* **83**, 1592-7 (1991).

78. Arad, M., Seidman, J.G. & Seidman, C.E. Phenotypic diversity in hypertrophic cardiomyopathy. *Hum Mol Genet* **11**, 2499-506 (2002).

79. Moolman, J.C. et al. Sudden death due to troponin T mutations. *J Am Coll Cardiol* **29**, 549-55 (1997).

80. Arad, M. et al. Gene mutations in apical hypertrophic cardiomyopathy. *Circulation* **112**, 2805-11 (2005).

81. Mogensen, J. et al. Alpha-cardiac actin is a novel disease gene in familial hypertrophic cardiomyopathy. *J Clin Invest* **103**, R39-43 (1999).

82. Olson, T.M., Karst, M.L., Whitby, F.G. & Driscoll, D.J. Myosin light chain mutation causes autosomal recessive cardiomyopathy with mid-cavitary hypertrophy and restrictive physiology. *Circulation* **105**, 2337-40 (2002).

83. Watkins, H. et al. A disease locus for familial hypertrophic cardiomyopathy maps to chromosome 1q3. *Nat Genet* **3**, 333-7 (1993).

84. Siu, B.L. et al. Familial dilated cardiomyopathy locus maps to chromosome 2q31. *Circulation* **99**, 1022-6 (1999).

85. Birmingham, N. et al. Mapping TNNT1, the gene that encodes cardiac troponin I in the human and the mouse. *Genomics* **30**, 620-2 (1995).

86. Blair, E. et al. Mutations in the gamma(2) subunit of AMP-activated protein kinase cause familial hypertrophic cardiomyopathy: evidence for the central role of energy compromise in disease pathogenesis. *Hum Mol Genet* **10**, 1215-20 (2001).

87. Watkins, H. et al. Mutations in the cardiac myosin binding protein-C gene on chromosome 11 cause familial hypertrophic cardiomyopathy. *Nat Genet* **11**, 434-7 (1995).

88. Geier, C. et al. Mutations in the human muscle LIM protein gene in families with hypertrophic cardiomyopathy. *Circulation* **107**, 1390-5 (2003).

89. Poetter, K. et al. Mutations in either the essential or regulatory light chains of myosin are associated with a rare myopathy in human heart and skeletal muscle. *Nat Genet* **13**, 63-9 (1996).

90. Thierfelder, L. et al. Alpha-tropomyosin and cardiac troponin T mutations cause familial hypertrophic cardiomyopathy: a disease of the sarcomere. *Cell* **77**, 701-12 (1994).

91. MacGeoch, C., Barton, P.J., Vallins, W.J., Bhavsar, P. & Spurr, N.K. The human cardiac troponin I locus: assignment to chromosome 19p13.2-19q13.2. *Hum Genet* **88**, 101-4 (1991).
92. Cullen, M.E., Dellow, K.A. & Barton, P.J. Structure and regulation of human troponin genes. *Mol Cell Biochem* **263**, 81-90 (2004).
93. Harada, K. & Morimoto, S. Inherited cardiomyopathies as a troponin disease. *Jpn J Physiol* **54**, 307-18 (2004).
94. Mesnard, L. et al. Human cardiac troponin T: cloning and expression of new isoforms in the normal and failing heart. *Circ Res* **76**, 687-92 (1995).
95. Anderson, P.A. et al. Molecular basis of human cardiac troponin T isoforms expressed in the developing, adult, and failing heart. *Circ Res* **76**, 681-6 (1995).
96. Michels, V.V. et al. The frequency of familial dilated cardiomyopathy in a series of patients with idiopathic dilated cardiomyopathy. *N Engl J Med* **326**, 77-82 (1992).
97. Arbustini, E. et al. Autosomal dominant dilated cardiomyopathy with atrioventricular block: a lamin A/C defect-related disease. *J Am Coll Cardiol* **39**, 981-90 (2002).
98. Krajinovic, M. et al. Linkage of familial dilated cardiomyopathy to chromosome 9. Heart Muscle Disease Study Group. *Am J Hum Genet* **57**, 846-52 (1995).
99. Vatta, M. et al. Mutations in Cypher/ZASP in patients with dilated cardiomyopathy and left ventricular non-compaction. *J Am Coll Cardiol* **42**, 2014-27 (2003).
100. Durand, J.B. et al. Localization of a gene responsible for familial dilated cardiomyopathy to chromosome 1q32. *Circulation* **92**, 3387-9 (1995).
101. McNair, W.P. et al. SCN5A mutation associated with dilated cardiomyopathy, conduction disorder, and arrhythmia. *Circulation* **110**, 2163-7 (2004).
102. Messina, D.N., Speer, M.C., Pericak-Vance, M.A. & McNally, E.M. Linkage of familial dilated cardiomyopathy with conduction defect and muscular dystrophy to chromosome 6q23. *Am J Hum Genet* **61**, 909-17 (1997).
103. Pelin, K. et al. Refined localisation of the genes for nebulin and titin on chromosome 2q allows the assignment of nebulin as a candidate gene for autosomal recessive nemaline myopathy. *Eur J Hum Genet* **5**, 229-34 (1997).
104. Jung, M. et al. Investigation of a family with autosomal dominant dilated cardiomyopathy defines a novel locus on chromosome 2q14-q22. *Am J Hum Genet* **65**, 1068-77 (1999).
105. Li, D. et al. Desmin mutation responsible for idiopathic dilated cardiomyopathy. *Circulation* **100**, 461-4 (1999).
106. Schonberger, J. et al. Mutation in the transcriptional coactivator EYA4 causes dilated cardiomyopathy and sensorineural hearing loss. *Nat Genet* **37**, 418-22 (2005).
107. Sylvius, N. et al. A new locus for autosomal dominant dilated cardiomyopathy identified on chromosome 6q12-q16. *Am J Hum Genet* **68**, 241-6 (2001).
108. Tsubata, S. et al. Mutations in the human delta-sarcoglycan gene in familial and sporadic dilated cardiomyopathy. *J Clin Invest* **106**, 655-62 (2000).
109. Knoll, R. et al. The cardiac mechanical stretch sensor machinery involves a Z disc complex that is defective in a subset of human dilated cardiomyopathy. *Cell* **111**, 943-55 (2002).
110. Bienengraeber, M. et al. ABCC9 mutations identified in human dilated cardiomyopathy disrupt catalytic KATP channel gating. *Nat Genet* **36**, 382-7 (2004).

111. Schmitt, J.P. et al. Dilated cardiomyopathy and heart failure caused by a mutation in phospholamban. *Science* **299**, 1410-3 (2003).
112. Schonberger, J. et al. A novel locus for autosomal-dominant dilated cardiomyopathy maps to chromosome 7q22.3-31.1. *Hum Genet* **118**, 451-7 (2005).
113. Olson, T.M., Michels, V.V., Thibodeau, S.N., Tai, Y.S. & Keating, M.T. Actin mutations in dilated cardiomyopathy, a heritable form of heart failure. *Science* **280**, 750-2 (1998).
114. Qin, H. et al. Localization of human cardiac beta-myosin heavy chain gene (MYH7) to chromosome 14q12 by in situ hybridization. *Cytogenet Cell Genet* **54**, 74-6 (1990).
115. Taylor, M.R. et al. Thymopoietin (lamina-associated polypeptide 2) gene mutation associated with dilated cardiomyopathy. *Hum Mutat* **26**, 566-74 (2005).
116. Li, D. et al. Mutations of presenilin genes in dilated cardiomyopathy and heart failure. *Am J Hum Genet* **79**, 1030-9 (2006).
117. Olson, T.M. et al. Metavinculin mutations alter actin interaction in dilated cardiomyopathy. *Circulation* **105**, 431-7 (2002).
118. Murakami, T. et al. Fukutin gene mutations cause dilated cardiomyopathy with minimal muscle weakness. *Ann Neurol* **60**, 597-602 (2006).
119. Daehmlow, S. et al. Novel mutations in sarcomeric protein genes in dilated cardiomyopathy. *Biochem Biophys Res Commun* **298**, 116-20 (2002).
120. Gemayel, C., Pelliccia, A. & Thompson, P.D. Arrhythmogenic right ventricular cardiomyopathy. *J Am Coll Cardiol* **38**, 1773-81 (2001).
121. Protonotarios, N. et al. Genotype-phenotype assessment in autosomal recessive arrhythmogenic right ventricular cardiomyopathy (Naxos disease) caused by a deletion in plakoglobin. *J Am Coll Cardiol* **38**, 1477-84 (2001).
122. Sen-Chowdhry, S., Syrris, P. & McKenna, W.J. Role of genetic analysis in the management of patients with arrhythmogenic right ventricular dysplasia cardiomyopathy. *J Am Coll Cardiol* **50**, 1813-21 (2007).
123. Rampazzo, A. et al. The gene for arrhythmogenic right ventricular cardiomyopathy maps to chromosome 14q23-q24. *Hum Mol Genet* **3**, 959-62 (1994).
124. Beffagna, G. et al. Regulatory mutations in transforming growth factor-beta3 gene cause arrhythmogenic right ventricular cardiomyopathy type 1. *Cardiovasc Res* **65**, 366-73 (2005).
125. Rampazzo, A. et al. A new locus for arrhythmogenic right ventricular cardiomyopathy (ARVD2) maps to chromosome 1q42-q43. *Hum Mol Genet* **4**, 2151-4 (1995).
126. Tiso, N. et al. Identification of mutations in the cardiac ryanodine receptor gene in families affected with arrhythmogenic right ventricular cardiomyopathy type 2 (ARVD2). *Hum Mol Genet* **10**, 189-94 (2001).
127. Rampazzo, A. et al. ARVD4, a new locus for arrhythmogenic right ventricular cardiomyopathy, maps to chromosome 2 long arm. *Genomics* **45**, 259-63 (1997).
128. Ahmad, F. et al. Localization of a gene responsible for arrhythmogenic right ventricular dysplasia to chromosome 3p23. *Circulation* **98**, 2791-5 (1998).
129. Melberg, A. et al. Autosomal dominant myofibrillar myopathy with arrhythmogenic right ventricular cardiomyopathy linked to chromosome 10q. *Ann Neurol* **46**, 684-92 (1999).

130. Rampazzo, A. et al. Mutation in human desmoplakin domain binding to plakoglobin causes a dominant form of arrhythmogenic right ventricular cardiomyopathy. *Am J Hum Genet* **71**, 1200-6 (2002).
131. Gerull, B. et al. Mutations in the desmosomal protein plakophilin-2 are common in arrhythmogenic right ventricular cardiomyopathy. *Nat Genet* **36**, 1162-4 (2004).
132. Syrris, P. et al. Clinical expression of plakophilin-2 mutations in familial arrhythmogenic right ventricular cardiomyopathy. *Circulation* **113**, 356-64 (2006).
133. Pilichou, K. et al. Mutations in desmoglein-2 gene are associated with arrhythmogenic right ventricular cardiomyopathy. *Circulation* **113**, 1171-9 (2006).
134. Syrris, P. et al. Arrhythmogenic right ventricular dysplasia cardiomyopathy associated with mutations in the desmosomal gene desmocollin-2. *Am J Hum Genet* **79**, 978-84 (2006).
135. Asimaki, A. et al. A novel dominant mutation in plakoglobin causes arrhythmogenic right ventricular cardiomyopathy. *Am J Hum Genet* **81**, 964-73 (2007).
136. Coonar, A.S. et al. Gene for arrhythmogenic right ventricular cardiomyopathy with diffuse nonepidermolytic palmoplantar keratoderma and woolly hair (Naxos disease) maps to 17q21. *Circulation* **97**, 2049-58 (1998).
137. Tristani-Firouzi, M. et al. Functional and clinical characterization of KCNJ2 mutations associated with LQT7 (Andersen syndrome). *J Clin Invest* **110**, 381-8 (2002).
138. Splawski, I. et al. Ca(V)1.2 calcium channel dysfunction causes a multisystem disorder including arrhythmia and autism. *Cell* **119**, 19-31 (2004).
139. Vatta, M. et al. Mutant caveolin-3 induces persistent late sodium current and is associated with long-QT syndrome. *Circulation* **114**, 2104-12 (2006).
140. Medeiros-Domingo, A. et al. SCN4B-encoded sodium channel beta4 subunit in congenital long-QT syndrome. *Circulation* **116**, 134-42 (2007).
141. Weiss, R. et al. Clinical and molecular heterogeneity in the Brugada syndrome: a novel gene locus on chromosome 3. *Circulation* **105**, 707-13 (2002).
142. London, B. et al. Mutation in glycerol-3-phosphate dehydrogenase 1 like gene (GPD1-L) decreases cardiac Na⁺ current and causes inherited arrhythmias. *Circulation* **116**, 2260-8 (2007).
143. Haghghi, K. et al. A mutation in the human phospholamban gene, deleting arginine 14, results in lethal, hereditary cardiomyopathy. *Proc Natl Acad Sci U S A* **103**, 1388-93 (2006).
144. Nyberg, M.T. et al. The variation of the sarcolipin gene (SLN) in atrial fibrillation, long QT syndrome and sudden arrhythmic death syndrome. *Clin Chim Acta* **375**, 87-91 (2007).
145. Kraev, A., Chumakov, I. & Carafoli, E. The organization of the human gene NCX1 encoding the sodium-calcium exchanger. *Genomics* **37**, 105-12 (1996).
146. Bowles, N.E., Bowles, K.R. & Towbin, J.A. The "final common pathway" hypothesis and inherited cardiovascular disease. The role of cytoskeletal proteins in dilated cardiomyopathy. *Herz* **25**, 168-75 (2000).
147. Yarbrough, T.L., Lu, T., Lee, H.C. & Shibata, E.F. Localization of cardiac sodium channels in caveolin-rich membrane domains: regulation of sodium current amplitude. *Circ Res* **90**, 443-9 (2002).

148. Martens, J.R., Sakamoto, N., Sullivan, S.A., Grobaski, T.D. & Tamkun, M.M. Isoform-specific localization of voltage-gated K⁺ channels to distinct lipid raft populations. Targeting of Kv1.5 to caveolae. *J Biol Chem* **276**, 8409-14 (2001).
149. Balijepalli, R.C., Foell, J.D., Hall, D.D., Hell, J.W. & Kamp, T.J. Localization of cardiac L-type Ca(2+) channels to a caveolar macromolecular signaling complex is required for beta(2)-adrenergic regulation. *Proc Natl Acad Sci U S A* **103**, 7500-5 (2006).
150. Ott, J. *Analysis of human genetic linkage*, xxiii, 382 p. (Johns Hopkins University Press, Baltimore ; London, 1999).
151. Young, L.J. Oxytocin and vasopressin as candidate genes for psychiatric disorders: lessons from animal models. *Am J Med Genet* **105**, 53-4 (2001).
152. Strachan, T., Strachan, T.H.m.g. & Read, A.P. *Human molecular genetics 3*, xxv, 674 p. (Garland Science, London, 2004).
153. Fantes, J. et al. Aniridia-associated cytogenetic rearrangements suggest that a position effect may cause the mutant phenotype. *Hum Mol Genet* **4**, 415-22 (1995).
154. Hearn, T. et al. Mutation of ALMS1, a large gene with a tandem repeat encoding 47 amino acids, causes Alstrom syndrome. *Nat Genet* **31**, 79-83 (2002).
155. Chevillard, C. et al. Localization of a potassium channel gene (KCNE1) to 21q22.1-q22.2 by in situ hybridization and somatic cell hybridization. *Genomics* **15**, 243-5 (1993).
156. Townsend, P.J., Barton, P.J., Yacoub, M.H. & Farza, H. Molecular cloning of human cardiac troponin T isoforms: expression in developing and failing heart. *J Mol Cell Cardiol* **27**, 2223-36 (1995).
157. Abello, M., Merino, J.L., Peinado, R. & Gnoatto, M. Negative flecainide test in Brugada syndrome patients with previous positive response. *Europace* **8**, 899-900 (2006).
158. Farza, H. et al. Genomic organisation, alternative splicing and polymorphisms of the human cardiac troponin T gene. *J Mol Cell Cardiol* **30**, 1247-53 (1998).
159. Koopmann, T.T. et al. Long QT syndrome caused by a large duplication in the KCNH2 (HERG) gene undetectable by current polymerase chain reaction-based exon-scanning methodologies. *Heart Rhythm* **3**, 52-5 (2006).
160. Fernandez, L. et al. Comparative study of three diagnostic approaches (FISH, STRs and MLPA) in 30 patients with 22q11.2 deletion syndrome. *Clin Genet* **68**, 373-8 (2005).